Craniofacial development chemical tools and molecular biology

Bolger, Triona

Awarding institution:
King's College London

Title: Craniofacial development
chemical tools and molecular biology

Author: Triona Bolger

Craniofacial development: chemical tools and molecular biology

Tríona Graínne Bolger

A thesis submitted for the degree
Doctor of Philosophy,
King's College London, University of London

Supervisor
Dr Karen J. Liu
Department of Craniofacial Development

2011

Acknowledgments

Clearly this project would never have happened if it weren't for the opportunity, support, advice and occasional kick in the ass from my supervisor Karen Liu. I don't think I can express how much more than science I have learnt from you in the last few years.

I am grateful also to Dr. Jeremy Green and Prof. Andrea Streit for always being willing to listen when I knocked on their doors.

A very special thank you is needed for Angela Gates, Dr. Chris Healy and Martin Chaperlin without whom CFD would grind to a halt. You collectively keep the ceiling up, wheels greased and world spinning, not to mention keep us supplied with tea, biscuits, home cooked dinners, reagents, calm words and working computers.

Lab members past and present, Lara, Hattie, Ashley, Gui, Eleni, John, Adam, Andrew, Laura and Abbey; work (and the Britannia) was a better place because of you all.

Heather Szabo Rogers you were an invaluable source of knowledge throughout the years and answered my innumerable daft questions with patience and generosity throughout. Congratulations on your two new roles, I am sure you'll be amazing in both.

Jacqui Tabler has been a great colleague, steadfast confidant and source of advice on topics ranging from food and flirtations to fibronectin. I expect your future to include greatness, ever-larger victory rolls and an even more expansive wardrobe of 40's fashion! Go forth and kick ass! I shall endeavor to keep you supplied with good tea!

Kirsty Wells, you kept me sane, listened to me practice those terrible early talks on the stairwell and prompted me to ever-brighter red hair. I don't think I would have survived the first year without you and I don't think I said thank you nearly enough. Good luck with your polka dot *in situs* and I hope to be kept abreast of the continued excellence in the Edinburgh chapter in your life.

Nisha Patel, though not my SG buddy could perhaps be considered a Wnt buddy? Thank you for the hugs, for my own little cookie fan club and for always sharing the funnier side of your life with me. I hope your adventures as a married woman bring you joy for the rest of your life.

Basil Yannakoudakis and Wills Barrell, thank you for putting up with my “final year” grumpiness and I’m happy to leave the transitioning lab in your capable hands. Wills – special thanks for the multitude of western blots you saved me from!

To Adam and Sarah, my bay mates and office mates in these last months, thanks for your patience and cheer!

To the fabulous Thames ladies, you have my eternal gratitude for reminding me that there was life outside a lab, for helping me (and in my heart, Kat) get a chance to race at Henley and for some fantastic parties along the way.
I am Thames Woman. Hear me Roar.

There are more friends to thank that I have pages of data but special thanks to Kira, Zoe and Bexy. You are my DULBC/TCD buddies who I think of whenever I need to remember that once upon a time, uni was fun!

To Ghis who gave me my first real home in London, I’m so glad I knocked on your door, I knew it was meant to be when I spotted the full shelf of books.

To Alan, who has waited patiently for me to be fun again. If I promise to bring Tree-with-free-time back, all the way from the Hill in Honesdale, can we have a BBQ soon, even if I have to come to Sydney for it?

To Soph T, who never said no to gossiping over breakfast and to bitching over weights.

To Kira and Angela, even knowing what you were letting yourself in for you still agreed to be my flatmates during this last year. Thanks for putting up with me.

Donal, what can I say. It seems that somewhere between coffee in the Ham café and breakfast in Fulham we grew up. You have been the most incredible friend and I’ll never not owe you.

Áine, now half a world away, as always you have a unfailing ability to put things in perspective that is greatly appreciated. I wish I were closer to you and your expanding brood of four legged family members! I know I drive you bonkers but thanks for always being at the other end of an email.

Mum (and second Mammy, Rita), my unfaltering fountains of support. I couldn't ask for more! Mum, if you are a tenth as proud of me as I am of you I consider myself a success. Thank you for now and always.

'If you can force your heart and nerve and sinew
To serve your turn long after they are gone,
And so hold on when there is nothing in you
Except the Will, which says to them: 'Hold on!'
Rudyard Kipling

Dad, whose guidance I cherish then, now and forever.

"For whatever we lose (like a you or a me)
it's always ourselves we find in the sea."
E. E. Cummings

TABLE OF CONTENTS

TABLE OF FIGURES

Formatted: Justified

Formatted: Justified, Right: -0.01 cm

Formatted: Justified

Formatted: Justified

TABLE OF TABLES

1. INTRODUCTION

1.1 The head: a vertebrate invention

In this project I have used *Xenopus laevis* to address the spatial and temporal requirements for various signaling pathways in organogenesis, specifically craniofacial development. Craniofacial structures of *Xenopus*, such as the cartilages, are analogous to those in other vertebrates. A significant portion of the vertebrate head is derived from the neural crest. Thus, this is also a study of neural crest development.

The vertebrate head can be defined by the presence of a number of specialised features including a segmented brain, complex sensory organs and others such as skull bones, teeth and facial muscles. This developmental biology project strives to understand how various signaling pathways regulate the development of this complex, multicellular, three-dimensional region. Moreover, I am interested in how the neural crest can contribute to these wide-ranging structures.

The unique features of the head help set vertebrates apart from cephalochordates, their closest non-vertebrate relatives (Stone and Hall, 2004) (Wada, 2001). One such close relative is *Amphioxus*, which has a notochord and a neural tube, but does not possess a complex brain or any complex facial structures. Crucially, it lacks the neural crest cells that comprise the head structures of vertebrates. In cephalochordate and urochordate embryos the cells in the border between the neural plate and the epidermis express several key genes required for vertebrate crest development (*Snail, Msx, Bmp2, Pax3*) (Meulemans and Bronner-Fraser, 2007; Yu et al., 2008). Unlike vertebrate crest, these cells are not migratory and do not have the same pluripotency of vertebrate neural crest cells (Holland and Holland, 2001). As such, the innovation of migratory neural crest cells is integral to the development of the head.

1.1.1 Craniofacial malformations

Errors in the development of cranial neural crest or in disruption in normal embryogenesis can result in a wide variety of craniofacial abnormalities. These abnormalities have far reaching implications for patients: the inability to eat, breathe, speak, or hear normally may result in severe difficulties during childhood that can persist into adulthood or, are sometimes fatal. Craniofacial abnormalities are among the most common birth defects and approximately one-third of all human congenital defects will present with craniofacial dysmorphologies. However, only a limited number of these disorders are well characterised and little is known about the etiology of these craniofacial disorders. Some are known to be primarily genetic in nature (e.g. Treacher Collins syndrome, Crouzon Syndrome or DiGeorge syndrome (Trainor, 2010; Trainor et al., 2009) (Reardon et al., 1994) (Wurdak et al., 2006)) while others are presumed to be caused by environmental factors (e.g. fetal alcohol syndrome (Ulleland, 1972)). Often multiple factors play roles in determining the severity of these disorders.

Recent advances in the generation of mouse and zebrafish mutants have shed some light on certain craniofacial syndromes. This said, generation of mutant models is time consuming and expensive. Though more models are now becoming available (e.g. Jackson laboratory genetic resource centre http://www.jax.org/), animal phenotypes may not be comparable to those in human patients. Mutant models have also been generated in forward mutagenesis screens (discussed later). These are extremely useful in shedding light on the requirements for specific genes. However, early defects can mask later roles in development and thus may not be ideal models for studying human dysmorphologies. For example, the *sonic hedgehog* (*SHH*) gene is known to be mutated in human craniofacial disorders. However, mice lacking *Shh* die early in gestation (Chiang et al., 1996). Conditional mutants, such as those generated by Cre-dependent gene excision, can bypass embryonic lethality (Sauer, 1987). Such inducible technologies are remarkably useful when looking at the function of a specific gene in a specific tissue, or, at a set time in development. This approach assumes availability of multiple transgenic mouse lines, which may be too expensive for most labs. In my project, we made use of *Xenopus* as an alternative model system for neural crest and craniofacial development.

1.2 The neural crest

The neural crest is a uniquely vertebrate, migratory cell population that arises in the dorsal region of the neural tube and contributes to both head and trunk. Neural crest (NC) arise bilaterally at the border of the non-neural ectoderm and the neural plate and can be identified by expression of a unique panel of genes, including *slug (snail2), snail, sox10, sox9, foxD3 and c-myc* (Linker et al., 2000; Mayor et al., 1995) (Sasai et al., 2001) (Spokony et al., 2002) (Nieto, 2002) (Honore et al., 2003). Neural crest cells are specified throughout the neural tube, posterior to the mid-hindbrain boundary. After neural tube closure, neural crest cells delaminate from the most dorsal region of the neural tube by undergoing an epithelial–mesenchymal transition (EMT). Crest cells then migrate throughout the embryo via distinct, conserved paths. After migration, neural crest cells populate specific regions along the length of the embryo and differentiate into multiple cell types during organogenesis. NC cells not only differentiate into skeletal elements of the head but are capable of forming connective tissue, Schwann cells, sensory ganglia, and melanocytes (Aybar et al., 2002) (Knecht and Bronner-Fraser, 2002) (Sauka-Spengler and Bronner-Fraser, 2008). Organs that receive a contribution from the neural crest include the optic vesicle, the inner ear, cranial nerves and the pharyngeal arches, where neural crest derived tissue form muscle, bone, and cartilage of the face (Le Douarin and Kalcheim, 1999).

As neural crest is integral to so many tissues, correct NC development is crucial for embryogenesis. Resulting phenotypes of improper NC development are dramatic and varied. They include cleft palate, intestinal aganglionosis (Hirschsprung's disease) and cancers such as neuroblastoma (Fuchs and Sommer, 2007; Tobin et al., 2008a). As such, neurocristopathies (disorders of the neural crest) are often pleiotrophic syndromes affecting many tissues. A more detailed understanding of neural crest development will, therefore, provide insight into a large number of human disorders.

1.2.1 Neural crest induction

A complex set of signaling pathways, discussed in more detail later, regulate induction of the neural crest (Aybar et al., 2002) (Knecht and Bronner-Fraser, 2002) (Sauka-Spengler and Bronner-Fraser, 2008).

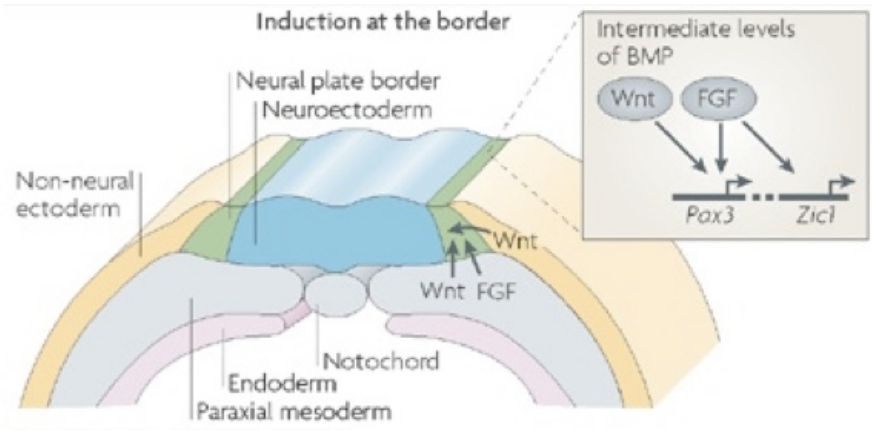

Figure 1.1 Some of the tissues and signals involved in neural crest induction
The induction of neural crest cells (in green) occurs at the border of the neural plate (blue) and the surface ectoderm (yellow). Neural crest induction depends on signaling between non-neural ectoderm and the neural plate. Signals from the paraxial mesoderm are also important.
(Sauka-Spengler and Bronner-Fraser, 2008)

As the neural tube elevates and closes, multiple signals specify the neural crest cells in the region between the neural plate and the surface non-neural ectoderm. Gradients of signaling factors are established during early embryogenesis. These include high-levels of BMP from the non-neural ectoderm, FGF from the paraxial mesoderm, and Wnt from the non-neural ectoderm and paraxial mesoderm (Figure 1.1) (Mancilla and Mayor, 1996) (Marchant et al., 1998) (García-Castro and Bronner-Fraser, 1999). A number of Wnts are required for neural crest during development. In *Xenopus* these include Wnt1, Wnt3A (in presumptive neural crest) and Wnt7b (in the neural plate and non-neural ectoderm) (Wu et al., 2005). Wnt8 is present in the underlying mesoderm and the Wnt receptor Frizzled (Fz3/9) is expressed in the

surrounding ectoderm (Wu et al., 2003). Wnt signaling in neural crest development is explored in detail later.

NC induction is initiated during early gastrula stages and may proceed during later neurula stages. Experiments in frog and chick embryos have shown that cell–cell interactions in the ectoderm are required to ensure NC development. There must be interaction between the non-neural ectoderm and the neural ectoderm (neural plate) in order to induce NC (Moury and Jacobson, 1990; Selleck and Bronner-Fraser, 1995) (Dickinson et al., 1995) (Mancilla and Mayor, 1996). Paraxial mesoderm is required to induce NC in the adjacent neural folds region (Selleck and Bronner-Fraser, 1995) (Bonstein et al., 1998). During gastrulation and early neurulation, this paraxial mesoderm lies beneath the presumptive neural crest. However, this interaction is not required during Zebrafish neural crest induction as excision of paraxial mesoderm does not cause loss of neural crest and MZoep ('maternal-zygotic one-eyed pinhead') mutants which lack paraxial mesoderm have normal neural crest (Ragland and Raible, 2004).

1.2.2 Neural crest delamination occurs via epithelial to mesenchymal transition

The neural crest arises from epithelial cells which are polarised and held together tightly by intercellular junctions (Tucker, 2004). The neural crest then delaminate in a process called epithelial to mesenchymal transition (EMT) during which the basal lamina of the dorsal neural tube breaks down, intercellular junctions weaken and cells are free to migrate (Tucker, 2004) (Kang and Svoboda, 2005). In the neural crest, delamination is tightly linked to the cell cycle. Neural crest cells delaminate during the S phase (Burstyn-Cohen et al., 2004). Wnt/β-catenin signaling is required indirectly, for controlling cell cycle progression from G1 to S phase by regulating the transcription of cyclin D1 (Tetsu and McCormick, 1999). This Wnt activity during delamination of the neural crest may be regulated by BMP (Burstyn-Cohen et al., 2004). Up regulation of BMP results in increased neural crest migration, a phenotype rescued with the addition of β-catenin. When β-catenin is over expressed, neural crest migration is lost (Burstyn-Cohen et al., 2004). *Slug*, a member of the snail family, is expressed in NC cells and promotes loss of epithelial characteristics as well as halting of cell cycle. These changes are crucial and have

also been found in metastatic cancer cells (Nieto, 2002; Vega et al., 2004). *Slug* is a transcriptional target of Wnt/β-catenin signaling (Vallin et al., 2001). In chick and *Xenopus*, inhibition of slug after neural crest induction results in neural crest cells failing to delaminate (Nieto et al., 1994).

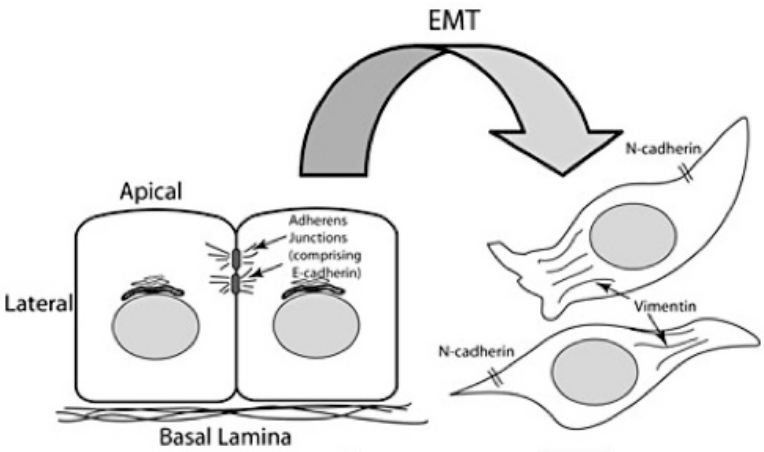

Figure 1.2 Delamination of Epithelial Cells
Epithelial cells are strictly polarised with apical, basal and lateral surfaces and are held tightly together with several types of intercellular junctions. The adherens junctions are composed of numerous E-cadherin molecules. In the transition from epithelial to mesenchymal cells, E-cadherin expression is downregulated, allowing attached epithelial cells to separate from each other and take on a mesenchymal phenotype. Mesenchymal cells can migrate through the extracellular matrix. In addition to loss of E-cadherin, there is often misregulated expression of N-cadherin in mesenchymal cells that has been linked to their increased motility.
Figure from (Doble and Woodgett, 2007)

1.2.3 Numerous external factors regulate migration of the neural crest

Trunk and cranial neural crest cells migrate along specific routes, unique to either population (Kuriyama and Mayor, 2008). Cranial neural crest cells migrate in a wave over a short period of time, compared to the more lengthy period of migration in the trunk neural crest cells (Hall, 2008) (Le Douarin and Kalcheim, 1999) (Théveneau et al., 2007). The paths taken by the migrating cells are specific and regulated by both attractive and repulsive forces, which are different depending on where the cells are located along the anterior-posterior (A-P) axis (Abzhanov et al., 2003). There are numerous molecules involved in generating the attractive or

repulsive forces, including semaphorins/neuropilins, ephs/ephrins, chemokines, complements and ADAMs such as ADAM13 (Alfandari et al., 2001; Carmona-Fontaine et al., 2011; Gammill et al., 2007; Olesnicky Killian et al., 2009; Rezzoug et al., 2011; Robinson et al., 1997; Smith et al., 1997)

Cranial neural crest paths are initially determined by rhombomeres of the developing brain. Neural crest cells arise from all the rhombomeres (r) of the chick brain, with some apoptosis is seen in the premigratory cells of r3 and r5 (Ellies et al., 2002). After delamination the neural crest cells (NCCs) sort into streams below the 2nd, 4th and 6th rhombomeres (Birgbauer et al., 1995). In *Xenopus*, organisation of the migratory streams occurs somewhat later and begins when the cells move into the branchial arches (Sadaghiani and Thiébaud, 1987; Smith et al., 1997). Prior to this the cells migrate close to the surface ectoderm in the embryo (Kuriyama and Mayor, 2008).

The cranial neural crest streams in the mouse are maintained by coordination of neuropilin 2 and semaphorin 3F expression (Gammill et al., 2007) (Eickholt et al., 1999). Rhombomeres and somites express semaphorin 3F while migrating neural crest cells express neuropilin 2 (Gammill et al., 2006; Osborne et al., 2005). Various Eph/ephrin combinations are found in mouse and chick and have been shown to regulate the migration of the neural crest cells around and through the anterior somites of the trunk (Santiago and Erickson, 2002). In both zebrafish and chick it has been shown that cranial neural crest cells express receptors Cxcr4 and Cxcr7 and that the expression the chemokine Sdf1 in pharyngeal arch is required for proper migration and subsequent differentiation of cranial crest (Olesnicky Killian et al., 2009; Rezzoug et al., 2011). Neural crest cells, upon first delamination, move as sheets of cells with contact between the cells that are important for proper migration. This cell-cell interaction requires close coordination between cells and recently it has been shown that the cells are not only receiving attractive and repulsive forces from their surrounding tissues but also from one another. These signals support the cohesive nature of the neural crest, are crucial for the collective migration and are mediated by the complement fragment C3a and its receptor C3aR (Carmona-Fontaine et al., 2011). Additionally, ADAMs have been found to have a role in regulating cranial neural crest migration (Seals and Courtneidge, 2003). Loss of ADAM13 in *Xenopus* cranial crest results in failure of these cells to migrate. Aberrant expression in trunk cells causes the NCCs to migrate into pathways they are normally prohibited from, suggesting the ADAMs are required for the cells to

interpret the permissive or repulsive messages in their surrounding (Alfandari et al., 2001). Alternatively, ADAM13 may be regulating the NCCs ability to travel on different extracellular matrices (Seals and Courtneidge, 2003)

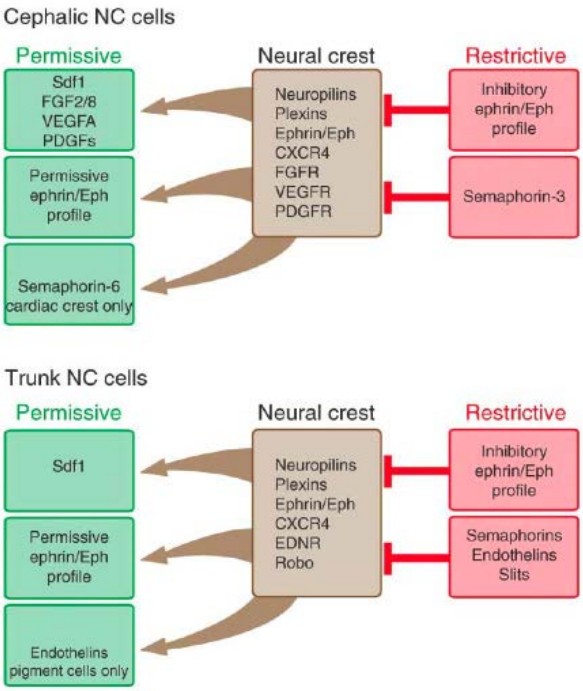

Figure 1.3 Signals guiding neural crest migration

Neural crest cells express a variety of cell surface receptors. The cephalic (cranial) and trunk crest express different receptors. The tissues surrounding the migrating crest have several positive (shown in green) and negative (shown in red) guidance cues. Certain molecules, such as ephrins/Eph may act as permissive or restrictive cues. Working together, these create the pathways for migration and maintain NC free regions in the body.
Figure from (Theveneau and Mayor, 2012)

Such attractive and repulsive forces work by regulating the direction of migration and either permitting or preventing cell migration in any given direction. In the case of semaphorins and chemokines, altering the cyctoskeletal support in the projection on the leading edge of the cell regulates direction of migration. Sema3 interaction with its neurophilin1 receptor induces growth cone collapse in neurons by activating GSK-3 at the cone edge (Eickholt et al., 2002), suggesting a potential role for GSK-3 in the leading edge of a migrating neural crest cell. Loss of semaphorin activity in

chick and zebrafish results in neural crest invading tissues that should be devoid of neural crest (Osborne et al., 2005) (Yu and Moens, 2005).

1.2.4 Differentiation of the Neural Crest

A number of factors have been implicated in the regulation of neural crest differentiation. These include the timing and route of their migration. Timing of neural crest delamination is important for the NC specification of in both chick and mouse (Serbedzija et al., 1994) (Henion and Weston, 1997) Lysinated rhodamine dextran tracing was used to label individual chick NCCs and all subsequent progeny. Injections performed early in the migration (E8-9) contributed to a much wider range of derivatives than those injected between stages E9-10 (Serbedzija et al., 1994). In mouse, in vitro clonal analysis was used to show that many neural crest cells are fate restricted, even in the premigratory stages. The later migrating cells express melanocyte markers, not found in cells that were migrating from the earlier explants (Henion and Weston, 1997). Late migrating neural crest cells in chick contribute significantly more than early migrating cells to skeletal elements of the face (Henion and Weston, 1997) while in mouse later emigration of cells results in dorsal fates such as dorsal root ganglia (Serbedzija et al., 1994). Melanocytes arise from the later migration of trunk neural crest (Wilson et al., 2004).

Neural crest cells traverse a number of different routes and these routes affect the differential fate of the cells (Wilson et al., 2004). The neural crest cells are exposed to a number of different factors that may affect survival and differentiation choices (Sieber-Blum and Zhang, 1997). Trunk neural crest cells migrate through either the ventral pathway to become neuronal and contribute to the dorsal root ganglia or take the more dorsal-lateral route to become cells such as melanocytes (Wilson et al., 2004). The importance of pathway was shown by quail/chick hybrid experiments when quail trunk cells were transplanted into the cranial region of a chick where they differentiated into cranial appropriate cholinergic neurons (Le Douarin and Kalcheim, 1999).

Though it is not yet clear exactly what *in vivo* signals each cell population is exposed to while migrating and how these cells coordinate these signals to determine their differentiation, some work in cell culture demonstrated that changes in exposure to certain signaling molecules, including various endothelins, Wnt signals, or

neurotrophins can alter fate decision in migrating NC cells (Sauka-Spengler and Bronner-Fraser, 2008). For example, increased Wnt/β–catenin signaling pushes NCCs to a neuronal cell fate (Lee et al., 2004).

1.3 Key signaling pathways in development

1.3.1 Hedgehog signaling

The hedgehog pathway (Hh) is highly conserved signaling pathway important in most organisms (Bürglin and Kuwabara, 2006). Much of the work identifying the key players took place in *Drosophila* (Ingham et al., 2011). Hh was first discovered in a mutagenesis screen identifying genes controlling the spatial organisation of the Drosophila body plan (Nüsslein-Volhard and Wieschaus, 1980). In mammals, three homologues of Hh have been identified: *sonic hedgehog (shh), indian hedgehog (ihh)* and *desert hedgegog (dhh)* (Echelard et al., 1993). Of these, *Shh* is the best studied and is of great importance during development. In mammals, inhibition of the Hedgehog pathway results in severe congenital anomalies, ranging from cyclopia and holoprosencephaly to milder effects such as a single maxillary incisor (Hu and Helms, 1999). Recent genome wide studies have identified numerous potential targets for Gli signaling. (Vokes et al., 2007) (Vokes et al., 2008)

1.3.1.1 Hedgehog ligands

All Hh ligands are initially secreted as large precursor molecules of approximately 45kDa in size that require significant post-translational modification (Lee et al., 1994) (Pepinsky et al., 1998). The first of these modifications involves cleavage of the immature peptide into two fragments: leaving an active 19kDa N-terminal fragment (Hh-N) and a 25kDa C-terminal fragment (Lee et al., 1994). The active signaling fragment is further modified by the addition of two lipid moieties. In a reaction unique to vertebrate Hedgehog, a cholesterol molecule is added to the C-terminal of Hh-N. This reaction is catalysed by the C-terminal fragment of the Hh peptide itself (Beachy et al., 1997). Additionally a cysteine residue at the N-terminal of Hh-N is palmitoylated (Pepinsky et al., 1998). In the absence of these lipid additions, Hedgehog signaling is lost (Lewis et al., 2001) (Chen et al., 2004).

1.3.1.2 *Hedgehog signal transduction*

Hedgehog has an unusual signal transduction. When mature Shh is secreted, it is sequestered by a 12-pass transmembrane receptor Patched (Ptc) (Marigo et al., 1996) (Stone et al., 1996) (Ingham et al., 1991). In vertebrates, two distinct Ptc receptors have been identified (Ptc1 and Ptc2). Both receptors bind the Shh ligand with similar affinity (Carpenter et al., 1998). In the absence of Shh ligand, Ptc associates with and inhibits a 7-pass G-protein coupled receptor Smoothened (Smo) (Stone et al., 1996). In the presence of ligand, Ptc inhibition is relieved, and Smoothened (Smo) activates downstream signaling.

1.3.1.3 *Intracellular signaling*

In *Drosophila*, the intracellular transducer of Hh signaling is the zinc finger transcription factor *cubitus interruptus* (*Ci*) (Alexandre et al., 1996). The vertebrate homologues of *Ci* are the *Gli* transcription factors. Three have been identified: *Gli1*, *Gli2* and *Gli3* (Hui et al., 1994). *Gli1* and *Gli2* are generally regarded as activator Glis; indeed Gli1 does not possess a repressor domain. This phosphorylation of Gli1 and Gli2 promotes their cytoplasmic degradation. In the absence of this phosphorylation they translocate to the nucleus and induce transcription of target genes (Sasaki et al., 1999). In contrast, phosphorylation of Gli3 results in its cleavage where it subsequently translocates to the nucleus to act as a transcriptional repressor. Hedgehog ligands block this repressor function by inhibiting Gli3 cleavage (Dai et al., 1999; Price and Kalderon, 2002). The Hedgehog signaling pathway is autoregulatory. Multiple components of the pathway, including Ptc1 and Gli1 is well established targets of Shh signaling (Ingham and McMahon, 2001).

1.3.1.4 Hedgehog signaling is linked to specific locations on the cell membrane

Recent evidence suggests that Hedgehog signaling in vertebrates is closely associated with primary cilia (Zaghloul and Katsanis, 2009). Here, in the absence of Shh signaling, Ptc is localised to the base of the cilium inhibiting Smo activity. On activation of Shh signaling, Ptc relocates and Smo moves in to the cilium (Wilson and Stainier, 2010) (Goetz et al., 2009) (Goetz and Anderson, 2010). Perturbations in ciliogenesis result in hedgehog-like defects (reviewed in (Fliegauf et al., 2007) (Park et al., 2006) (Brugmann et al., 2010)).

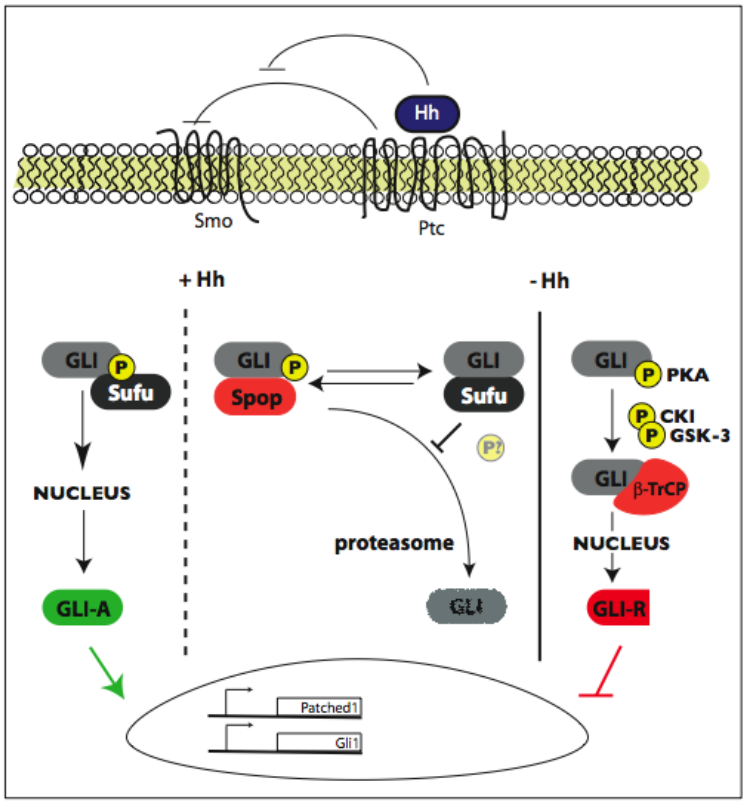

Figure 1.4 Hh signaling

Extracellular Hh ligand binds to the 11 transmembrane receptor protein *patched (ptc)*. This relieves the inhibition of *smoothened (Smo)* by *ptc*, allowing smo to signal through a series of intracellular proteins resulting in activation of the downstream Gli family of transcription factors: *Gli1, 2* and *3*. In the absence of Hh ligand *ptc* inhibits *smo*, preventing activation of hedgehog signaling. Gli is phosphorylated by glycogen synthase kinase (GSK-3), protein kinase A (PKA) and protein kinase CK1 (CK1). The results in the cleavage of Gli into a repressor form which enters the nucleus and inhibits Hh target gene expression. Intracellularly, in the presence of Hh ligand, full length *Gli* interacts with supressor of fused (SuFu), is phosphorylated and can translocate to the nucleus where it activates downstream transcription of targets including *patched1* or *gli1*. Further regulation of *Gli* activity involves its interaction with Spop which targets *Gli* for proteosomal degradation. This degradation can be inhibited by SuFu.

1.3.2 Roles for Hedgehog signaling in development

Hedgehogs are absolutely required for normal embryonic development. The role of Shh in craniofacial development is especially well documented. In humans and mice, loss of function mutations in *Shh* are responsible for holoprosencephaly, a disorder characterised by a failure of the forebrain to divide and defects in the facial midline (Roessler et al., 1996). Over activation of the Shh pathway, either through overexpression of *Shh*, or the loss of *Ptc* (leading to constitutive activation of Smo), is also developmentally deleterious. In humans, mutations in PTC are associated with basal cell nevus syndrome, a disorder causing developmental defects and tumors, especially basal cell carcinomas (BCCs). Similarly, mice overexpressing Shh in the skin develop BCCs (Johnson et al., 1996) (Oro et al., 1997).

Shh is an especially interesting ligand because it can participate in either short or long range signaling depending on the biological context. Because the mature peptide is associated with lipid modifications, Shh was originally believed to be membrane associated and therefore only able to signal at short range. However, it has now been shown that a highly stable multimeric form of Shh is capable of free diffusion and thus can act as a morphogen (Goetz et al., 2006) (Zeng et al., 2001). A classic example of Shh's ability to act as a morphogen is during vertebrate limb development, demonstrated through experiments using the chicken limb. Prior to digit patterning, Shh is expressed in a defined region (the "zone of polarising activity") of the posterior limb bud (Riddle et al., 1993). This results in the formation of a gradient of Shh along the posterior to anterior axis of the developing limb (Lewis et al., 2001). This gradient plays an important role in specifying the anterior-posterior pattern of the limb and in the types of digits that are formed (Yang et al., 1997). Gradients in hedgehog signaling are also known to regulate the dorsal-ventral identity of neurons from the neural tube. Shh expression from the ventral notochord creates a ventral-dorsal gradient in signal strength what results in the specification of discrete neuronal identities (Briscoe, 2004; Briscoe et al., 2001)

1.3.3 Hedgehog is essential for neural crest development

Hedgehog signaling has two crucial roles in neural crest development, ensuring survival and regulating differentiation. Shh from the anterior endoderm and prechordal plate is required for the survival of neural crest cells early in the migration of the cranial crest population (Ahlgren and Bronner-Fraser, 1999) (Brito et al., 2006) (Jeong et al., 2004). Inhibition of Shh by removal of source tissue or by blocking of signal using antibodies causes increased NCC death and craniofacial defects.

Later, Shh signaling plays a role in regulation of the differentiation of the neural crest into cartilage and neurons. NCCs that have migrated into the face require signaling from underlying tissues for proper morphogenic movements and cranial cartilage patterning (Wada et al., 2005). Neural crest cells that populate the gut depend on Shh signaling to proliferate and generate the enteric nervous system (Fu et al., 2004). Cell culture assays have shown that Shh signaling has the potential to orient NCC migration in the gut by restricting its migration (Fu et al., 2004). It may also regulate the differentiation into neurons (Fu et al., 2004; Ungos et al., 2003) (Calloni et al., 2007).

1.3.4 Wnt signaling

The Wnts are a family of secreted, highly conserved, cysteine-rich glycoproteins involved in many key aspects of morphogenesis and embryonic development. The pathway is used repeatedly throughout development with temporal and spatial requirements during development of many organs (Wodarz and Nusse, 1998).

The name Wnt was coined based on the phenotype in *Drosophila melanogaster* (wingless) and the homologous region in the mouse Int1 locus. These two genes, mouse Wnt-1, first identified in 1982 (Nusse and Varmus, 1982) and Wingless, identified in 1987 (Cabrera et al., 1987) (Rijsewijk et al., 1987) were just the first genes identified in what would become the Wnt family. Mutations in various Wnt genes have shown the importance of this pathway in processes ranging from segmentation in *Drosophila*, to gut development in *C.elegans* and axis formation in *Xenopus* (Wodarz and Nusse, 1998).

There are two Wnt signaling pathways, the canonical and the non-canonical pathway (see Figure 1.3). Outlined below are the two segments of the non-canonical pathways (in green and brown, Figure 1.3) and the canonical pathway (in blue, Figure 1.3). Recently, it has been shown that traditional assumptions attributing Wnt ligand/Frizzled receptor combinations to specific branches of Wnt pathways may be erroneous. Wnt 11, long assumed to be required solely for non-canonical signaling, can induce β-catenin signaling during axis formation in *Xenopus*, a canonical Wnt function (Tao et al., 2005). The question of how the signal is correctly interpreted by the cell upon binding of a Wnt ligand is therefore still open to debate, though it is likely that the regulation of cell membrane complexes play a large role. (Cha et al., 2009) (Cha et al., 2008)

1.3.4.1 Canonical Wnt signaling

The canonical Wnt pathway is mediated by β-catenin with Wnt ligands activating a series of complex signaling cascades. In resting cells, an inhibitory "destruction" complex phosphorylates the transcriptional co-activator β-catenin, targeting it for degradation. This complex is comprised of Axin, glycogen synthase kinase-3 (GSK-3) and other proteins. Upon binding of Wnt ligands to Frizzled cell-surface receptors and the transmembrane protein LRP, the intracellular signaling phospho-protein, Dishevelled, inhibits the destruction complex. GSK-3 no longer phosphorylates β-catenin, thereby halting the ubiquitination and subsequent degradation of β-catenin via proteolytic degradation. β–catenin is then free to accumulate in the cell, translocate to the nucleus where it replaces the inhibitory molecule Groucho in a complex with T-cell specific transcription factor (Tcf) or lymphoid enhancer-binding factor 1 (Lef) transcription factors. This β-catenin-Tcf/Lef transcription complex then induces target gene transcription (Salic et al., 2000) (Logan and Nusse, 2004). Target genes are widespread, and the Wnt homepage, kept by the Nusse lab at Stanford University, lists over 120 Wnt target genes http://www.stanford.edu/group/nusselab/cgi-bin/wnt/

1.3.4.2 Non-canonical Wnt signaling

Wnt signaling independent of β-catenin constitutes the non-canonical Wnt signaling pathways. These include Wnt/calcium signaling, Wnt/JNK signaling and Wnt/PCP signaling (Rao and Kühl, 2010).

Planer cell polarity (PCP) signaling is responsible for asymmetrical and polarised localisation of proteins in cells including epithelia, giving rise to daughter cells with different cellular components, reviewed in (Dale et al., 2009). Wnt/JNK signaling involves the activation of small GTPases, which include Rac, Rho and JNK itself and like PCP signaling, regulates polarised cell movements (reviewed in (Rao and Kühl, 2010)).

Wnt/calcium signaling relies on mediation by G-proteins to release a wave of calcium ions. When released, this activates Ca++ dependent downstream targets that include calcineurin, reviewed in (Rao and Kühl, 2010). Wnt/Ca+ signaling is thought to have a role in mediating canonical Wnt activity in dorsal-ventral patterning of the early *Xenopus* embryo as dominant negative NF-AT mutants have ectopic dorsal structures and non-inhibitable NF-AT mutants lose anterior structures (Saneyoshi et al., 2002).

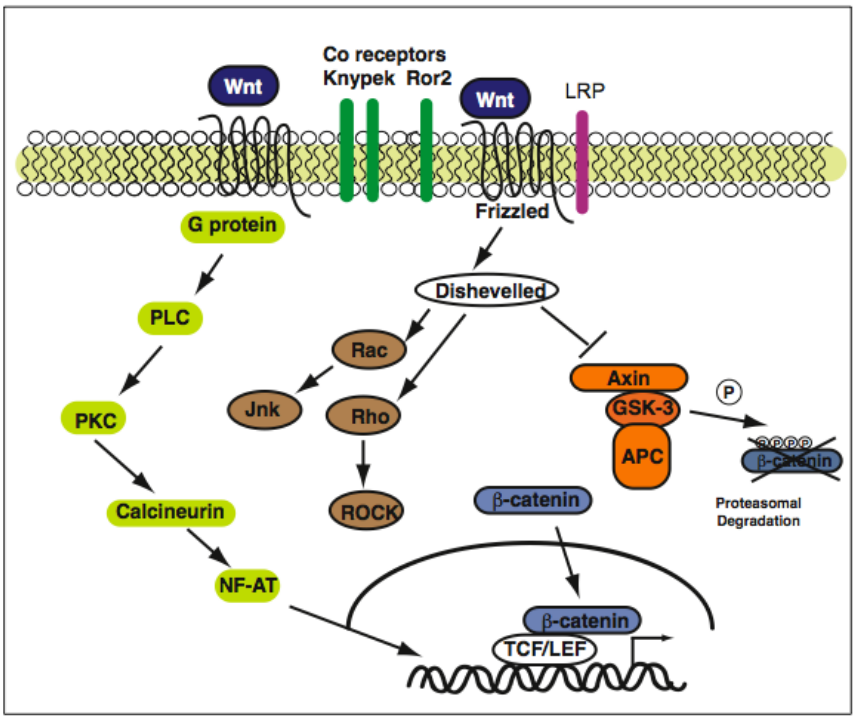

Figure 1.5 Wnt signaling

WNT-Ca2+ signalling pathway (in green above) is mediated by G proteins and phospholipases. Activation results in transient increases in cytoplasmic calcium that activates the kinase PKC (protein kinase C) and the phosphatase calcineurin. This in turn activates NF-AT which can supress signaling through β-catenin (discussed below). Planar cell polarity (PCP) signaling (in brown above) activates the small GTPases RHO (RAS homologue gene-family member) and RAC1 (Ras-related C3 botulinum toxin substrate 1). These activate JNK (Jun N-terminal kinase) and ROCK (RHO-associated coiled-coil-containing protein kinase 1). The canonical signaling pathway modulated levels of β-catenin in the cell. In resting cells, an inhibitory "destruction" complex phosphorylates the transcriptional co-activator β-catenin, targeting it for degradation. This complex is comprised of Axin, glycogen synthase kinase-3 (GSK-3) and other proteins. Binding of Wnt ligand to the Frizzled receptors on the cell surface inhibits the phosphorylation complex, allowing β-catenin to accumulate and enter the nucleus, where it binds to LEF/TCF factors and induces target gene transcription.

1.3.5 Wnt signaling is important throughout development

The Wnt pathway is another signaling pathway that is used repeatedly in development. Most important for this project is the role of Wnt in the induction of two uniquely vertebrate structures: the head and the neural crest.

Specification of axial identity in the embryo is determined by a concerted effort from numerous genes. The details regarding this patterning were first discovered in the 1920's with the identification of "the organiser", a region of the early gastrula that is patterned before the rest of the embryo and induces primary induction of the dorsal/ventral axis. The organiser is found in the anterior portion of the dorsal blastopore lip in the early *Xenopus* gastrula (Harland, 2008). In the 1950's it was shown that this early event is preceded by anterior/posterior axis formation. It was found that a gradient of an unknown signal confers increasingly posterior tissue identity with increased signal strength (Harland and Gerhart, 1997). This signal was later identified to be Wnt and it was found that properly regulated Wnt signaling is crucial for anterior-posterior (A-P) identity (Domingos et al., 2001). During gastrulation in vertebrates this difference in Wnt signaling translates into a body plan, instructing the developing embryo where the "head" and "tail" should be. In fact, a high level of posterior Wnt signaling combined with inhibition of Wnt in the anterior is a conserved principle of vertebrate axial development (Yamaguchi, 2001).

A number of Wnt inhibitors including Cerberus (cer), Dickkopf (Dkk), and Frzb are secreted by the anterior in the gastrula. Together, they maintain Wnt inhibition, thereby, acting as an inducer of head structures (Glinka et al., 1998) (Kazanskaya et al., 2000) (Mao et al., 2001). Alterations to the inhibition of Wnt in the anterior, such as loss of dkk-1 or over expression of non-inhibitable β–catenin, result in increased anterior Wnt signaling. This shift causes a loss of head structures (Heasman et al., 1994). Dkk-1 mutant mice display a range of microcephaly with null mutants losing anterior head structures completely (MacDonald et al., 2004). Conversely, when β–catenin is knocked down with antisense morpholino oligonucleotides (MO) injection or overexpression of glycogen synthase kinase -3 (GSK-3, an inhibitor of Wnt signaling), expression of the anterior head marker, *Xhex,* is expanded and ectopic cement glands are induced (Heasman et al., 2000).

1.3.6 The many roles for Wnt signaling in neural crest induction

In every biological model system examined, Wnt signaling is required for NC induction (Dorsky et al., 1998) (Brault et al., 2001) (García-Castro et al., 2002; Ikeya et al., 1997; Saint-Jeannet et al., 1997) (Chang and Hemmati-Brivanlou, 1998) (Lewis et al., 2004) (LaBonne and Bronner-Fraser, 1998) (Steventon et al., 2005). Studies in *Xenopus* show that regulation of Wnt signal is required at two time points, first in the induction of neural tissue then in regionalization of neural tissue. Wnt is then directly responsible for the expression neural crest specific genes. The first is during early gastrulation when Wnt/β−catenin signaling and BMP signaling are inhibited in the ectoderm to allow specification of neural tissue. Later, Wnt signals that determine both anterior–posterior and mediolateral positioning are required for neural crest induction. At this point in the early neurula, *Wnt8a* is expressed in the lateral and ventral mesoderm underlying the presumptive neural crest (Christian et al., 1991). *Wnt1* and *Wnt3a* are expressed in the ectoderm in the same region as *slug* (Wolda et al., 1993). Wnt activity is required for induction of the neural crest. Indeed *slug*, the earliest neural crest specific marker, has Lef/β−catenin binding sites in its promoter region and is directly regulated by Wnt signaling (Vallin et al., 2001). The anterior neural plate, where neural crest is not induced, actively prevents Wnt signaling with expression of Wnt inhibitors in the underlying prechordal mesoderm such as dickkopf-1 (dkk-1) (Carmona-Fontaine et al., 2007).

In *Xenopus* and chick embryos, overexpressing components of the canonical Wnt pathway like frizzled, Lrp6, or β-catenin expanded the region fated to be NC as did ectopic expression of canonical Wnt ligands (Chang and Hemmati-Brivanlou, 1998) (LaBonne and Bronner-Fraser, 1998) (Saint-Jeannet et al., 1997). In contrast, inhibiting Wnt signaling by over expressing GSK-3 reduces induction of the NC (Saint-Jeannet et al., 1997).

1.3.7 BMP signaling

Bone Morphogenetic Proteins (BMPs), are members of the Transforming Growth Factor β (TGFβ) family of ligands. BMP signaling regulates a hugely diverse range of events in the developing embryo. The BMP family of secreted signaling molecules consists of over 20 identified members. The BMPs, with the exception of BMP1 (a metalloprotease, an enzyme where the catalytic activity requires a metal ion, typically zinc), belong to the TGFβ super family along with the TGFβs and activins. Within the family of secreted growth factors, the BMPs can be further divided according to their homology to ancestral genes. *BMP2* and *BMP4* are grouped together as the *decapentaplegic (dpp)* subfamily due to their homology with the *Drosophila dpp* gene. *BMP5* to *8* are the 60A subfamily because they are homologous to *Drosophila 60A* (Kingsley, 1994) (Massagué, 2000).

The BMPs act through the BMP receptors (BMPRs), transmembrane proteins with specific serine-threonine kinase activity. The receptors consist of a ligand binding extracellular domain and an intracellular domain associated with kinase activity. There are two types of receptors BMPRI and BMPRII respectively with Type 1 receptors having higher affinity for BMP binding (Wrana et al., 1994) (Kirsch et al., 2000).

BMP ligands are dimers and the monomers containing binding sites for Type I and Type II receptors. For signaling to proceed the Bmp ligand must bind to Type I and Type II receptors, forming a multimeric complex. The Type II receptor phosphorylates serine-threonine residues within a conserved intracellular region of the bound Type I receptor (Wrana et al., 1994), stimulating the Type I receptor kinase activity. This causes the phosphorylation of the cytoplasmic signaling molecules, Receptor-activated Smads (RSmads). BMP receptors phosphorylate specific RSmads (1, 5 and 8), distinct from those RSmads2 and 3 involved in TGF and activin signaling. Phosphorylation induces RSmads to form a complex with an unphosphorylated co-Smad, Smad4. This complex then translocates to the nucleus, where it is able to affect the transcription of target genes (Massagué and Chen, 2000).

BMP signaling, like most intracellular signaling pathways, is highly regulated. To overcome the problems of specificity given the few signaling molecules used downstream of BMP, nuclear cofactors are incorporated to modulate transcriptional control by the Smad complex once it has entered the nucleus (Massagué and Wotton, 2000). Negative regulation of the pathway occurs at the point of ligand-receptor binding. Soluble proteins such as Noggin and Chordin prevent binding of BMPs to their receptors (Abreu et al., 2002; Massagué and Wotton, 2000). These signals can be induced as a result of other signaling pathways or by BMP itself. It should be noted that BMP signaling can occur in a Smad independent manner such as the mitogen activated protein kinase MAPK cascade, not discussed further in this thesis (Derynck and Zhang, 2003). It is now believed that BMP signaling, using SMADS to relay signals to the nucleus, draws on a large number of co-factors that modify gene targets depending on the cellular environment

1.3.8 BMP signaling in development

The BMPs, initially discovered to play a role in bone formation, have since been shown to have diverse functions during vertebrate and invertebrate embryogenesis (Hogan, 1996; Urist, 1965). BMPs are required in early embryonic development, when *Bmp4* and inhibitors *Chordin* and *Noggin* are expressed in an opposing fashion in the early embryonic mesoderm, where they regulate dorsal-ventral patterning (Hogan, 1996). The BMP agonists *Chordin* and *Noggin* have roles in developmental events as diverse as forebrain development, mandibular outgrowth and left-right asymmetry (Bachiller et al., 2000; Mine et al., 2008; Stottmann et al., 2001).

In establishing the left and right body plan, levels of BMP signaling are regulated by expression of the antagonists *Noggin* and *Chordin*. Errors in the this patterning result in erroneous development of such asymmetric organs as the heart, lungs, liver, spleen and intestines as w ell as the vascular system (Mine et al., 2008). Later roles include regulation of the outgrowth of the mandible. Here both *Noggin* and *Chordin* are expressed in the developing branchial arches. Loss of both genes results in hypoplasia of the developing mandible due to cell death of the cells in this region (Stottmann et al., 2001).

1.4 Biological screens

Numerous model organisms have been used for scientific research over time but amphibia have long been popular for developmental biology research. As such, *in vivo* chemical screens have been performed for generations. Sea urchin eggs, newt spawn and frog spawn were popular choices for these early experiments. However, researchers performing these early screens noted that these experiments could only be performed during spring when spawn was available. It would be another few decades before frog spawning would be induced using hormone preparations, discussed below.

1.4.1 Why is *Xenopus* a model organism?

Xenopus is an aquatic, externally developing animal with large clutches, making it particularly suited to screening experiments. The 1mm eggs are easily cultured in 96 well plates and the tadpoles do not require feeding for many days.

Today the most commonly used research organisms are yeast, *C. elegans*, *Drosophila*, zebrafish, *Xenopus laevis* and *tropicalis*, chick and mouse. Each offers advantages and disadvantages but for this project I will describe zebrafish and *Xenopus*, which are well suited to chemical screens addressing temporal requirements of signaling in development of vertebrate organs. Both are aquatic, externally developing animals with reasonable clutch sizes (100-200 for zebrafish and 1000+ for *Xenopus*) and zebrafish offers most of the same early advantages as *Xenopus*. The critical time points in neural crest development are identified and occur stereotypically, offering the opportunity to manipulate signaling during specific key events in development (LaBonne and Bronner-Fraser, 1999) (Henion et al., 1996) (Kelsh et al., 1996; Neuhauss et al., 1996) (Chang and Hemmati-Brivanlou, 1998).

1.4.2 *Xenopus laevis*: history of a research model

Xenopus laevis is often lauded as a great animal model for early embryological studies; however, it was not an obvious choice for a developmental model. A South African native, *Xenopus* was initially studied as a comparative curiosity. As a short-

tongued frog, it is distinct from those found readily in Europe (including the popular *Rana*) yet it became the dominant embryological research model during the 50's and 60's. This was predominantly due to two factors: 1) *Xenopus* became a popular and trustworthy laboratory readout for pregnancy in post-war Europe and US, so numerous colonies in hospital labs provided readily accessible eggs to researchers year round; 2) during this time, researchers were making great strides in techniques that allowed biochemical and cellular questions to be addressed. Therefore, the use of *Xenopus* was expanded beyond developmental biologists by researchers in other fields (reviewed in (Gurdon and Hopwood, 2000)).

Xenopus eggs are well suited for use in chemical screens. Their large size and robust nature makes them ideal for early manipulations. The predictable, temperature sensitive development of *Xenopus*, is a useful tool for studying discrete developmental events. Together these traits offer the researcher the opportunity to have 1000's of embryos developing in unison that can be cultured in a multitude of conditions.

In this project, I demonstrate the utility of *Xenopus* for chemical screens (chapters three to four). In chapter five, I describe a novel role for Hedgehog signaling in specification of the primary mouth. Chapter six defines a role for glycogen synthase kinase 3 (GSK-3) in neural crest migration and contributions to craniofacial development. Finally, in chapter seven, I describe collaborative work defining interactions between Gli proteins and GSK-3, which uncover previously an unknown role for GSK-3 in *Hedgehog* signaling.

2 MATERIALS AND METHODS

2.1 Embryo collection

Xenopus laevis live in fresh water and sexually mature females can be induced to lay hundreds of eggs. Embryos were obtained by inducing ovulation via injection of 350 – 500 units of human Chorionic Gonadotropin (hCG) into the dorsal lymph sac approximately 16 hours before eggs were required. Eggs were then collected by gentle "squeezing" and were fertilised by *in vitro* fertilisation using a piece of testis isolated from a male. Males were sacrificed by an overdose of the anaesthetic MS-222 (50% in H2O) injected into the dorsal lymph sac. Isolated testes were stored at 4°C in 1XMR (Marc's Ringer) and 0.050mg/ml gentamicin antibiotic. A small piece of testis was cut and macerated in the Petri dish containing eggs with 0.5ml dechlorinated tap water. Embryos were flooded with 1/3X MR and transferred to incubators at appropriate temperatures. The jelly coat was removed from the eggs after the first cleavage by incubating in 2% cysteine pH8 (Smith and Slack, 1983) for 3-4mins followed by 5 washes in H2O and a final 3 washes in 1/3xMMR. The embryos are grown in 1/3xMMR at 14°c or 19°c to the appropriate stage in accordance with Nieuwkoop and Faber, 1967. Unfertilised, dead or dying embryos were removed and media was changed regularly to maintain clean conditions.

2.2 Fixation

Embryos were fixed in MEMFA for 1 hour at room temperature or overnight at 4°C. Embryos were then washed twice in MeOH and stored in MeOH. Samples were stored at -20°C until processing. Post processing, embryos were fixed overnight in MEMFA and stored at room temperature in MeOH unless otherwise stated.

2.3 DNA preparation

To transform bacterial cells 1µg of plasmid DNA was added to a 25µl volume of DH1α competent cells and incubated on ice for 20 minutes. The cell solution was then heat shocked at 42°C for 1 minute and returned to ice for 2 minutes. 200µl of LB media were added to the solution, 100µl of which is spread on a 50mg/mL ampicillin LB agar plate and this was grown overnight at 37°C. A single colony was

then picked using a clean pipette tip. This tip was placed in a flask of LB media containing 50ug/ml ampicillin and incubated over night (no more than 16 hours) at 37°C on a shaker. When the colony reached appropriate density, measured by loss of transparency of the LB media, the recombinant plasmid DNA was isolated using the Qiagen plasmid mini or midi kit and protocol.

2.4 DNA restriction digests

10µg circular Mini or Midi prep DNA was cut using a restriction endonuclease (source: Promega or NEB) in a 1 x reaction buffer mix at 37°C for 2 hrs:

10µg DNA
5µl 5 x Buffer
2µl Restriction enzyme
Made to 50µl H2O

DNA was analysed using agarose gel electrophoresis to confirm that it had been completely linearised as DNA templates for RNA transcription must be fully linearised for efficient transcription. If DNA was not fully linearised 2µl enzyme was added and the reaction was incubated at 37°C for a further 2hrs. The DNA was cleaned using Qiagen mini or midi prep kit. DNA was treated with Proteinase K (sigma), phenol chloroform extracted and ethanol precipitated then the DNA resuspended in nuclease free water to give a concentration of 1µg/µl.

2.5 RNA synthesis

Synthetic capped mRNA for microinjection was made using the mMessage mMachine kit (Ambion) and DNA templates listed in table below. mRNA was eluted and cleaned using NucAway Spin Columns (Ambion) before elution in 100µl RNA-ase free/nuclease free H2O. 5µl was taken for qualitative analysis on a 1% TAE/agarose gel. 0.1µl of ethidium bromide was added to allow visualisation of the DNA on an electrophoresis gel. The 5.1µl was denatured at 85°C for 10mins and run out on the agarose gel to ensure mRNA was correct length and good quality. A second aliquot of 5µl was made up to 100µl using RNase free H2O and quantified using a spectrophotometer.

2.6 In situ hybridisation probe synthesis

Antisense RNA probes were prepared using appropriately linearised plasmids as templates and transcribed with SP6 or T7 polymerases (Promega) as described by Harland and Weintraub 1985. Plasmids were linearised using the indicated restriction enzymes and incubated at 37°C for 2hours. Proteins from this linearisation were removed by PK treatment at 55°C for 15mins and the now linear template cleaned using phenol : chloroform extraction. Templates were resuspended in DNase free H2O at a concentration of 1ug/µl. Dig labeled *in situ* hybridisation probes were synthesised using DIG-Labeling Mix (Roche), precipitated in half volume 8M LiCl at -80°C and washed in 70% EtOH. The pellet was resuspended in 55µl H2O. 2.5µl were taken and run on a gel as above. 2.5µl was also taken and quantified as above. The remaining volume was added to hybridisation buffer at 1ug/ml for a 1X stock. See probe synthesis table for template details.

Probe	Linearised with	Run from	Reference
GSK-3α	EcoR1	T7	Cloned from EST AccNo:BG364215
GSK-3β	EcoR1	SP6	Harland lab collection No. 675
Twist	EcoR1	T7	(Hopwood et al., 1989)
Slug	Nco1	SP6	(Grammer et al., 2000)
Sox9	Sal1	T7	Liu lab collection No: 25
Otx2	Not1	T7	Monsoro-burq lab collection No.303
Six1	No1	T7	Monsoro-burq lab collection No.1771
Krox 20	Not1	T3	
Pax6	EcoR1	SP6	Monsoro-burq lab collection No.522
Ptc-2	Not1	T7	AccNo: AB037688
Shh	Ecor1	T7	

Table 2.1: Probe synthesis

2.7 Microinjection

De-jellied embryos were put onto the mesh grid in a petri dish filled with 1/3xMMR and 2% Ficoll. Ficoll is a high molecular weight polysaccharide and is used in this media to remove the fluid from within the vitelline membrane via an osmotic gradient. This makes the embryo easier to inject and reduces the volume of cellular leakage, resulting from injection. Build up of cellular fluids between the embryo and vitelline membrane can kill the embryo. The micropipettes were calibrated by injecting mRNA into the surface of a dish of mineral oil and measuring the diameter of the ejected mRNA using an eyepiece graticule. The desired injection volumes were crudely changed by trimming the micropipette using forceps and finely adjusted by changing pressure and duration of expulsion. To express mRNA in the whole embryo or large regions of the embryo, embryos were injected at the 2 or 4 cell stage.

To keep expression restricted to specific tissues, such as the neural crest, embryos were injected at the 32cell stage using the 32-cell stage fate map as a guide. Lineage labeling was performed by co injection of mini ruby dextran.

2.8 Drug screen

Embryos are collected and fertilised, dejellied and washed into 1/3X MMR. Drug dilutions of the required concentrations are made in culture media (Table 3.1) and embryos are transferred into 24 well plates. For the initial screen two concentrations of each drug were made and 10 embryos were cultured per well. Initial examination of phenotypes was catalogued in embryos exposed to drug at 2-cell stage and allowed to develop stage 45. No wash out was performed and the drug solution was not refreshed. Embryos were monitored daily and dead embryos removed.

Further treatments were performed using those drugs that generated interesting phenotypes (Table 3.2). To establish whether the perturbed pathway had roles at distinct times in development and whether the phenotypes seen at stage 45 could be attributed to perturbations at specific time points in development, embryos were exposed to drug during short periods. Embryos were transferred to 24 well plates, 10 per well and exposed to 1/3x MMR solution containing drug at 1) 2 cell stage until stage 45, 2) at stage 12.5 until stage 19, 3) at stage 19 until stage 37 or 4) stage 37 until stage 45. Embryos were kept in 1/3X MMR before the drug treatment. Drug was added at the appropriate stage by transferring the embryos to a new well containing the appropriate 1/3x MMR/drug solution. To remove the drug the media containing the drug was drawn off, the embryos rinsed 3 times in fresh 1/3x MMR before finally transferring them to a new 24 well plate with fresh 1/3x MMR. All embryos were allowed to develop to stage 45. In control embryos the same washes were performed to ensure that if the handling caused any phenotypes, they would be identifiable in the controls.

Certain parameters were established to ensure that experimental phenotypes were indeed a result of the drug, not caused by natural defects or illness. In any given batch of embryos, if 30% or more of the controls developed atypically the batch was discounted. This was crucially important as on many occasions the control embryos developed with severe anterior defects (lack of a cement gland, narrow head etc). Such batches were not scored in the experiments. If 30% of more of the controls

died the batch was also discounted. These measures did result in the loss of numerous experiments but were essential in protecting the results from any variation due to changes in the maternal environment, disease or stress that could have adversely affected the embryo quality.

2.9 Wholemount mRNA in situ hybridisation (WISH)

Embryos for whole mount mRNA *in situ* hybridisation were prepared by collecting at the appropriate stage. Embryos were fixed in MEMFA for 1 hour at room temperature, the vitelline membrane was removed and the embryos bleached in 0.5x SSC, 5% formamide, 1% H_2O_2 then dehydrated into methanol and stored at -20°C until further processing. Embryos older than stage 28 were first anesthetised in 0.1% benzocaine then fixed. All *in situ* hybridisations were developed in BM purple substrate. Whole-mount *in situ* hybridisation was done according to Harland 1991 with the following modifications: Proteinase K step and post PK fixation step were removed so WISH was performed as follows:

Day 1.

Embryo were bleached using solution of 1% H2O2, 5% formamide in MeOH in clear glass bottles under bright light. Embryos were not rolled during bleaching as this often caused damage to the brittle embryos. The samples were then rehydrated step wise from 100% MeOH into 100% PBS+0.1% Tween (Ptw) at RT (5 mins at each step 75%MeOH/25% H_2O, 50%MeOH/50% H_2O, 25%MeOH/75% PTw, then 100% in PTw). Embryos were then washed 3x5mins in PTw at room temperature before being sorted into baskets. These baskets, made from eppendorfs with the bottom cut off and fine pore mesh glued on, can hold up to 10 embryos and allow for easy handling of the samples throughout the various washes.

Once separated, embryos were incubated 2x5 mins in 0.1M triethanolamine pH 7-8 before addition of acetic anhydride (12.5µl in 5mls). This acetic anhydride addition was repeated and incubated for 5mins at RT. Embryos were washed in PTw 2x5mins at RT them transferred to hybridisation solution at 60°C for 1hour. This pre-probe hybridisation was removed and replaced with 0.5ml of probe solution (1µg/ml probe) and hybridised overnight at 60°C.

Day 2.

Probe was removed, stored for future use at -20°C, and embryos were returned to the pre-hybridisation solution at 60°C for 10mins.

Embryos were washed in 2xSSC at 60°C for 3x20mins then incubated in 2xSSC with RNAse A (20µg/ml) and RNAse T1 (10µg/ml) for 30mins at 37°C. This was followed by a 10min wash in 2xSSC at RT and 2x30min washed in 0.2xSSC at 60°C.

Embryos were then washed in maleic acid buffer (MAB) for 2x10min at RT before incubation in MAB+2%BMB blocking agent (Boehringer Mannheim Blocking solution) either o/n for 1hr at RT. Anti-digoxygenin AP antibody was added to this (1:3000) and the embryos incubated o/n at 4°C.

Day 3:

Embryos were washed in MAB for 1x5 hours followed by 2x5min washes in alkaline phosphatase buffer. Baskets were then transferred to a 48 well plate, 0.5ml of BM purple (Boehringer Mannheim) added to each well and the whole dish covered with tinfoil to allow the colour to develop in the dark. If probes had been used previously, the first 30mins of development was done at 37°C as this increased the rate of reaction. Alternatively this was done at RT and the colour checked every 30-40mins. Once the stain has reached the required depth the process was stopped by a MAB wash (5 mins RT). Embryos were then post-fixed in bouins fix o/n at 4°C. This turned the embryos bright yellow and numerous washes in PTw were required to remove the yellow colour. When embryos had returned to the appropriate colour (purple stain with white background) they were photographed. This could be done in PTw or if a visualisation of a deeper stain was required, embryos were dehydrated into 100% MeOH and washed into benzyl benzoate/benzyl alcohol (BB:BA) clearing agent. This was only performed in glass watch clock dishes and embryos were not kept in BB:BA for extensive periods as it will cause the purple stain to fade. Embryos were then washed into MeOH for long-term storage.

2.10 Wholemount immunohistochemistry

Embryos were aged to the appropriate stages, dissected out of their vitelline membranes and fixed in MEMFA for 1hour at room temperature, the vitelline membrane was removed and the embryos bleached in 0.5x SSC, 5% formamide, 1% H2O2dehydrated into methanol and stored at -20°C until further processing. Embryos older than stage 28 were first anesthetised in 0.1% benzocaine before fixation. Embryos were rehydrated in stepwise fashion; 75% MeOH, 50% MeOH, 25% MeOH to PBS. Embryos were washed in 1xPBS+0.1% tween and preblocked in 1xPBS+0.1% tween with 10% heat inactivated goat serum. Embryos were incubated

with primary antibodies overnight at 4°C. Embryos were washed for 3x2hours in 1xPBS+0,1% tween at room temperature then incubated with secondary antibodies overnight at 4°C. Alexa 514 fluorophore is preferable as it is distinct from the autofluorescence of the gut. Embryos developed with fluorescent secondary antibodies were photographed after 3x 2hour washes in 1xPBS+0.1% tween. Non-fluorescent staining was done using HRP conjugated antibodies and DAB. Embryos being stained with DAB were bleached prior to primary antibody incubation.

2.11 Immunohistochemistry on wax sections

Embryos for sectioning were dehydrated into 100% MeOH then embedded using the following protocol:

Solution	***Wash duration***
100% IMS	0:30
100% IMS	0:30
Xylene	0:30
Xylene	0:30
Xylene	0:30
Ultraplast Wax	0:30
Ultraplast Wax	0:30
Ultraplast Wax	0:30

Sections were cut 11μM thick and were mounted on slides in a 3 slide sequential manner. As each ribbon was mounted, the first section was placed on slide 1, the second on slide 2 and the third on slide 3. This was repeated until all sections were mounted. Sections were mounted onto flat cool slides wet with a small amount of 30% EtOH: 70% water. When the slide was full they were transferred to a hot rack at 40°C and baked until the slides were dry (2-3 hours). If the sections were not smoothing out, additional EtOH : water solution could be added to help remove wrinkles. When dry, slides were moved to an oven and baked overnight at 40°C. They were stored in covered trays at 4°C until stained.

Slides were dewaxed in histoclear 2x 2mins followed be rehydration in a stepwise fashion (5 min washes in 100%. 90%, 80%, 70%, 50%, 30%, EtOH). Slides were washed in PBS 2x2mins then PTx for 5mins. Antigen retrieval was achieved by microwaving the samples for 4x4mins in 10mM sodium citrate. Solutions were topped up between heating with pure H2O. The slides and solution was then cooled on ice and when RT, washed back into PBS 2x 2mins. To block, slides were placed in slide trays, lying flat and covered with sufficient PBT + 10% sheep serum to cover.

Cover slips of appropriately trimmed parafilm were overlaid and the slides incubated at room temperature for 40mins. Block solution was drawn off using a fine tipped plastic pipette and the primary antibody added in the same manner as the block. The slides were incubated at 1:300 primary antibody in block solution overnight at 4°C. Slides were washed in PBT 3x 10mins then blocked again as before. Secondary antibody was applied as primary at 1:300 + DAPI at 1;1000, cover slipped and kept dark for 1hr at RT. Slides were washed in PBT 4x10mins then PBS 2x 5mins. Slides were mounted with mowiol and protected by placing appropriate sized glass coverslips over the slides.

2.12 Wholemount cartilage staining

Stage 45+ embryos were fixed in MEMFA for 1 hour at room temperature before washing into EtOH. Embryos can be stored at -20°C at this stage. For cartilage staining embryos were washing into a 0.15% alcian blue solution (70% EtOH/30% acetic acid) and left to wash at room temperature for 3 days. Solution may be replaced during the 3 days if the Alcian blue dye precipitates. When suitably stained, embryos were rinsed 3x 15 mins in 95% EtOH. Rehydration was done stepwise into 2% KOH then washed from 2%KOH stepwise into 80% glycerol/20% 2%KOH, 1 hour per wash before washing overnight into the final solution. Dissection of cartilages was then performed to increase visibility of craniofacial cartilages.

2.13 Western blotting

Western blots were used to detect protein levels in *Xenopus* lysates. Embryos were collected at the appropriate stages and frozen in minimal liquid at -80°C. Lysates were prepared by homogenizing embryos into RIPA (radioimmunoprecipitation assay buffer). Lysates were spun down for 10mins. The supernatant was removed carefully leaving a pellet and fatty layer. This was repeated twice more. An equal amount of SDS loading buffer was added to the remaining supernatant and the proteins denatured at 90°C for 5mins before quick spin. This sample can stored at -20°C.

Samples, equal to ¼ of an embryo were loaded into a well of a 4-12% gradient gel, run at 160V for 45 mins. Semi dry transfer onto PVDF membrane was performed at 15V for 45mins. Membranes were rinsed in water then methanol before drying

completely. Membranes can be stored by dehydration in MeOH before probing. To probe for protein, membranes were rehydrated by a wash in MeOH, clean water then TBS. Membranes were blocked incubating in a 50-ml conical tube containing TBS + 10% fat free milk (Cell signaling no:9999) and 0.1% bovine serum albumin (BSA) on a automatic roller at RT for 1hour. Primary antibody was applied at 1:200 – 1:1000 depending on the antibody in block solution and blots left overnight at 4°C. Membranes were washed in TBSTw for 3x 20 mins then blocked again as before. Secondary antibody was applied as primary at 1:30,000 – 1:50,000 depending on primary antibody and incubated at RT for 1hour. Membranes were washed 3x 20mins TBSTw then developed using immobilon western chemiluminescent HRP substrate (Immobolin kit no: WKBL S01 00).

2.14 Hematoxylin and Eosin staining

Hematoxylin is a stain that marks basophilic structures such as chromatin or ribosomes a deep purple, providing a clear view of the cell nuclei. Eosin is an acidic stain that stains acidicophilic structures red. It stains the cell membranes clearly. (Ehrlich, 1886). Slide mounted sections were dewaxed with 2x10 minute Histo-clearTM washes and rehydrated stepwise in ethanol washes (100%, 90%, 70% and 50%) for 2 minutes each. Slides were washed in distilled water before a 10min incubation in Erhlich's Haematoxylin (Solemedia). Excess haematoxylin was removed by washing the samples for 10 minutes under running water. For Eosin staining to contrast, slides were rinsed in distilled water and then submerged in acid alcohol for 15 seconds. Slides were then stained with 0.5% aqueous Eosin (Lamb) for 2 minutes, washed in distilled water and dehydrated stepwise in a series of two minute ethanol washes (70%, 90% and two 100%). Sections were air-dried for 1 hour before being cover-slipped (VWR) with DePex (Solemedia).

2.15 Luciferase assay

Embryos were injected in both blastomeres at the 2-cell stage with either SuperTopFlash (STF) or GliBS reporter construct (ref). Embryos were cultured in various conditions to stage 14 before being transferred individually to wells in a 96 well plate. Lysates were prepared by pipetting up and down rapidly in 50µl of 1x passive lysis buffer (promega kit E1910). 25µl of lysate was transferred to a suitable

white 96 well plate, which was placed in the luminometer. Automatic injections were set up to add 25µl of luciferase assay regent 1 (LAR1) to each well. Firefly luciferase activity was measured for each well in the plate. Regents from dual-luciferase reporter assay kit E1910 from Promega were used.

2.16 Imaging

Images were taken using a Nikon SMZ1500, a stereomicroscope with a zoom range of 0.75x to 11.25x and edited using Adobe Photoshop.

2.16.1 Confocal imaging

Single-photon microscopy was performed using a Leica TCS SP5 DM16000 confocal microscope. Appropriate lasers were used according to the secondary fluorophores used during immunostaining. Alexa 488 was excited with the Argon laser (488), Alexa 568 and To-PRO was excited using the DPSS 561 laser and DAPI was excited using the 405 diode. Collection filters were set using the Leica defaults where 488 emissions were collected between 496 and 558µM, 568 emissions were colleted from 596-712µM. Images were captured using a HCXPLAPO CS 0.7na dry X20 or oil wet X40 objective.

2.17 Data analysis and statistics

In all of the screening experiments, at least 21 samples were assessed for each condition. All screening figures show representative samples. The minimum number of embryos examined per treatment are provided in the figure legends.

For quantitative measurements of embryo dimensions, 12 embryos were chosen at random from each condition. The mean, as well as error bars denoting the standard error of the mean (SEM), are shown for each measurement. P values were generated using the Student's t-test.

Where the percentage of embryos displaying a specific phenotype is shown, the number is rounded to the closest whole number.

2.18 List of solutions

1X Modified Marcs Ringer Solution

100mM	NaCL
2mM	KCL
1mM	MgCl2
2mM	CaCL2
5mM	HEPES. pH 7.5

Stored at room temperature in 5L drums. 1/3xMMR was used for general embryo culture and 1/3xMMR + 2% Ficoll was used for embryo manipulations.

10X PBS (pH 7.5)

80mM	Na_2HPO_4
20mM	$NaH_2PO4.2(H_2O)$
100mM	NaCl

Made with nuclease free H2O. pH adjusted and autoclaved.

PBSTw (PTw)

1X PBS + 0.1% Tween

PBSTx (PTx)

1X PBS + 0.1% Triton 20

TBSTw

1X TBS + 0.1% Tween

20X SSC:

3M	NaCl
0.3M	Tri-sodium citrate

pH adjusted to 7.5 with NaOH, autoclaved and stored at room temperature.

MEMFA fixative

0.1M	MOPS pH 7.4
2mM	EGTA
1mM	Magnesium sulphate
3.7%	Formaldehyde

Hybridisation buffer:

50%	Formamide (molecular grade)
5X	SSC
5mg/ml	Torula RNA (stock at 25mg/ml in 50% Formamide (molecular grade))
100µl/ml	Heparin
1 X	Denhardts solution
0.1%	Tween-20
0.1%	Chaps
0.25mM	EDTA

Alkaline Phosphatase Buffer:

100mM	Tris-HCL pH 9.5
50mM	$MgCl_2$
100mM	NaCl
5mM	Levamisole
0.1%	Tween-20

Frozen in 50mls aliquots. The levamisole, which inhibits endogenous alkaline phosphatases, is stable in solution for only a limited time so added fresh when defrosted.

1M Tris-HCL (pH 9.5)

12.1g	Tris in 100mls

Bleach

6ml	H_20
3.33ml	30% H_2O_2
0.5ml	Formamide (molecular grade)
0.25ml	20XSSC

Mowiol:

2.4g	Mowiol 4-88 (Polyvinylalcohol 4-88)
6.0g	Glycerol
mix well	
6.0ml	H_20
Leave at room temperature for 2 hours	
12ml	0.2M Tris-HCL (pH 8.5)

Incubate at 50°C for 10 minutes and mix further. Incubate at 50°C overnight until dissolved. Centrifuge at 5000rpm for 15minutes, collect and store supernatant at -20°C.

LB Media:

4g	Tryptone
4g	NaCl
2g	Yeast Extract
400ml	dH_2O

autoclaved, cooled to ~50°C and 1µg/ml ampicillin added.

LB agar plates:

1.5% Agar was added to above LB and Autoclaved. Agar was cooled and poured into 90mm Petri dishes. Plates were set at 37°C overnight.

3 CHEMICAL SCREEN PART 1: Temporal perturbations uncover novel requirements for known signaling pathways.

3.1 Summary

The aim of the following two chapters is to identify pathways involved in the development of neural crest derived tissues, focusing on craniofacial structures. The morphogenesis of the head requires three-dimensional coordination of different tissues such as cartilage, bone, muscle and nerves. As this process is impossible to study in isolated cells, I used an *in vivo Xenopus laevis* screen to identify signaling pathways controlling development of these structures. I designed a small pilot screen where tadpoles were cultured in media containing small molecules. I chose a set of compounds with known biological activity, including drugs that act on canonical Wnt signaling, non canonical Wnt signaling, hedgehog signaling and FGF. By applying drugs at different stages of development I was able to perturb signaling during very specific developmental processes, uncovering previously unknown requirements for these well-studied pathways.

3.2 Introduction

3.2.1 Biological screens

"Screening" has long been used to identify what certain molecules can do and what processes specific pathways regulate. Historically, the most common types of screens in developmental biology have been chemical screens, expression cloning (overexpression of protein in cells as an activity assay) or genetic screens.

In classic work using *Drosophila,* forward genetic screens (when a mutagenised parent is created and subsequent generations are interbred to identify random mutations) have been used extensively to isolate developmentally important genes (Nüsslein-Volhard and Wieschaus, 1980). Genetic screens like these have been

incredibly successful in identifying key genes and building understanding of gene networks in development. However, there are limitations. Identification of the gene that has been mutated can be very labour intensive and costly, inhibiting its extensive use in higher organisms such as vertebrates. More recently, technological advances in genome wide sequencing has allowed ENU generated mouse mutants to be screened with great effect (Hrabé de Angelis et al., 2000; Nolan et al., 2000) (Anderson, 2000). While these mutants have contributed much to our understanding of development and disease, they are hampered by the irreversible nature of the mutations. Many pathways are used and reused throughout development and mutations in those pathways may present a phenotype at the earliest use of that gene. Study of the later requirements may be difficult if early phenotypes mask the later requirements or if the mutation causes early lethality.

Expression cloning screens have been successfully used to identify kinase substrates (Stukenberg et al., 1997), pathway components (Andrésson and Ruderman, 1998) and novel developmentally active molecules (Smith and Harland, 1992). Screens such as these can be used to identify single proteins from a vast pool, allowing rapid identification of active molecules (McCormick, 1987). Expression screens are often performed in *Xenopus* or zebrafish by overexpressing pools of mRNA. This provides insight into what a protein can do rather than what it does in *vivo*. However, once a molecule of interest has been identified, lower levels of the protein, dominant negative mutants and inhibitors can be injected to study the in *vivo* function.

Chemical screens have been used in drug discovery to detect activity of chemicals for over 40 years. Application of chemicals to the assay medium of choice (proteins, cells, embryos etc) allow for a large number of compounds to be tested for activity in a rapid, controlled and reproducible manner. These chemical screens can be performed using libraries of compounds that may share predicted activity (such as kinase inhibitors) or a common origin (natural products or variations of a single molecular backbone). In developmental biology, this type of screen has been used to rapidly assay phenotypic changes in the presence of various small molecules (reviewed in (Wheeler and Brändli, 2009)). When combined with an externally developing aquatic animal such as zebrafish or *Xenopus*, this technique can be applied at any stage in their development, allowing us to assess temporal requirements of a pathway. *Xenopus* and zebrafish possess similar advantages in their application to such screens and both have proven highly useful in numerous previous chemical screens. However *Xenopus* has a significantly longer shared

evolutionary history with mammals than zebrafish (approximately 100 million years) and have many similarities in both organ development and physiology (Wheeler and Brändli, 2009).

Chemical screens themselves have limitations. Off-target drug interactions can lead to non-specific phenotypes and should be overlooked. Such phenotypes are not due to perturbation of the pathway of interest and can be misleading when interpreting results. However, it is often possible to address this by using more than one compound that perturbs the pathway in a similar manner. These compounds may act at a different point in the pathway or in different way to inhibit or activate the pathway. In this way it is possible to confirm the phenotype is due to the predicted effect of the drug, not due to some unknown and usually unidentifiable off target effect. Where this isn't possible, perhaps because there are no other small molecules available, further confirmation of the phenotype can be done in later analysis using other well-developed molecular techniques such as injection of morpholino oligonucleotides (MOs) to inhibit specific protein synthesis. MOs (discussed in greater detail in Chapter 6) inhibit the synthesis of individual proteins and need to be injected or otherwise transfected into the animal. As such they are not as well suited for large-scale screens but can be used in conjunction with a small molecule screen to great effect.

It is also important to recognise that the pharmacokinetics of drugs in media used to culture *Xenopus* embryos is typically unknown. The half-life of the small molecule, its stability at temperatures in which the embryo is viable, the ability of the drug to be absorbed into the embryo, as well as the metabolism of the drug will all impact the results of the screen. Despite these limitations, chemical screens provide extremely powerful ways to identify compounds that have bioactivity and to address their role in multiple organ, tissue or cell development. A recent example demonstrates the use of a small-scale chemical screen to assess activity of compounds believed to perturb TGF-β signaling. Novel effects of pyridines were identified along with confirmation that these compounds have strong bioactivity (Dush et al., 2011). Our screen is similar and assesses phenotypic changes resulting from incubation in the presence of the small molecules at specific time points in development.

3.3 Results

3.3.1 Development of a small molecule screen to identify pathways involved in neural crest development

In this project, I devised a small-scale screen using a number of compounds that would affect pathways we knew to be important in development, including epidermal growth factor (EGF), calcineurin, fibroblast growth factor (FGF), canonical and non-canonical Wnt and Hedgehog (see table 3.1: Chemicals). By selecting targets in pathways that are used repeatedly in development (e.g. Wnt and Hedgehog) I aim to highlight how a small screen could be used to identify novel requirements. Additionally I used two compounds with unknown targets and intended to determine if any insights into their mechanism could be elucidated by the phenotypes they induced. One has been suggested to inhibit Wnt signaling (pyrimidine) (Liu et al., 2005). The second is the anti-malaria drug artestunate; its mode of action is unknown (MIMS, Monthly Index of Medical Specialities). If this project was successful I anticipated that such a screen could be scaled up, using *Xenopus* as a model for craniofacial or neural crest development.

This screen was conducted in two parts. I performed an initial primary screen where embryos were incubated from the 2-cell stage in two concentrations of drug. The aim here was to identify which compounds caused phenotypes and to select the most effective concentration. When the appropriate compounds and concentrations were identified I performed a secondary screen with drug additions at later stages, chosen to address the requirement of that target molecule during specific stages in neural crest development. These stages were described in more detail in the introduction. Neural crest induction begins prior to stage 12.5 with slug expression evident from stage 9 (Nieto et al., 1994). By stage 19 the NCCs are undergoing EMT and beginning to migrate from the dorsal neural tube. At stage 26 the first of these cells have reached their destinations and early steps in differentiation are under way. By stage 37 the majority of NCCs have delaminated and further specification is occurring.

3.3.2 Setting up the screen and identifying early phenotypes:

In our pilot study, I set out to test 15 chemicals acting in signaling pathways known to be important in early development (Table 3.1). Initially, embryos were treated with two doses of each compound, applied from the 2-cell stage onwards (schematic in Figure 3.1A). The embryos were cultured in multi-well plates so overall health, developmental progression and morphological changes were readily assessed in live animals. Animals were grown to feeding tadpole stages (stage 45, Figure 3.1B-C). At this point, tadpoles were assessed for effects on the gut, eyes and overall morphology (Figure 3.1B-C and Table 3.2). Changes to musculature were assessed by immunohistochemistry (schematic, Figure 3.1C), and some tadpoles were then processed for cartilage staining, marked by alcian blue (Figure 3.1C). The primary screen highlighted the large variety of phenotypes that could be identified using *Xenopus* as a model; these phenotypes are outlined in table 3.2.

In order to refine the temporal requirements, I performed a secondary screen where drugs were applied at specific time points during neural crest development. The stages chosen were: stage 12.5, after induction of neural crest; stage 19, during early migration of the neural crest and at two stages of differentiation, stage 27 and stage 37 (schematic in Figure 1A). At stage 27, the neural crest has migrated into the facial mesenchyme and by stage 37 chondrogenic condensations become apparent. Compounds were washed out at the end of the treatment stage and embryos were transferred to new multiwell plates in fresh, untreated media. However, we did not assess efficiency of washout.

Drug	Target	Lowest Conc'	Effect	Highest Conc'	Effect
Artesunate	Unknown	10uM		100uM	✓
BIO	GSK3	5uM	✓	50uM	✓
Cyclopamine	Smoothened	5uM	✓	250uM	✓
Cyclosporin	Calcineurin	10uM		100uM	
Gefitnib	EGFR tyrosine kinase	10uM		100uM	
IWR	Axin	10uM	✓	100uM	✓
LY294002	PI3K	10uM		100uM	○
Purmorphamine	Smoothened	10uM	✓	500uM	✓
Pyrimidine	Unknown	0.1uM		10uM	✓
QS11	Porcupine	10uM		100uM	
Rho Kinase inhibitor 111 (Rockout)	Rho Kinase	10uM		100uM	✓
SB202190	p38 MAP kinase	10uM		100uM	
SU5402	VEGFR2/FGFR1	10uM		100uM	✓
U0126	MEK1/MEK2	10uM		100uM	
Y29632	Rho kinase	10uM		100uM	✓

✓ phenotype ○ lethal

Table 1: Small molecules used in this screen

.

Shown here are drugs with target proteins, if known. Each compound was initially tested at the two concentrations listed. Also noted are presence or absence of observable phenotyes, as well as lethality.

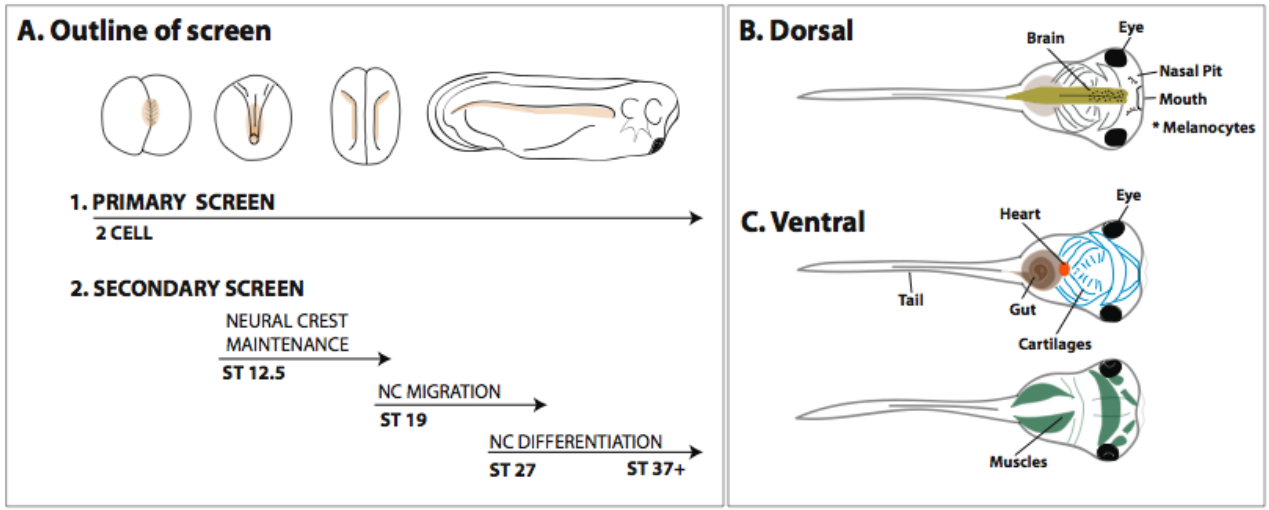

Figure 3.1: Screen set up and analysis

The primary screen was performed at the 2-cell stage. Embryos were allowed to develop to stage 45 (3.1A). The secondary screen was performed at time points known to be important in neural crest development; stage 12.5 for neural crest maintenance; stage 19 for neural crest migration and stage 27 for neural crest differentiation. All animals were grown to stage 45 (3.1B). Tadpoles were examined for changes to the heart, eyes, cartilage (visualized in the translucent tadpole or stained with alcian blue) and for changes to the body length or tailfin (3.1C). The muscles in the tadpole were visualized by immunohistochemistry using 12 101 antibody (3.1C).

Compound	Conc.	Face	Gut	Pigment	Mouth	Edema	Body length	Tailfin	Midline
Artesunate	100μM		✔				✔		
BIO	15μM	✔	✔	✔	✔	✔	✔	✔	✔
Cyclopamine	250μM	✔	✔	✔	✔	✔	✔		✔
Cyclosporin	100μM			✔		✔			
IWR	100μM	✔	✔		✔	✔		✔	✔
Purmorphamine	100μM	✔	✔		✔	✔			✔
Pyrimidine compound	10μM	✔				✔	✔		✔
QS11	100μM	✔							
Rho kinase inhibitor 3	100μM	✔	✔			✔	✔		✔
SU5402	100μM						✔	✔	
Y29632	100μM						✔		

Table 3.2: Phenotypes scored in the primary screen

In the primary screen tadpoles were scored for changes to the following structures: face, gut, melanocytes, primary mouth, edema, body axis extension, tailfin thickness and changes to the midline.

3.3.3 Early perturbations result in axis truncations

It was strikingly apparent that drug treatments resulted in very severe defects in the elongation of the tadpole. This phenotype was only seen when the embryos were treated early. Anterior-posterior (A-P) determination occurs very early in *Xenopus* embryos, during gastrulation (Slack and Tannahill, 1992) (Lane and Sheets, 2000), but in the majority of the shortened tadpoles there appeared to be a reduction in the number of somites, rather than any perturbation in initial A-P patterning. The exception was in the 2-cell BIO treated tadpole where there were dramatic perturbations in anterior structures (discussed chapter 6) (Figure 3.2D).

Dramatically shortened tadpoles were seen in either 2-cell treatments (Figure 3.2C, D and G) or those incubated in drug between stages 12.5 and 19 (Figure 3.2E&H). Fibroblast growth factor (FGF) inhibition, using SU5402, at the 2-cell stage truncated the posterior extension of the tadpole while the face remained unaffected (Figure 3.2C). In embryos treated during the same period with the hedgehog agonist purmorphamine the body axis was similarly shortened (Figure 3.2G). GSK-3 inhibition using BIO and up regulation of hedgehog with purmorphamine during stages 12.5-19 resulted in a somewhat less severe truncation than the 2-cell but some reduction in the length of the tail was seen. In the stage 19+ treatments no elongation defects were scored (Figure 3.2F & E). Changes in the somites can also lead to truncations. Somite development is perturbed in the embryos exposed to SU5402, BIO and purmorphamine from 2-cell (Figure 3.2C, D and G). The more anterior somites lack the correct chevron shape (schematised in the tail, Figure 3.2A) and are thicker than those in the WT (Figure 3.2B). Those towards the posterior of the tail are prematurely very thin.

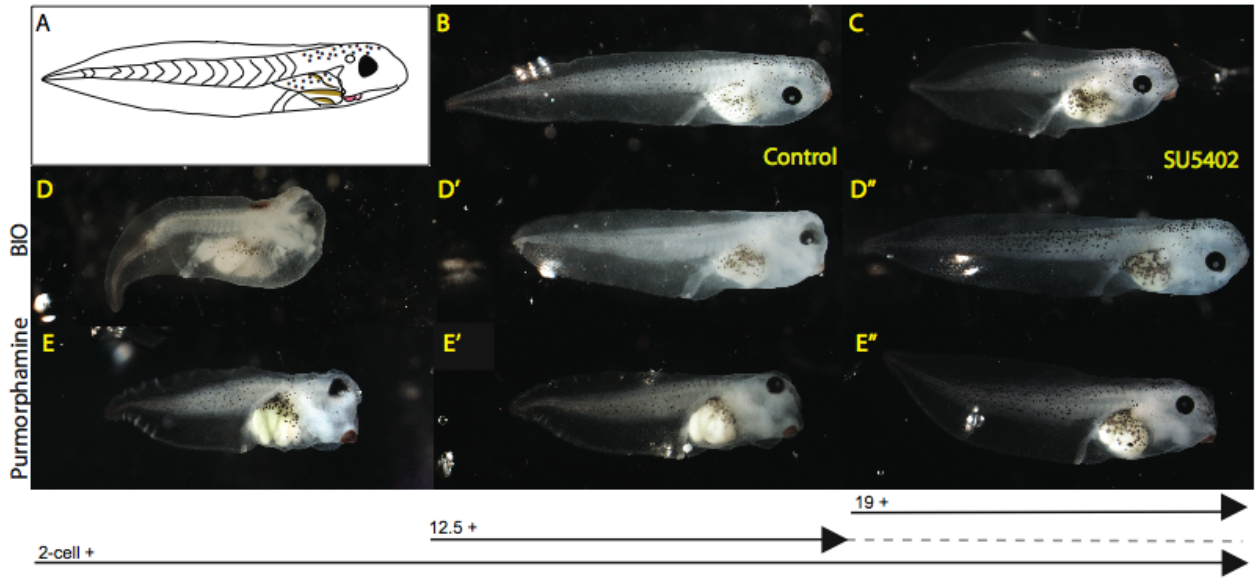

Figure 3.2 Early perturbations cause axial truncations

Schematic of lateral stage 45 tadpole (3.2 A). WT stage 45 tadpole (3.2B). 100μM FGF inhibitor SU5402 treatement at 2cell severely shortens the tadpoles while not changing the facial structures (3.2C). 15μMBIO at 2 cell (3.2D) and between stages 12.5 - 19 (3.2D') truncates the posterior tadpole. Incubations between stages 19 - 37 do not shorten the tadpole (3.2D"). 100μM purmorphamine truncates the tadpole when applied at 2cell stage (3.2E) and between stages 12.5 - 19 (3.2E'). Later treatments are only slightly perturbed (3.2E").

3.3.3.1 *Two compounds altered the height of the neural crest derived tailfin*

The tailfin is made up of neural crest cells that migrate out of the neural tube towards the posterior (Collazo et al., 1993). Two drug treatments, IWR and cyclosporin, were found to change the size of tail fin when scored in stage 45 tadpoles. Inhibition of Wnt signaling using Inhibitor of Wnt Receptor (IWR) from the 2-cell stage throughout development resulted in a dramatic loss of tailfin above and below the body (Figure 3.3C) compared to WT (Figure 3.3A-B). When drug was applied at stage 12.5 and a washout performed at stage 19 a similarly severe phenotype was observed (Figure 3.3E). The dorsal-ventral extent of the tailfin in both these treatments was 0.5x that of the WT (all measurements were taken a uniform distance from the tail tip, site shown in yellow). However, this phenotype was not found in later treatments (stages 19-37, Figure 3.3G and stage 37-45, Figure 3.3I). Consistent with roles for Wnt, early IWR treatment may be causing a global reduction in neural crest derived tissues (discussed in Figure 4.3). In the later treatments these phenotypes are less severe (see almost phenotypically normal tadpole when treated at stage 37, Figure 3.3I).

Cyclosporin treatment resulted in a marginal but measurable thickening of the dorsal tailfin (Note, measurements, shown in red, were taken above the proctodeum (Figure 3.3D, F, H & J).

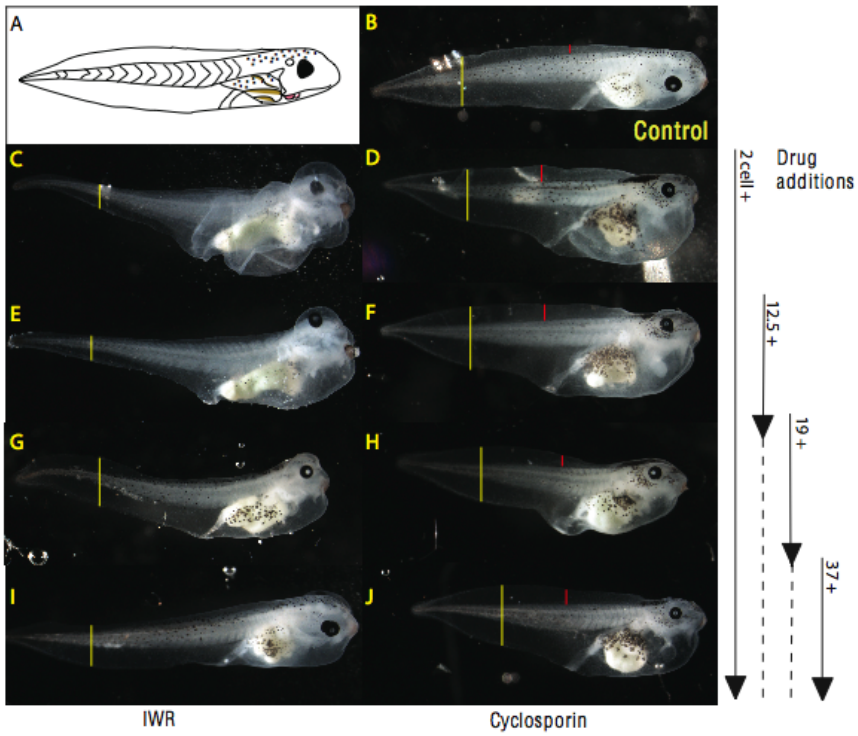

Figure 3.3 IWR and cyclosporin application perturbs development of the NC derived tail fin

(Fig 3.3A) Lateral schematic of a stage 45 tadpole, illustrating the extension of the tail fin.
(Fig 3.3B) Control tadpole. Depth of tailfins were measured a uniform distance from the tail tip (yellow lines).
(Fig 3.3 C-E)100μM IWR treatment from 2-cell and between stages 12.5-19 caused 50% decrease in tail fin depth compared to control embryos (Fig 3.3B) (yellow lines).
(Fig 3.3E-G) IWR treatment from stage 19 or stage 37 had no effect on tail fin depth in stage 45 tadpoles. A small increase in tail fin depth was observed in 100μM cyclosporin treated tadpoles.
(Fig 3.3B, D, F, H & J) The depth of the dorsal fin was measured directly above the proctodeum (red lines).
In cyclopsorin treated tadpoles the dorsal tailfin is between 1.9x and 2.1x the depth in all treatments (Fig 3.3D, F, H & J) compared to control (Fig 3.3B)
(n=12 in each condition shown).

3.3.4 Melanocytes are dramatically altered.

The melanocytes arise in the dorsal neural tube and migrate as unpigmented cells to populate many organs before differentiating into pigmented, mature melanocytes (Douarin, 1999). These cells are specific type of chromatophore that possess specialized vesicles called melanosomes which contain eumelanin, a type of melanin that appears black or brown (Wasmeier et al., 2008). In the developing embryo, melanocytes are often variable in both size and number, even within tadpoles from the same clutch. Some striking phenotypes were observed but it should be noted that I did not differentiate between a loss of melanocytes and a loss of melanosomes. Nor did I look to see whether the melanocyte cell shape itself was changed or whether the lack of a starred shape was caused by changes to diffusion of melanosomes in the cell.

Figure 3.4 shows close up images of the melanocytes in embryos from a number of treatments. Two treatments resulted in melanocytes that appeared smaller and more rounded (BIO, Figure 3.4B and purmorphamine, Figure 3.4E), while tadpoles treated with the Hedgehog inhibitor cyclopamine showed an absence of melanocytes (Figure 3.3D). In contrast, cyclosporin treatment caused an increase in the number of trunk-derived melanocytes seen in both the cranial and caudal regions of the tadpole (Figure 3.4C).

Both the cyclopamine and BIO phenotypes were stronger in response to continuous treatment; in contrast, cyclosporin was effective in all treatments (Figure 3.5B-C and F-G). These tadpoles showed excessive melanocytes delaminating in huge numbers from the neural tube throughout all the treatment stages examined (Figure 3.5F-K).

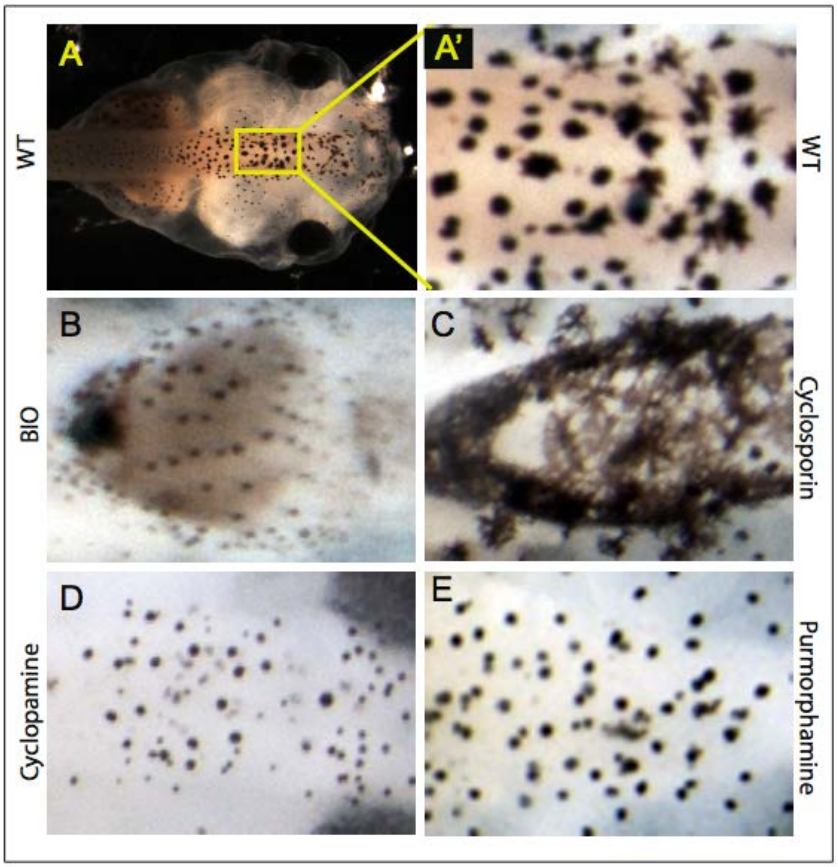

Figure 3.4: Melanocytes are strongly changed in certain drug treatments.

(3.4A) WT stage 45 dorsal view, yellow box shows region in 3A'-E.
(3A') Close up of melanocytes in WT. Note varied morphologies of melanocytes.
(3B) 15μM BIO reduces the number of melanocytes and inhibits the starred shape.
(3C) 100μM cyclosporin causes a drastic increase in the number of melanocytesfrom the dorsal neural tube. Melanocytes appear more dendritic.
(3D-E) 250μM cyclopamine and 100μM purmophamine reduce the number and size of melanocytes.
(n≥9 for all conditions shown).

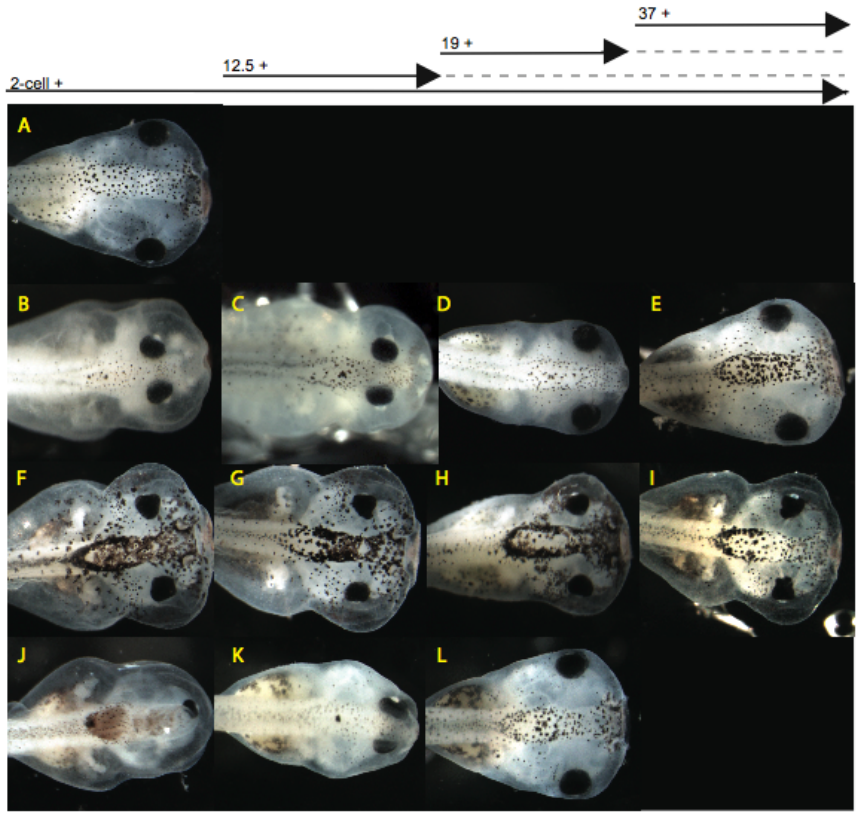

Figure 3.5 Early drug treatments most strongly affect melanocyte production

(3.5A) In the stage 45 control tadpole melanocytes have migrated from the dorsal neural tube and are visible all over the tadpole.
(3.5B) 2-cell 100uM cyclopamine treatment at reduces the number of melanocytes drastically.
(3.5C-D) Treatment between stages 12.5 - 19 and 19-37 reduces the numbers, though less dramatically, with some obvious in the neural region.
(3.5E) Treatments after stage 37 results in an animal that appears WT.
(3.5F-I) 100uM cyclosporin treatment dramatically increases the number of melanocytes in all treatments.
(3.5J)-K 5uM BIO treatment at 2-cell stage causes loss of melanocytes as does incubation between stages 12.5 - 19.
(3.5L) Later application has no effect on the tadpole.
($n \geq 24$ for all conditions shown).

3.4 Discussion & Conclusions

A large number of morphological phenotypes were identified in this chemical screen, some novel and some well characterized. Perturbations during early stages, such as many of those described here, can be used to complement other approaches, such as mRNA overexpression or knockdown of gene activity by antisense morpholino oligonucleotide (MO) injection. Treatment at these stages can be used to rapidly identify molecules that have activity in the embryo and in some cases can be used to test pathway specificity.

3.4.1 Well characterized phenotypes can be identified and confirmed rapidly

One of the first developmental processes to be explored in detail in *Xenopus* was A-P patterning. There are a number of pathways known to be crucial for proper extension of the embryo (Lane and Sheets, 2000) (Slack and Tannahill, 1992). FGF signaling is one such pathway; therefore, the stunted tadpoles (Figure 3.2C) were unsurprising. However, in later stages FGF is thought to be required for patterning of craniofacial structures (Bachler and Neubüser, 2001) (Johnston and Bronsky, 1995) (Nie et al., 2006) (Szabo-Rogers et al., 2008) so it was surprising that the 2-cell treatment did not affect the development of the anterior structures or face. In these experiments, compounds were added at the 2-cell stage, with no reapplication. It is possible that the activity of the drug has diminished before patterning the face. In the future treatment at later time points may give hints to both the requirements of FGF signaling in the head and to the *in vivo* pharmacokinetics and pharmacodynamics of SU5402.

3.4.2 Interesting changes to the melanocytes suggest more than one mechanism has been altered

Inhibition of hedgehog signaling during early development causes a dramatic loss of NCC (Brito et al., 2006). I hypothesize that the severe loss of melanocytes, along with the obvious changes to the cranial structures in the embryos treated from 2 cell and stages 12.5 with cyclopamine derive from an increase in apoptosis of neural crest cells

due to lack of caudal endoderm sonic signaling (Figure 3.5C-D) (Ahlgren and Bronner-Fraser, 1999). BIO had a similarly severe early phenotype though the presence of more craniofacial tissue when compared to cyclopamine treated suggested a different mechanism affecting the melanocytes.

Cyclosporin A treatment had an interesting effect on melanocyte proliferation (Figure.3.5F-I). Actually, regulation of calcineurin activity is used in a variety of human treatments for pigmentation disorders. Vitiligo is caused by the production of antibodies against the patient's own melanin. This autoimmune disorder results in white patches of skin due to the destruction of melanin. It can be treated with topical application of calcineurin inhibitors that act to inhibit the immune system (Leitner et al., 2011) (Gawkrodger et al., 2010). Another role for the drug-induced suppression of calcineurin in the immune system is in prevention of transplant rejection. Various calcineurin inhibitors including cyclosporin A have been used in transplant therapy (Taïeb, 2005). However, this treatment can be a double-edged sword as calcineurin inhibition can also induce melanoma in organ transplant recipients (Walsh et al., 2011). Furthermore, calcineurin may play a role in delamination and some data suggest that calcineurin inhibition by cyclosporin A is responsible for nephrotoxicity in transplant recipients (Slattery et al., 2005). Collectively these data suggest that the hyper pigmentation seen in the cyclosporin treated tadpoles may be due to either an increase in melanin production in the developing melanocytes or due to an increase in the number of neural crest cells delaminating from the neuroepithelium.

This assay has shown that studying the various stages in neural crest development can be done rapidly and with ease. Important signaling pathways in the development of your favourite structure can be readily assigned a temporal window that, in the case of the phenotypes that may mimic one of the many neurocristopathies, can allude to the developmental process affected. Our data demonstrate a straightforward method to examine the development of organ systems and tissues that are developing concurrently, important in pleiotropic syndromes. Future studies can incorporate other molecular approaches such as transgenic techniques. Traditional protein studies are well established in *Xenopus*. Combined with drug assays this provides potential for rapid validation of drug-protein interactions with the added bonus of *in vivo* vertebrate biology.

4 CHEMICAL SCREEN PART 2: Novel roles for well studied pathways

4.1 Introduction

This chapter will focus on the more novel phenotypes that I encountered in the chemical screen, with an in-depth focus on modulators of the Wnt and Hedgehog pathways. These include changes to the eye, craniofacial structures and to the guts. We know that NC contributions are crucial for eye and facial formation. In addition, the gut was highlighted as it displayed phenotypes with numerous clear temporal implications in signaling, highlighting one of the strengths of this screen.

In *Xenopus* the neural crest migrates in three streams which give rise to distinct portions of the craniofacial cartilage, the branchial stream (which splits into two), the hyoid stream and the mandibular stream. The mandibular stream is *Hox*-negative and comes from rostral rhombencephalic and mesencephalic region of the brain. It migrates into the first arch before differentiating into the lower and upper jaw cartilages (Meckel's and the palatoquadrate respectively). A small number of cells from this anterior stream contribute to the posterior region of the palatoquadrate. The *Hox*-positive streams are the more posterior, originating from rhombomeres 4 to 7. These streams colonise the second, third, and fourth arches where they give rise to the hyoid skeleton (Sadaghiani and Thiébaud, 1987) (Baltzinger et al., 2005).

Though much of the early work to identify the tissues that receive neural crest contribution was done in chick, *Xenopus* has a well-characterised cell lineage. Not only has lineage tracing been used to follow the development of each cell in the 32/64 cell embryo through development, allowing specific targeting to tissues in the later tadpole, but the contributions of each neural crest stream to the face are known (Sadaghiani and Thiébaud, 1987) (Baltzinger et al., 2005). This allows us to determine from the changes in the face which of the neural crest streams have been most severely affected.

The contribution of the neural crest to the eyes is less clear-cut but the mesenchymal and choroid layers, along with the cornea of the eye are derived from the mandibular crest stream (Nagy et al., 2006) (Sadaghiani and Thiébaud, 1987). Neural crest cells not only contribute to the structures of the eye but may also be important in patterning their development (Grocott et al., 2011).

Neural crest cells colonize the developing gut in a rostro-caudal wave after entering the foregut following migration from the neural tube (Burns and Douarin, 1998) (Nagy et al., 2006). Here, they differentiate into the neurons of the enteric nervous system. It is clear that failure of this tissue to migrate correctly (described in *Xenopus* (Collazo et al., 1993)) results in defects in later gut development and is implicated in a number of human birth defects, including Hirshsprung's (Epperlein et al., 1990) (Tobin et al., 2008b). Although I have not scored for any potential changes in the innervations of the gut, I describe the phenotypes found in the gut as an interesting illustration of temporal requirements for a certain signaling pathway in a multistep development of single organ.

4.2 Results

4.2.1 Midline defects were associated with close-set eyes in early treatments

By stage 45 the eyes are mobile and set wide on either side of the face. They have obvious lenses and darkly pigmented retinal epithelia. Many of the compounds caused defects in eye development, ranging from alterations to size and positioning to micropthalmia and cyclopia. Some of these defects were associated with midline defects that changed the positioning of the eyes, discussed in Figure 4.1.

I found that in a number of these treatments, phenotypes decreased in severity with later additions of the compounds. This was most evident with GSK-3 inhibition using BIO where the 2-cell stage resulted in a cyclopic embryo (yellow star, Figure 4.1E). In the stage 12.5 – 19 treatment two eyes were obvious, even though they remained very close to the brain (green arrow, Figure 4.1F). By the stage 19-37 treatments tadpoles looked normal (Figure 4.1G). Hh inhibition using cyclopamine causes a dramatic narrowing of the midline in the 2-cell, stage 12.5-19 and stage 19-37 treatments (green arrow, Figure 4.1B-D) though the midline was less dramatically decreased in the latter treatment. In the first two treatments the eyes remained close to the brain. By stage 19 I saw proper separation of the eyes away from the midline. IWR treatment also causes a severe midline defect in the 2-cell treatment (green arrow, Figure 4.1H) and, like in cyclopamine treatment, this resulted in eyes that remain close to the brain. When applied between stages 12.5-19 the phenotype looks remarkably similar with the same close-set eyes. With application during stages 19-37 the severity decreases (Figure 4.1I-J).

Along with changes in the positioning of the eyes (presence/absence of eyes and proximity to the brain) some morphological changes were identified. The early up regulation of Hedgehog signaling with purmorphamine causes poorly patterned pigmented retinal epithelia along with a narrowed midline (as discussed above & Figure 4.1) but the compact, pigmented nature of the eyes when embryos were incubated

between stages 12.5-19 treatments were unaffected. In later treatments this disorganised retina does not occur (Figure 4.1K-M).

Wnt inhibition also caused lens defects in the two earlier exposures. There is severe edema in IWR treated tadpoles and the swelling pulls the lens from the eyes as they are attached to the skin (red arrow, Figure 4.1H-J). Rho/Rac inhibition shows a similar lens defect the same two treatments (red arrow, Figure 4.1N-P) along with micropthalmia in the tadpole cultured in drug from 2-cell (yellow arrow, Figure 4.1N).

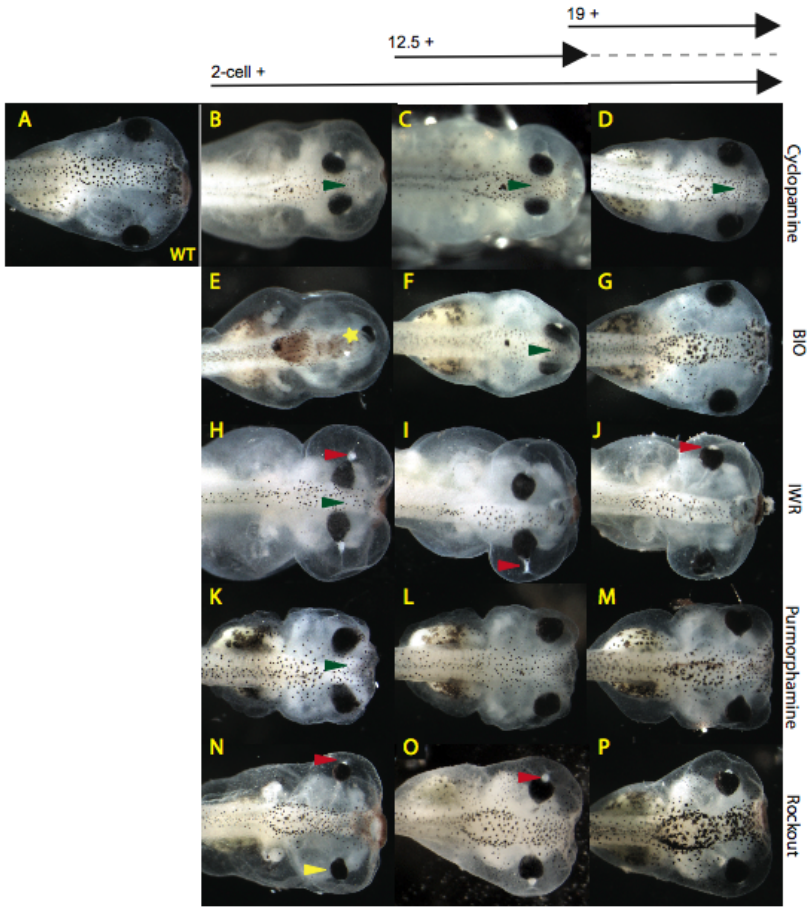

Figure 4.1 Various eye phenotypes were observed

(Fig 4.1A) Stage 45 WT.
(Figure 4.1B-D) Close set eyes, indicated by green arrowheads, are seen in all 250μM cyclopamine treatments as well as (Figure 4.1F)15μM BIO between stages 12.5 – 19, (Figure 4.1H) 100μM IWR as well as 100μM purmorphamine (Figure 4.1K).
(Figure 4.1L) Less severe midline defects were seen in purmorphamine treatments between stages 19 - 37.
(Figure 4.1E, yellow star) In tadpoles treated with BIO at the 2-cell cyclopia is seen. Lens detachment defects (red arrowheads) occurred with purmorphamine (Figure 4.1H-J) and 100μM Rockout (Figure 4.1N-O) incubation.
Rockout treatment at the 2-cell stage caused micropthalmia (Fig 4.1N, yellow arrowhead).
(n≥21 for all conditions shown).

4.2.2 A closer look at the changes to the eyes

In order to further assess the changes to the eye, I examined coronal sections of treated tadpoles (Figure 4.2). Sections through BIO-treated tadpoles at stage 45 show a cyclopic eye (arrowhead) below the brain (arrow) (Figure 4.2C) with little other tissue seen in the anterior of those embryos. When treated with the Wnt inhibitor, IWR, tadpoles have narrowed midlines with eyes that are relatively well patterned. The lenses appear to have failed to detach from the overlying epithelium and as the edema distorts the skin the lens is pulled from the attached eye (Figure 4.2D). Finally, in two other conditions with narrowed midlines, the eyes remain close to the brain (cyclopamine and purmorphamine, Figure 4.2E - 4.2F). In cyclopamine treatments the eyes appear close-set but appropriately patterned with the lens, ganglion cell layer, nuclear cell layer and pigmented retinal epithelium obvious (Figure 4.2E). In contrast, over activation of hedgehog signaling by purmorphamine treatment strongly affects eye formation, resulting in disorganised structures that remain contiguous with the brain (Figure 4.2F).

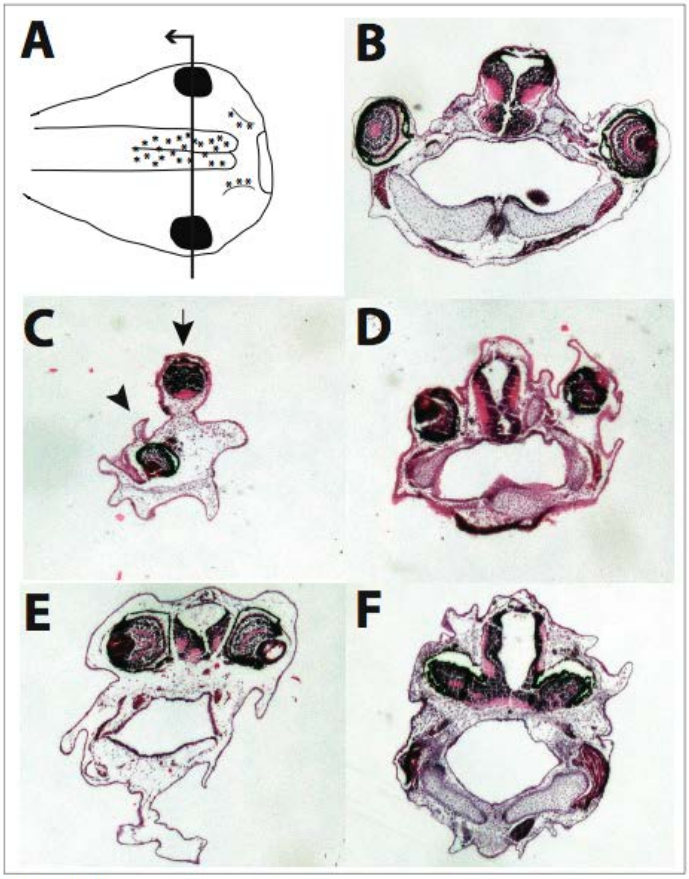

Figure 4.2 Wnt and Hh perturbations affect eye structure

(Fig 4.2A) Schematic showing plane of section. Hematoxylin and eosin stained section WT tadpole.
(Fig 4.2B) Note eyes with complex layered structure with the lens, pigmented retina and optic nerve visible. 2cell stage 15μM BIO treatment causes cyclopic embryo that retains a lens but has poorly patterned pigmented retina (arrowhead indicating single eye, arrow pointing to brain, Fig 4.2C).
(Fig 4.2D) 100μM IWR causes loss of patterning in the retina and lens defects.
(Fig 4.2E & F) 250μM cyclopamine and 100μM purmorphamine treatments result in embryos with narrow midline.
(Fig 4.2F) In purmorphamine treatments the eyes are very poorly patterned with no continuous pigmented retina.
(n=3 for all conditions shown).

4.2.3 Hedgehog and Wnt are important in craniofacial cartilages

To confirm Wnt and Hh effects on craniofacial cartilage I stained the stage 45 tadpoles with Alcian blue, which binds to acidic mucopolysaccharides and glycosaminoglycans in cartilage (Figure 4.3). These cartilages develop from neural crest, which emerge from the neural tube to populate the developing face (schematic Figure 4.3A-C). Because affected cartilages suggested that defects in subsets of neural crest streams might correlate with loss of specific facial cartilages, I decided to examine the NC during migratory stages using *twist* expression.

Activation of Wnt by BIO resulted in a strong reduction in anterior cartilages (Figure 4.3E-J). Affected tissues included Meckel's cartilage, the parahyoid and anterior ethmoid plate; however, the gill cartilages were relatively unperturbed (Figure 4.3E-J). This suggested that the anterior-most streams (schematised in red and yellow, Figure 4.3A-C) are the most sensitive to changes in GSK-3 activity. Indeed, *in situ* hybridisation for *twist* mRNA revealed dramatic loss of these tissues (Figure 4.3O).

In contrast, I found that Wnt inhibition by IWR resulted in cartilages that appeared reasonably well patterned. However, upon dissection, I found them to be less structurally solid than their control counterparts (note less intense staining in the parahyoid, Figure 4.3F-K). The infrarostral cartilage is absent in the IWR treated tadpoles (see Figure 4.3C) but Meckel's cartilage appears normal (Figure 4.3K). Consistent with these observations, I found that streams of *twist* positive cells were not as well defined; however, the amount of *twist* positive tissues does not appear reduced (Figure 4.3P).

Inhibition of Hedgehog by cyclopamine treatment caused the most catastrophic loss of cranial cartilages, leaving only a remnant of the posterior parahyoid and the otic capsules (Figure 4.3G-L). When I examined *twist* expression, I found some loss of posterior neural crest streams; however, the neural crest flanking the eye appears to be migrating along the appropriate path (yellow, Figure 4.3A and 4.3Q). These data suggest that Hedgehog signaling may not be required during migration and may play additional roles in the neural crest, including survival (Brito et al., 2006) (Ahlgren and Bronner-Fraser, 1999).

However, when Hedgehog signaling is activated by purmorphamine, the cartilages are largely unaffected. The infrarostral cartilage is lost though this may be due to the widened midline, discussed below (Figure 4.3H-M). Neural crest migration appears largely normal; although perhaps the streams are not as defined (Figure 4.3R).

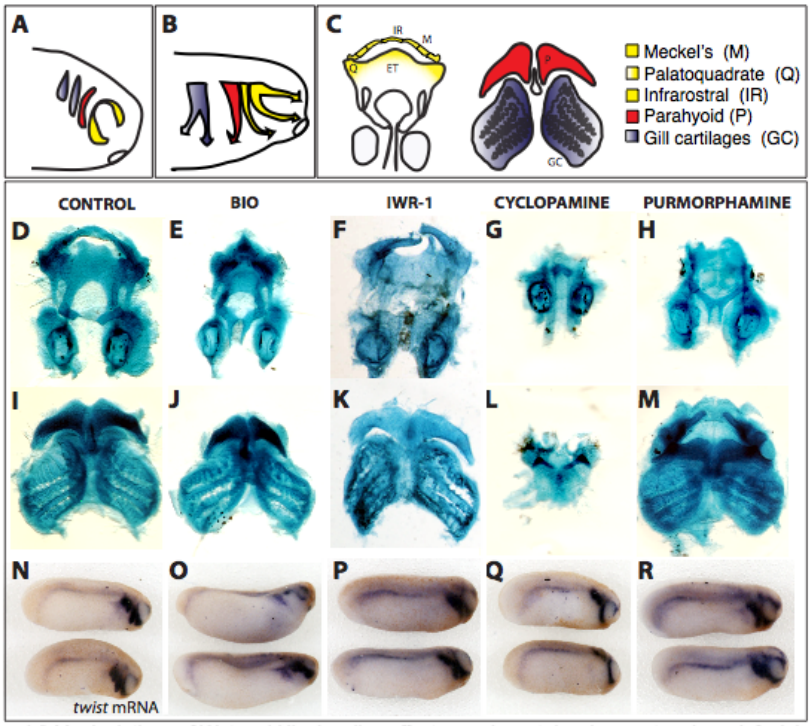

Figure 4.3 Manipulations of Wnt and Hh signaling affect neural crest development and craniofacial cartilages.

(Fig 4.3A-C) Schematic of Xenopus NC migration and subsequent contribution to cartilages. Lateral view. At stage 23, neural crest is migrating from the dorsal neural tube (Fig 4.3A).
(Fig 4.3B) By stage 28, the neural crest has populated the branchial arches. (Fig 4.3C) Schematized lineage of the craniofacial cartilages.
(Fig 4.3D-I) Colors correlate with streams in A and B. Alcian blue stained cartilage dissected from a WT stage 45 tadpole. (Fig 4.3N) Control embryo stained by in situ hybridization for twist mRNA to mark migrating neural crest.
(Fig 4.3E-J) 2 cell 15μM BIO treated tadpole with anterior cartilage defect. (Fig 4.3O) The ethmoid plate is narrowed, Meckel's cartilage is absent and the parahyoid smaller. Twist in situ reveals clear loss of anterior migratory streams.
(Fig 4.3F-K) Cartilages dissected from 100μM IWR treated tadpole appear normal though the infrarostral (IR) cartilage is missing. Cartilages are thinner; note relative intensity of Alcian blue staining. (Fig 4.3P) Twist expression is relatively normal.
(Fig 4.3G-L) Incubation with 250μM cyclopamine caused a catastrophic loss of cranial cartilages. Only the cartilage surrounding the ossicles and a remnant from the parahyoid remain. (Fig 4.3Q) Twist expression is primarily reduced in the posterior streams.
(Fig 4.3H-M) Tadpoles treated with 100μM purmorphamine had clear midline defects, resulting in a loss of the infrarostral and palatoquadrate. (Fig 4.3R) Purmorphamine treatment resulted in less well-defined but largely normal twist expression.
(n≥12 for all conditions shown).

4.2.4 Some of the phenotypes were subtle

In three of the drug incubations I noticed that the infrarostral cartilage was absent despite an apparent overall normal patterning of the cartilage. In three cases, there was no midline defect, in contrast to purmorphamine treatments discussed above. Alsterpaullone (Figure 4.4B) and pyrimidine (Figure 4.4D) caused no other apparent phenotypes so it came as a surprise to see such a specific absence of cartilage. It was also missing in IWR treatments as discussed (Figure 4.4C).

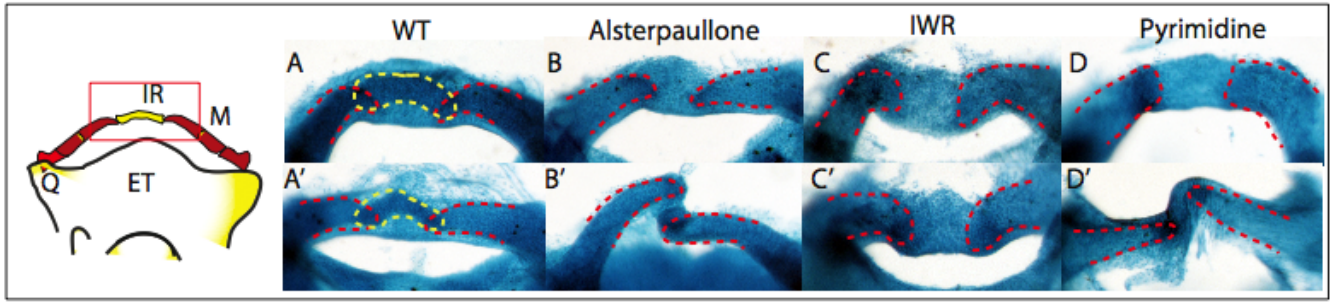

Figure 4.4 In certain drug treatments the infrarostral cartilage was lost

(Fig 4.4A) Schematic of stage 45 cartilages, infrarostral cartilage (IR, yellow) at anterior, flanked by Meckels cartilages (red) shown in WT.
(Fig 4.4B-B') The IR is lost in 100μM alsterpaullone treatment, (Fig 4.4C-C') 100μM IWR treatment and (Fig 4.4D-D') 1μM pyrimidine treatment.
(n≥7 for all conditions shown).

4.2.5 The craniofacial muscles are also affected

As described above, craniofacial cartilages are strongly affected by perturbation of Wnt and Hh signaling. Given the intimately linked nature of the cartilages and craniofacial muscles, I decided to examine changes to the presence and positioning of these muscles.

I looked for changes by immunohistochemistry using an antibody that recognises skeletal muscle (Figure 4.5/4.6). A schematic of the anatomy and WT tadpoles show the normal musculature (4.5A-C'). Drug treated tadpoles are examined in Figure 4.6. In the BIO treated tadpoles, changes to the head muscles correlate with the anterior cartilage defects described above. Unsurprisingly, given the cyclopic nature of the tadpoles, the optic muscle complex is severely affected (red arrowhead, Figure 4.6B). The levator mandibulae complex is not apparent. Extension of the muscles in the truncated mandibular region is shorter: note the intermandibularis posterior, interhyoideus and constrictor branchialis complex (yellow arrow, yellow arrow head and blue arrowhead respectively, Figure 4.5M). In IWR treatment the majority of muscles are decreased in size, with the abdominal muscles most severely affected (red arrowhead, Figure4.6H). The hyoangularis and intermandibularis muscles are also much shorter. Thus, activation of Wnt signaling results in concurrent changes in facial cartilage and muscle, while inhibition has minimal effects.

Inhibition of Hedghog signaling results in a striking loss of head muscles. The majority of the dorsal muscles are absent, with only the interhyoideus and a diminished orbitohyoideus remaining (Figure 4.5O). On the contrary, the axial muscles are largely normal (note the abdominal muscles in Figure 4.5I and the somites in Figure 4.5N). Purmorphamine treatment does not result in the loss of any of the craniofacial muscles. However, the interhyoideus muscle is discontinuous at the midline (red arrowhead, Figure 4.5 J).

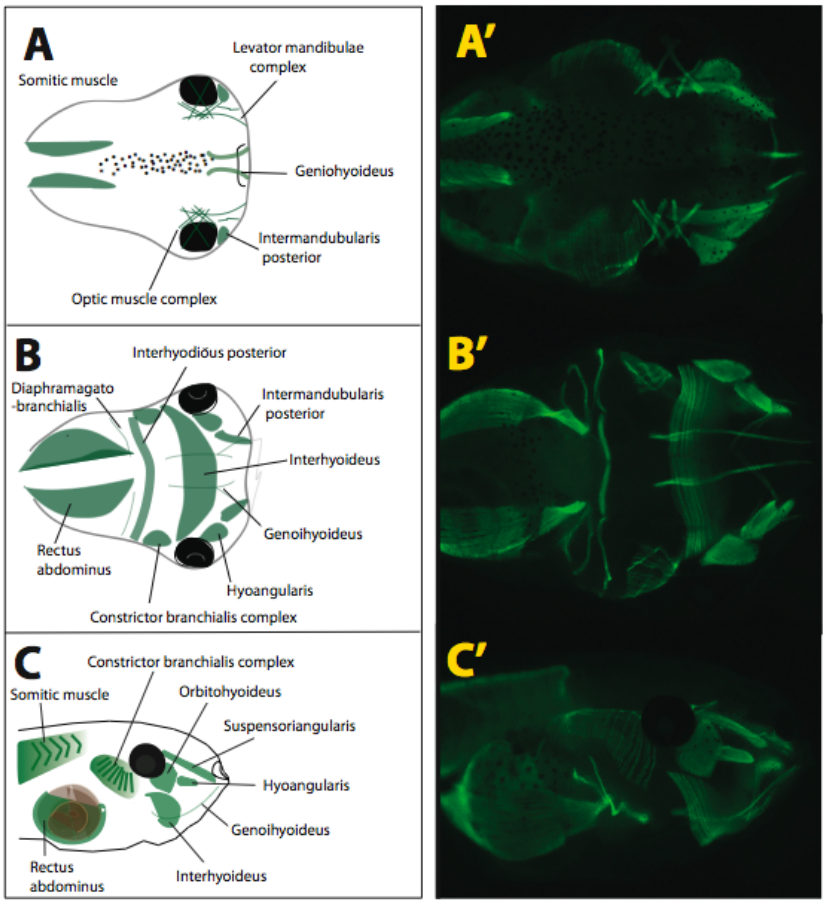

Figure 4.5 Schematic of stage 45 Xenopus craniofacial muscles

Schematic of stage 45 WT tadpole facial muscles with names; (dorsal view Fig 4.5A, ventral view Fig 4.5A′, lateral view Fig 4.5A″) stained with muscle marker 12/101.
(n=3 for all conditions shown).

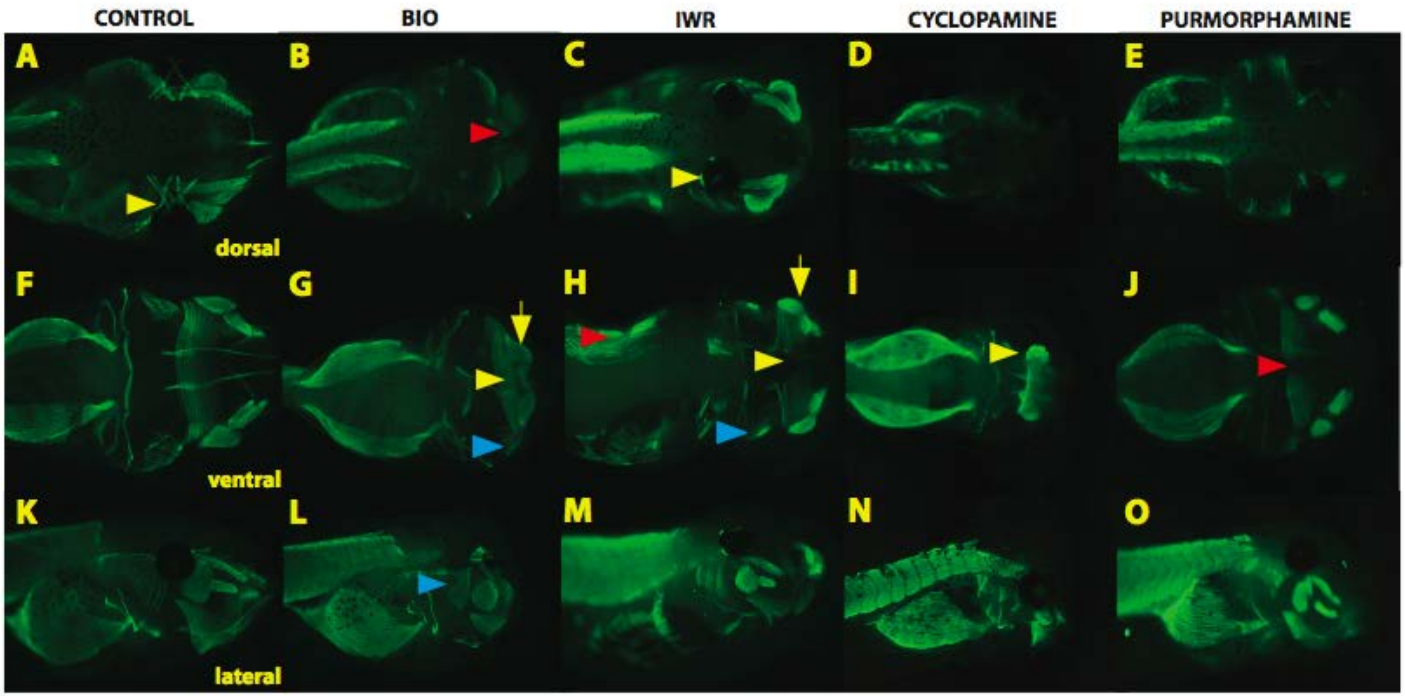
CONTROL
BIO
IWR
CYCLOPAMINE
PURMORPHAMINE
A
B
C
D
E
dorsal
F
G
H
I
J
ventral
K
L
M
N
O
lateral

Figure 4.6 Craniofacial muscles are displaced but not absent.

(Fig 4.6A, F, K) Stage 45 tadpoles stained with immunohistohemistry using 12 101 on WT and embryos treated from 2cell with (Fig 4.6B, G, L) 15μM BIO treated, (Fig 4.6C, H, M)100μM IWR, (Fig 4.6D, I, N) 50μM cyclopamine and (Fig 4.6E, J, O) 100μM purmorphamine tadpoles.
The ocular muscles were strongly affected in all treatments (Fig 4.6B-E) with both patterning and size changed, most strongly in cyclopic BIO treatment tadpole (red arrowhead, Fig 4.6B).
The intermandibularis posterior, interhyoideus and constrictor branchialis complex are reduced (yellow arrow, yellow arrow head and blue arrowhead respectively, Fig 4.6G).
In IWR treatment the muscles appears to cross the eye (yellow arrowhead, Fig 4.6C) rather than attaching to the posterior eye (yellow arrowhead, Fig 4.6A).
Extension of the muscles in the truncated mandibular region is shorter: note the intermandibularis posterior, interhyoideus and constrictor branchialis complex (yellow arrow, yellow arrow head and blue arrowhead respectively, Figure 4.6H).
In IWR treatment the majority of muscles are decreased in size, with the abdominal muscles most severely affected (red arrowhead, Fig 4.6H).
Cyclopamine treatment causes a striking loss of majority of the dorsal muscles, with only the interhyoideus and a diminished orbitohyoideus remaining (yellow arrowhead, Fig 4.6I). The axial muscles are largely normal (Fig 4.6N).
Purmorphamine treatment does not result in the loss of any of the craniofacial muscles. However, the interhyoideus muscle is discontinuous at the midline (red arrowhead, Fig 4.6J).
(n≥9 for all conditions shown).

4.2.6 Early perturbations most strongly affect gut development

In tadpoles, the gut develops stereotypically (Nieuwkoop, 1994). By stage 45, the tightly coiled gut is easily visible (WT 4.7A) but little is known about the signaling mechanisms required for correct patterning in the development of the visceral mesoderm. The coiling of the gut was affected in numerous drug treatments. Several manipulations led to an absence of gut coiling, loss of gut coiling, delayed gut coiling or gut elongation phenotypes. The wide variety of phenotypes and the large number of compounds that affected development suggest that the complex process of gut development was affected at different stages in these treatments and that different processes have been altered.

Typical development of the gut begins very early. This screen has not examined changes in the patterning of the endoderm in the early development (Chalmers and Slack, 2000) nor have we looked at the possibility that treatments were perturbing left right symmetry in the embryos (Dush et al., 2011). Instead, I have focused on whether the intestinal tubes coiled (described in detail by (Nieuwkoop, 1994)).

Initial treatment with three of our compounds resulted in very dramatic elongated gut phenotypes: IWR (Figure 4.7F-I), cyclopamine (Figure 4.7B-E) and rockout (Figure 4.7J-M). For cyclopamine and IWR, these phenotypes were also evident in the refined treatments (stage 12.5 – 19, Figure 4.7C & G). In these phenotypes it appears that the gut tissue has extended along the elongating body axis without any attempted independent coiling and maturation (Figure 4.7B-C & 4.3F) (Chalmers and Slack, 2000). This trend continued in the latter two treatments (Figure 4.7L-M). IWR application at stage 19 resulted in an attempted at gut coiling. However, stage 37 treatments were largely benign (Figure 4.7E). In contrast, by stage 12.5-19, inhibition of Rho kinase by Rockout only caused a delay: though the guts were coiled, they appeared more like that of stage 43 tadpoles (Figure 4.7K).

Not all the treatments caused elongated phenotypes. In cyclosporin treatment guts have very little differentiated tissue in the abdomen. This phenotype results from all stages of treatment (Figure 4.7N-Q). Purmorphamine has yet another type of gut phenotype. Hedgehog agonism causes a gut that is appropriately positioned yet the coiling is

disorganised (Figure 4.7R-T). This phenotype was present in all the treatment windows examined.

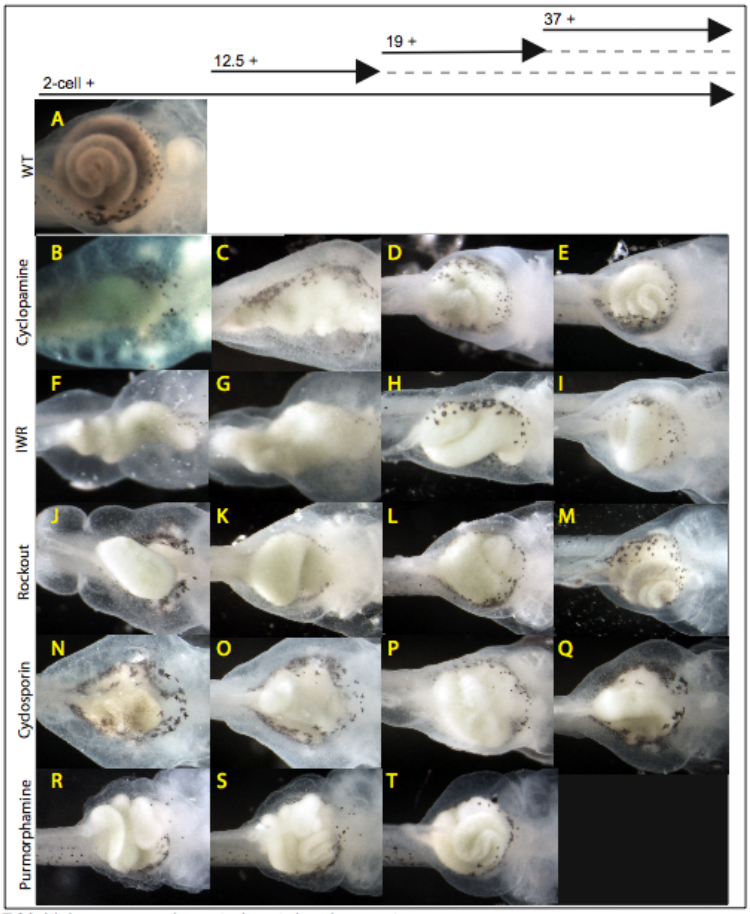

Figure 4.7 Multiple compounds perturb gut development

(Figure 4.7A) Ventral view, WT tadpole gut at stage 45. (Figure 4.7B, F, J, N&R) Embryos treated at 2cell, (Figure 4.7C, G, K, O&S) stages 12.5 - 19, (Figure 4.7 D, H, L, P&T) stages 19 - 37 and (Figure 4.7E, I, M&Q) stages 37 - 45.
(Figure 4.7B-C) 100μM cyclopamine treatment caused uncoiled, extended guts in the two early treatments. (Figure 4.7D) Between stages 19-37 coiling was present and by stage 37 no changes were seen (Figure 4.7E).
(Figure 4.7 F-G) 100μM IWR incubation had severe phenotypes in the two early treatments and decreasing severity with later drug application (Figure 4.7H-I). (Figure 4.7 J) 2cell treatment with 100μM Rockout caused elongated guts. (Figure 4.7K) In treatments between stage 12.5 - 19 and between stages 19 - 37 (Figure 4.7L) some gut coiling was observed.
(Figure 4.7M) By stage 37, Rockout caused no change to gut coiling. (Figure 4.7N-Q) Cyclopsorin and (Figure 4.7R-T) purmorphamine application halted proper gut coiling in all stages treated.
(n≥21).

4.2.7 Wnt signaling is required throughout development of the gut.

I chose to look more closely at the effects that both the edema and the delayed coiling of the gut (discussed in previous figure) have on the proper differentiation of abdominal structures and muscles (Chalmers and Slack, 2000). As described above, I found the progressively less severe phenotype in later treatments suggests that Wnt signaling is most important during initial stages of gut development. Treatment of 2-cell embryos caused severe edema and an extended and predominately undifferentiated gut, clearly seen in sections through the gut (Figure 4.8G&L). Addition of compound at stage 12.5 resulted in an extended, uncoiled gut similar to that from the 2-cell treatment (Figure 4.8C). However, when I sectioned these animals, I found that the later treatment resulted in increasingly differentiated tissues within the intestines (Figure 4.8H). Treatments beginning at stage 19 still resulted in poorly patterned guts but some coiling was evident, while the edema is much reduced (Figure 4.8D&I). By stage 27, treated guts appeared delayed, rather than disrupted; tissue complexity in the abdomen was almost WT (Figure 4.8E&J).

Concurrently, I examined the body wall muscles. The abdominal muscles begin to develop at stage 31 when undifferentiated cells coalesce from the trunk myotomes. These cell clumps migrate beneath the epidermis and at stage 39 begin to broaden into sheets of muscle that extends from the pericardium to the proctodeum (Lynch, 1990). The trunk myotomes appear disorganised in the IWR treatment so it may be that this disorganisation has delayed or perturbed the ventral migration of the cells that will become the body wall muscles (Martin and Harland, 2001). The *rectus abdominal* muscle lies along the lateral side of the gut in stage 45 tadpoles as a tightly associated sheath (arrow, Figure 4.8K). In IWR-1-endo treatment, along with changes to gut coiling I see disruption in this sheath of muscle (Figure 4.8BL-O). I found diffuse abdominal muscles in severely affected tadpoles; these animals were also edematous. (Figure 4.8L-O). Later additions of IWR-1-endo resulted in nearly normal muscles (Figure 4.8N-O).

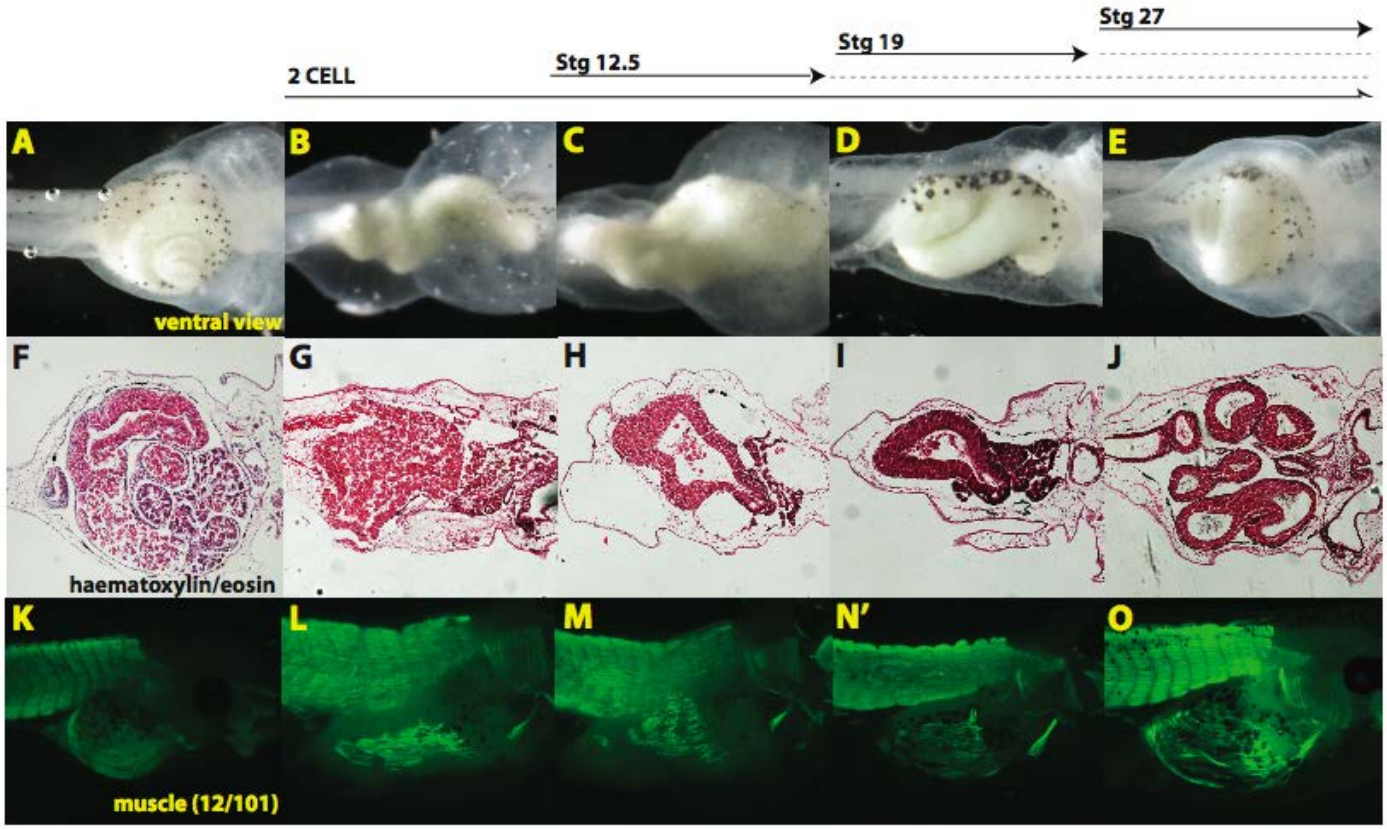
Stg 27
Stg 19
Stg 12.5
2 CELL
A
B
C
D
E
ventral view
F
G
H
I
J
haematoxylin/eosin
K
L
M
N'
O
muscle (12/101)

Figure 4.8 Wnt signaling is important throughout Gut development

(Fig 4.8B, G &L)Tadpoles were treated with 100μM IWR from 2 cell, (Fig 4.8C, H & M) between stages 12.5 - 19, (Fig 4.8D, I & N) stages 19 - 37 and (Fig 4.8 E, J & O) stages 37 - 45 and the development of their gut coiling compared to WT (Figure 4.8A, F & K).
(Figure 4.8F-J) Coronal sections were taken through the abdomen and H&E staining performed.
(Figure 4.8K-O) 12/101 muscle marker was used to analyse the abdominal muscles. At all stages inhibition of Wnt results in a loss of proper gut patterning.
(Fig 4.8B) The most severe phenoypes were found with 2-cell treatment and the severity of the phenotypes decreased over time (Fig 4.8C-E).
(Fig 4.8F) In the WT complex abdominal structures are apparent. (Fig 4.8G) In the 2cell treated this is completely lost. Some differentiation appears to have taken place in the treatements between stages 12.5 - 19 (Fig 4.8H) and 19 - 37 (Fig 4.8I).
(Fig 4.8J) The tadpoles treated from stage 37, while not normal, have the some complex structure.
(Fig 4.8K-O) Analysis of the abdominal muscles shows that the development of these muscles is closely related to overall gut development.
(n≥21 for all conditions shown).

4.3 Discussion and Conclusions

This chapter has demonstrated that a large number of phenotypes can be assessed in a rapid and reproducible manner using *Xenopus* as a model for craniofacial and neural crest development. By applying small molecules to the embryos at discrete time points I was able to determine temporal requirements for various signaling pathways in the development of numerous organs. Though this screen was aimed at developmental stages that were important to neural crest development, such a screen could be adapted to study any process of interest.

When we examined the tadpoles treated at various stages for changes to the head shape and to the eyes it was apparent that the most severe changes occurred with the early perturbations. In order for a tadpole to develop a true cyclopic phenotype the induction of the prechordal plate of the division of the forebrain must be affected. It has been well established in chickens and in *Xenopus* that Shh is a key regulator in the division of the eye field (Li et al., 1997) (Pera and Kessel, 1997) though in *Xenopus* is it suggested that Shh signaling is not required for the correct specification of the floor plate (Peyrot et al., 2011). As only the embryos treated with BIO at two cell stage developed true cyclopic phenotypes, I would postulate that this region is likely unaffected in the cyclopamine treated tadpoles, as the eye field retains its division (Chow and Lang, 2001). The BIO phenotype will be further addressed in chapter 4.

Many of the eye phenotypes scored in the drug tadpoles could be attributed to changes to the midline. The most interesting change to the eyes came with the overactivation of Hedgehog using purmorphamine, where I saw changes to the layers of the eye and a loss of compact pigmented epithelial retina. This correlates with studies in zebrafish which have shown that Hedgehog signaling is required for the dorsal-ventral patterning of the eye and that overactivation of Hh signaling results in a loss of dorsal retinal identity and a fusion of pigmented epithelium with the forebrain (Take-uchi et al., 2003).

There were dramatic changes to the craniofacial cartilages and I have shown that apparently similar phenotypes can be readily attributed to distinct developmental processes. For example, changes to cranial structures may arise because of defects in neural crest migration (BIO, discussed chapter 5), potential defects in tissue survival (cyclopamine) or changes to underlying morphology (midline expansion, purmorphamine). However, the loss of the infrarostral cartilage was an interesting and subtle phenotype that came as a surprise. To the best of my knowledge this small cartilage is derived in the same manner as Meckel's cartilage. In fact, in salamanders or newts, it has been proposed that the infrarostral cartilage is a specialised anterior part of Meckel's (Svensson and Haas, 2005). The *Xenopus bagpipe* ortholog *zampogna* is expressed in the mesenchymal cells of the future infrarostral cartilage so it would be interesting to see if expression of this gene is altered in IWR and other treatments. This would suggest that the infrarostral cartilage is regulated and develops in a manner independent of Meckel's cartilage.

Assays of this nature can reveal links between seemingly disparate phenotypes such as loss of muscle and cartilage. Conversely, phenotypes that appear obviously linked, such as deformed gut and abdominal muscle, may be uncoupled. While Wnt signaling is clearly required throughout the coiling of the gut it is also needed for proper development of the abdominal muscles (Martin and Harland, 2001). Furthermore, if the epidermal layer is disrupted due to structural changes or pressure from edema then the muscle precursor aggregates may be unable to migrate to the correct position. Given the relatively late development of this muscle sheet I would postulate that the severely malformed muscles in early treated tadpoles are closely associated with the observed edema.

The majority of the phenotypes were found most commonly or to be more severe in the 2-cell stage treatments, suggesting that the drugs are acting on early embryonic processes. In particular, changes to the gut may be due to a loss of left-right patterning that renders the embryo incapable of looping the elongating gut. Should this need to be addressed in more detail, the expression pattern of genes that are expressed in an asymmetric L-R pattern, such as *nodal*, could be examined (Dush et al., 2011).

5 HEDGEHOG SIGNALING DETERMINES THE SIZE OF THE PRIMARY MOUTH

5.1 Summary

One interesting and unexpected phenotype that came out of the chemical screen was the effect that Hedgehog (Hh) perturbations had on the size of the primary mouth. I found that inhibition of Hedgehog signaling resulted in a reduced or imperforated mouth while increasing of hedgehog signaling dramatically increases the size of the mouth.

In vertebrates, patterning of the mouth is a multi-step process requiring interactions between numerous tissue types. Here I define the primary mouth as the initial opening of the alimentary canal and the secondary mouth as the complex mouth structure including palette, teeth, tongue etc. Though there is some understanding of important steps in formation of the secondary mouth structures, less is known about molecules that control initiation of oral perforation. The formation of the primary mouth in a number of vertebrate models has been well characterised (Takahama et al., 1988) (Waterman, 1977) (Waterman and Schoenwolf, 1980). Development of the primary mouth in *Xenopus* has been elegantly described by recent work from Dickinson and Sive (Dickinson and Sive, 2006). Although Hedgehog signaling has a well-characterised role in the development of the vertebrate secondary mouth, nothing is known about its role in primary mouth development, or in regulating the perforation of the buccopharyngeal membrane, an essential step in primary mouth formation.

In vertebrates the mouth opening forms as a result of contact between the invaginating stomodeal ectoderm and the underlying endoderm. In an analogous process, ectodermal-endodermal interactions also precede the opening of the hindgut, followed by dissolution of a membrane. The formation of the cloacal membrane occurs with the loss of mesodermal cells and basement membrane proteins separating the ectoderm and endoderm cells (Hassoun et al., 2010). While there are no previous data suggesting that Hh has a role in the dissolution of the buccopharyngeal membrane, there are some indications that Hh signaling may be important in regulating formation and dissolution

of the cloacal membrane (Mo et al., 2001) (Perriton et al., 2002) (Parkin et al., 2009) (Seifert et al., 2009). *Shh* mutants have a persistent cloacal membrane, demonstrating an early role for Hedgehog in cloacal septation (Haraguchi et al., 2007). Aberrant levels in Hedgehog signaling in *Gli2*$^{-/-}$ and *Gli3*$^{-/-}$ mouse mutants also lead to dorsal cloacal membrane persistence in a dose responsive manner (Kimmel et al., 2000) (Mo et al., 2001). Persistence of this membrane in humans is associated with numerous anorectal anomalies, most common in females (Kim et al., 2001) (Levitt et al., 2011; Rosen et al., 2002).

In human patients some syndromes that present with anorectal defects have been identified as having mutations in the Hedgehog pathway. In the case of Pallister-Hall syndrome there is a mutation in Gli3 (Kang et al., 1997). Indeed, VACTERL is used as a clinical diagnosis of non-random birth defects (names derives from vertebral defects (V), anal atresia (A), tracheoesophageal fistula with esophageal atresia (TE), radial and renal dysplasia (R)) and many of these have been attributed to mutations in the hedgehog effector genes (Doray et al., 1999; Kim et al., 2001; Topf et al., 1993).

As Hedgehog signaling is known to play important roles in facial patterning and is expressed in the right tissues at appropriate times I hypothesized that Hh levels might also affect primary mouth development. To address this I used small molecules to alter levels of Hedgehog signaling and analyzed the tadpoles at feeding stages (stage 45). My results showed that increasing the levels of Hh signaling with the Hh agonist purmorphamine resulted in a dramatically expanded mouth. This appears to be due to premature contact between the two tissue layers. Conversely, treatment with the Hh inhibitor cyclopamine reduced the size of the oral opening in a dose-dependent manner, with high doses leading to a complete loss of the mouth. In this case, there appears to be a persistence of intervening mesenchymal tissues, preventing breakdown of the epithelia.

5.2 Results

5.2.1 Levels of Hedgehog signaling determine size of the primary mouth

In the primary screen outlined in chapter 3 I described the effect of Hedgehog manipulations on overall tadpole morphology. Consistent with previous reports, I found that treatment with cyclopamine (up to 250µM) resulted in tadpoles with narrower cranial width and shorter heads (Figure 5.1B) when compared to controls (Figure 5.1A) (Chen et al., 2002). Though the cyclopamine treatment led to significantly smaller heads, I found, to our surprise, that incubation in purmorphamine, the Hh agonist, resulted in broadly similar phenotypes (Figure 5.1C). To gauge the width of the head, I took two measurements at stage 45: between the eyes and at the widest point in the head (schematic, Figure 5.1D). Both measurements were important as there was often significant edema seen around the face that distorted the width of face. Measuring between the eyes gave me a representation of both the reduction in distance between the eyes but also of overall loss of facial growth in embryos where the eyes were still separate. However this distinction was not pursued.

To determine the extent of facial growth, I measured the length of the face from behind the eyes as well as the distance from the front of the eyes to the most anterior point (schematic Figure 5.1E). In both treatments the tadpoles were statistically significantly shortened in all dimensions in comparison to EtOH, the drug vehicle control (*, Figure 5.1D-E $P<0.001$). No statistically significant difference was found between the cyclopamine and purmorphamine treatment.

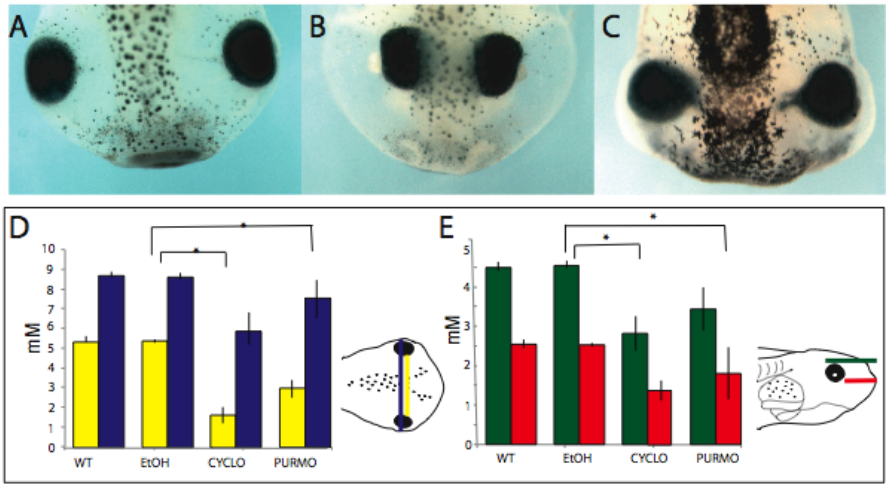

Figure 5.1 Perturbations in Hh signaling negatively affect the width and length of the Xenopus head

(Fig 5.1A, B and C) Dorsal views of stage 45 untreated, 250μM cyclopamine or 100μM purmorphamine treated embryos.
(Fig 5.1D, blue and yellow lines respectively) The width of the widest point of the head at the level of the eyes, and the width between the eyes was used to measure the width of the head.
(Fig 5.1D) Cyclopamine and purmorphamine treatment significantly decreased the width of the tadpole heads
((blue line) p=9.83124E-10, (yellow line) p=8.53855E-12).
(Fig 5.1C, green and red lines, respectively) Head length was measured from the anterior most point of the head to either the posterior or anterior extent of the eye.
(Fig 5.1E) Cyclopamine and purmorphamine treatment significantly decreased head length
((green line) p=2.63227E-14, (red line) p=5.42094E-11).
(n=12 for all conditions shown).

5.2.2 Hedgehog regulates mouth size in a dose responsive manner

One huge advantage of a drug manipulation in this manner is the ability to precisely regulate the dose added to the media. As such I varied the dose and tested to see if modulating the amounts of Hedgehog signaling resulted in a graded response in the size of the mouth. To do this, I applied a range of concentrations of both cyclopamine and purmorphamine treatments beginning at stage 2. Embryos were treated with 250μM cyclopamine (Figure 5.2A), 50μM cyclopamine (Figure 5.2B) and 5μM cyclopamine (Figure 5.2C) to decrease Hedgehog signaling. To increase Hedgehog signaling I treated the embryos with 2μM purmorphamine (Figure 5.2E), 20μM purmorphamine (Figure 5.2F) and 100μM purmorphamine (Figure 5.2G). I found dose of drug correlated with a clear graded response in the size of the mouth (Figure 5.2).

5.2.3 The size of the mouth is plastic until late in development

The WT mouth at stage 45 is approximately the width of the nasal pits and just dorsal to the cement gland, (schematised in Figure 5.2M). As mentioned, early treatment with cyclopamine at the 2-cell stage results in a mouth that doesn't perforate, although in some embryos a keyhole depression is apparent (outlined in red, Figure 5.2I). Treatment from stage 12.5-19 dramatically reduced the size of the mouth (Figure 5.2J), as did treatment from stage 19 to 37 (Figure 5.2K). Treatments at stage 37 have no effect on mouth width, suggesting that the requirement for hedgehog signaling on mouth size occurs prior to this stage (Fig 5.2L). In contrast, maintaining Hedgehog activation is sufficient to increase the size of the mouth. Treatment with purmorphamine from the two-cell stage narrows the head but hugely expands the mouth (Fig 5.2N) when compared to the control (Figure 5.2H). This expansion is seen in all later treatments, with decreasing severity (Figure 5.2 O-Q)). Unlike the stage 37-cyclopamine treatments, purmorphamine continues to affect the width of the mouth in the later treatment (Figure 5.2Q). This suggests that while the initial development of the mouth requires early hedgehog signaling the mouth size can be expanded late into development by an increase in Hh.

It should be noted that in the embryos where an expansion of the mouth was seen, the mouth cavity was not as greatly expanded so it is possible to see both the most exterior edge (red dotted line, Figure 5.2) and on occasion the inside of the mouth cavity which is highlighted with a yellow dotted line (Figure 5.2N-Q).

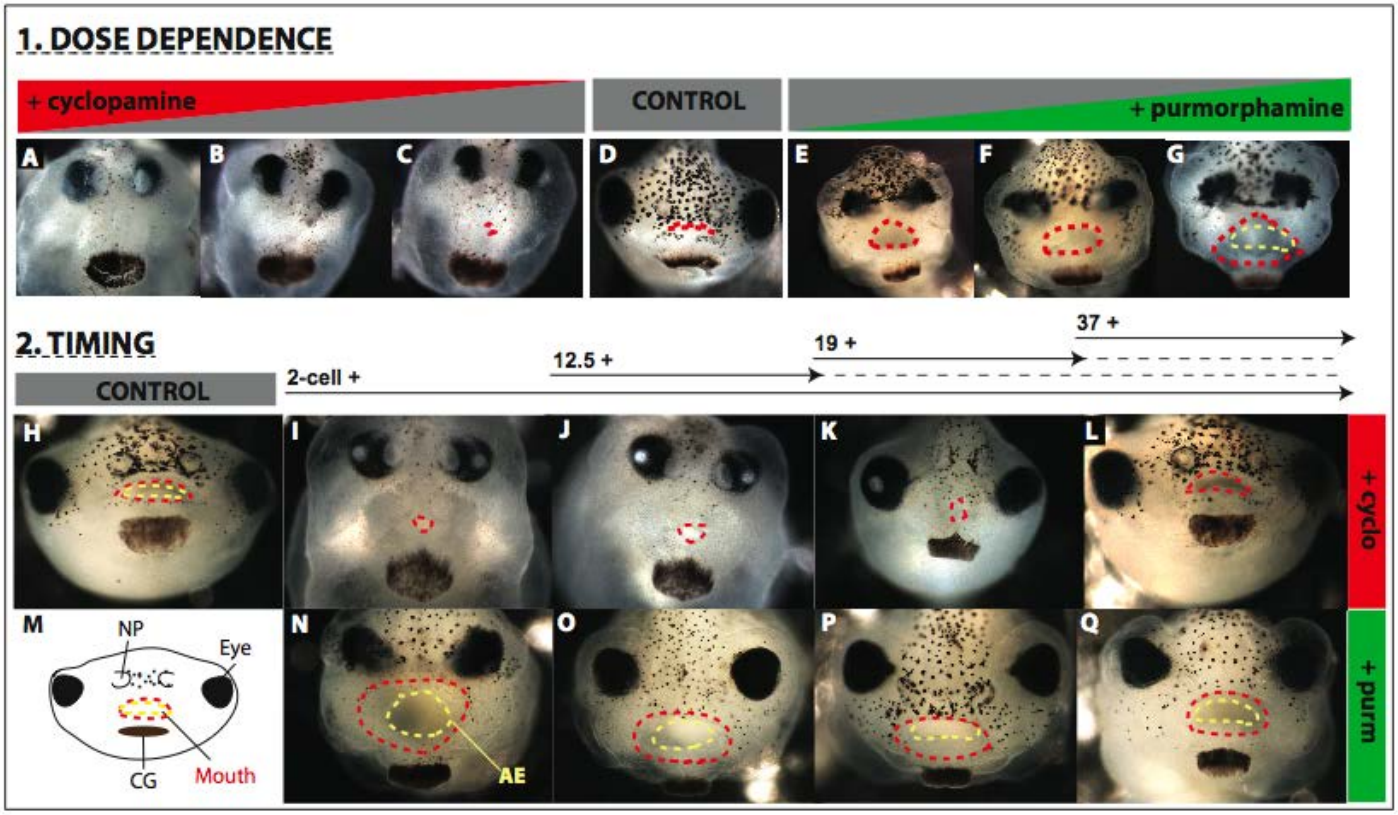
1. DOSE DEPENDENCE
+ cyclopamine
CONTROL
+ purmorphamine
A
B
C
D
E
F
G
2. TIMING
CONTROL
2-cell +
12.5 +
19 +
37 +
H
I
J
K
L
+ cyclo
M
NP
Eye
CG
Mouth
N
O
P
Q
AE
+ purm

Figure 5.2 Development of the mouth is sensitive to both dose and timing of hedgehog signaling.

(5.2 A-C) Frontal views of tadpoles exposed to 250μM, 50μM and 5μM cyclopamine from the 2-cell stage and grown to stage 45. Note loss of mouth in high doses (Figure 5.2A-B) and small, perforated "keyhole" mouth (Figure 5.2C).
(5.2D) Control vehicle treated tadpole in 0.01% EtOH control
(5.2E-G) Frontal views of tadpoles treated with 1μM, 10μM or 100μM purmorphamine and grown to stage 45. Note increased mouth size with increasing concentrations of purmorphamine.

(5.2H-Q) Timing of drug sensitivity.
(5.2H) Vehicle treated control tadpole, stage 45.
(5.2I-L) Treatment with 50μM cyclopamine at indicated stages. All treatments up to stage 37 with cyclopamine reduces the mouth size (5.2I-K). Treatments after stage 37 (5.2L) do not affect mouth size or perforation.
(5.2N-Q) All treatments with 100μM purmorphamine lead to a larger mouth.
External edge of mouth opening outlined with red dotted line; internal edge of mouth opening outlined with yellow dotted line.
($n \geq 35$ in all treatments).

Formatted: Not Highlight

5.2.4 *Xenopus* mouth develops in a stereotypical manner

Dickinson and Sive document the normal development of the mouth, describing how the mesoderm between the endoderm and ectoderm is removed and the primary mouth opens. They report that the first obvious sign of mouth formation occurs from stage 22, marked by the dissolution of the basement membrane that separates the ectodermal cell population from the endoderm cells (Dickinson 2006). Following this the depression called the stomodeum can be visualized. This depression deepens as apoptosis and cell intermingling thin the ectoderm/endoderm tissue during mid-stage 30's (Dickinson 2006). By early stage 40's this membrane has dissolved and the mouth is open. It has been shown that the endoderm is required not for induction of the stomodeum but for the perforation of the mouth opening (Dickinson and Sive, 2006). Hedgehog ligand is in the anterior endoderm; therefore, I hypothesized that the duration of Hh reception might be critical to the size of the oral opening.

As outlined in Figure 5.5, contact between the endoderm and ectoderm followed by dissolution of the basement membrane and apoptosis are required to form a correctly perforated primary mouth. To pinpoint the effects of Hh modulation on the oral opening, I examined a staged series of treated tadpoles (Fig 5.3). When I sectioned embryos at stage 22 and performed H&E staining on the samples I found that the amount of mesenchymal tissue between the endodermal and ectodermal epithelial sheets is doubled in cyclopamine treatment (yellow line, Fig 5.3G) compared to WT (yellow line, Figure 5.3A). This intervening tissue is decreased in purmorphamine treatments (yellow line, Figure 5.3M). This pattern continues in the stage 26 sections (yellow lines, Figure 5.3B,H&N). In all these embryos the ectoderm is a double-layered epithelium and appears unaffected by the treatments. At these stages the endoderm should be a continuous epithelial sheath (black arrowhead, Figure 5.3A-C & M-N) but in the cyclopamine treatment this structural integrity is absent at stages 22 and 26 (black arrowhead, Figure 5.3 G-H).

By stage 28 there is premature contact between the endoderm and ectoderm in the purmorphamine treated tadpoles (blue arrowhead, Figure 5.3O); compare this to mesenchymal tissue still found between these two tissues in the WT (black arrowhead, Figure 5.3C). At stages 28 and 30, the cyclopamine treated animals that I examined had

very disorganised endoderm with many loose cells apparent in the developing gut (black arrow, Figure 5.3J-K). Previous work from the Sive lab (Dickinson & Sive, DB, 2000) has shown that the presence of the endoderm is required for the perforation of the mouth. Indeed, the phenotype they describe, embryos lacking in a perforated mouth but with a small depression present, was found in a subset of our cyclopamine treated embryos. In others (30% n=42), I saw no depression at all (Fig 5.2).

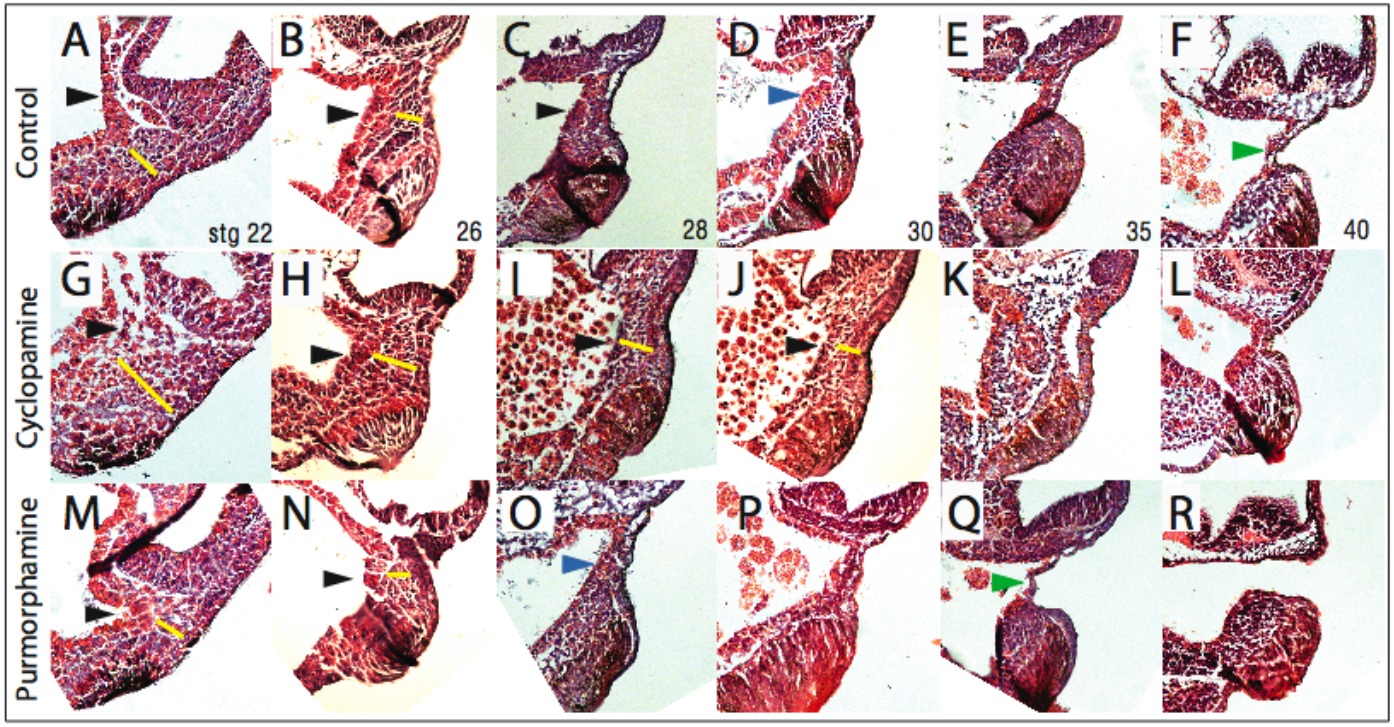

Figure 5.3 Perturbations in Hh signalling alter ectoderm and endoderm of the prospective primary mouth.

(Fig 5.3 A-F) Saggital H&E stained sections of untreated stage 22, 26, 28, 30, 35, 40 tadpoles incubated with (Fig G-L) 250uM cyclopamine, (Fig 5.3M-R) 100uM purmorphamine from the 2-cell stage.
(Fig 5.3A and B, yellow line) In control embryos mesenchyme between the ectoderm and endoderm of the primary mouth (black arrowheads) thins between stages 22 and 26 and begins to abut from stage 30 (blue arrowhead, Fig 5.3D). (Fig 5.3F, green arrowhead) From stage 40 the ectoderm-endoderm bilayer thins before perforating.
(Fig 5.3G-J, yellow lines) Thicker and persistent mesenchyme within the presumptive primary mouth was observed in cyclopamine treated tadpoles compared to controls.
(Figure 5.3O, blue arrowhead) (Fig 5.3P and green arrowhead in 5.3P) In purmorphamine treated tadpoles the ectoderm and endoderm abut by stage 28.
(Fig 5.3F) The mesenchyme within the presumptive mouth region thins and perforates prematurely compared to controls. (n=5 for all conditions shown).

5.2.5 Dramatic alterations to fibronectin suggests a mechanism for changes to the mouth

Dickinson and Sive demonstrate clearly the loss of basement membrane over time in the developing stomodeum. This is critical for the perforation of the mouth, as the cells must lose the basal lamina so that the abutting ectoderm and endoderm cells can intercalate before dissolution. I found that changes in Hedgehog signaling resulted in altered fibronectin deposition (Figure 5.4). In WT conditions at stage 22, the mouth region is already losing fibronectin from the basement membrane at the site of the invaginating stomodeal depression (between yellow arrows, Figure 5.4A&D) compared to epithelium of the tissue below the cement gland. In cyclopamine treated tadpoles, the cells in the stomodeum have not lost this basement membrane (blue arrow, Figure 5.4B) but in purmorphamine treatments fibronectin levels are already reduced in this region, suggesting advanced progression in the formation of a mouth (yellow arrows, Figure 5.5C&F).

The disorganised endoderm is also obvious at this stage in the cyclopamine treated embryos. The endoderm at this stage should be epithelial and characterized by long columnar cells. β−catenin staining in the cells shows the lack of columnar cells in the endoderm of the cyclopamine treated (Figure 5.4H) compared to the ectoderm of the same sample or the endoderm of the WT (Figure 5.4G). In the purmorphamine treatments, the β−catenin localisation is mildly altered but the cell shape clearly shows the epithelial nature of the endoderm in this treatment (Figure 5.4I).

At stage 26 the basement membrane should be absent from the region of the mouth (Dickinson and Sive, 2006). This was clear in the WT tadpoles at this stage (yellow arrow, Figure 5.4J). In cyclopamine treated tadpoles there was residual fibronectin expression suggesting maintenance of a basal identity in the cells of the stomodeum (Figure 5.4K). If this is the case then no intercalation of the endoderm and ectoderm cells would be able to occur and the mouth would be unable to perforate. In contrast, purmorphamine incubation led the extensive disorganisation of the fibronectin staining suggests that the region where the endoderm and ectoderm cells can mingle and thin is enlarged, allowing for the formation of a drastically enlarged mouth (Figure 5.4L). This

thinning is required for the interaction of the two tissue types, resulting in perforation of the membrane (Waterman, 1985). Furthermore, it is possible that these changes lead to the inability of this tissue to displace to mesenchymal tissue between the endoderm and ectoderm. It is unknown whether this occurs through an active or passive process.

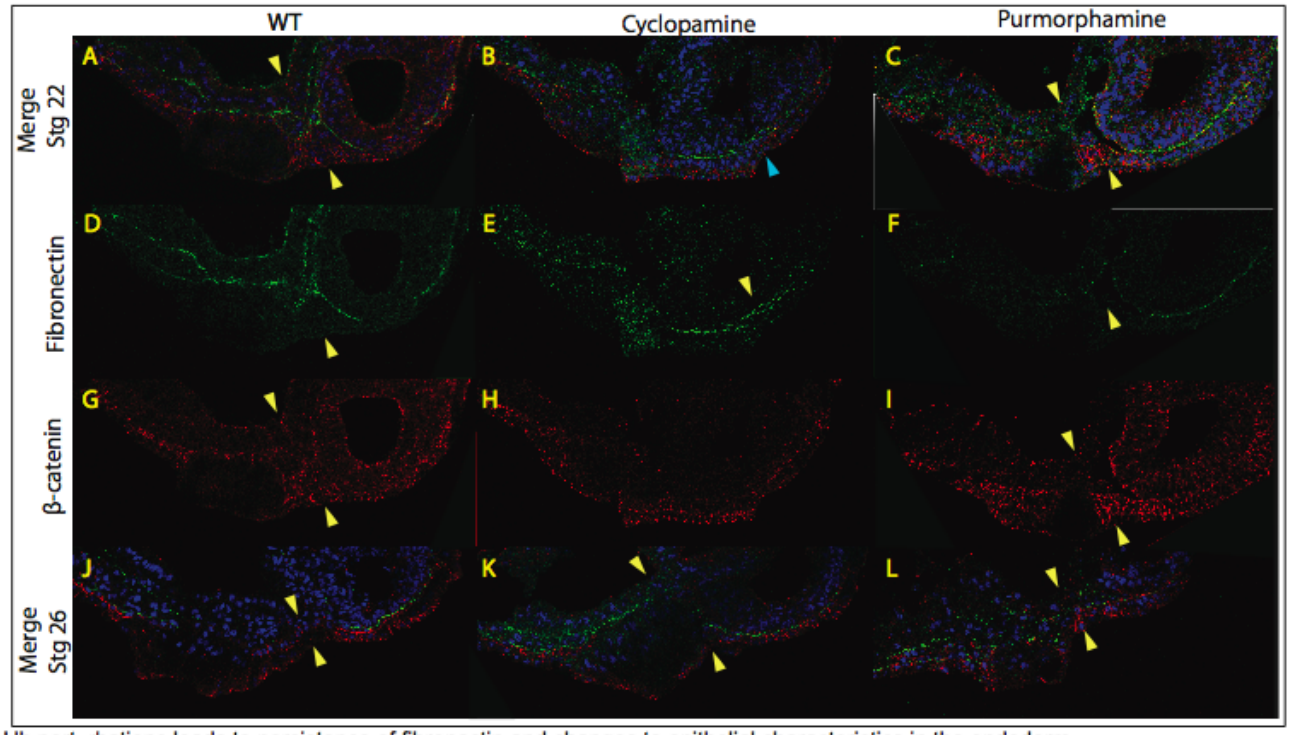

Fig 5.4 Hh perturbations leads to persistence of fibronectin and changes to epithelial characteristics in the endoderm

(Fig 5.4A-I) Immunohistochemistry was performed to examine the localisation of fibronectin (in green) and β-catenin (in red) in saggital sections of 22 embryo and (Fig 5.4J-L) stage 26 embryos,
(Fig 5,4B,E&H) 250uM cyclopamine treated from 2cell and (Fig 5.4C,F&I) 100uM purmorphamine treated from 2cell embryos.
(Fig 5.4D, yellow arrows) At stage 22 fibronectin is in the basement membrane of the presumptive mouth of WT and (yellow arrows, Fig 5.4E) cyclopamine treated but (yellow arrows, Figure 5.4F) dissolving in purmorphamine treated embryos.
(Fig 5.4H) β-catenin localisation in endoderm shows cell shape changes in cyclopamine treated compared to WT (Fig 5.4G).
(Fig 5.4J) At stage 26 basement membrane is dissolving in the WT and (Fig 5.4L) purmorphamine treated but remains in the cyclopamine treated (Fig 5.4K). Separate channels not shown for Fig 5.4J-L. (n=3 for all conditions shown).

5.2.6 Hedgehog is upstream of Wnt in regulating the levels of fibronectin in the developing mouth

Dickinson and Sive clearly demonstrated that the levels of Wnt protein in the developing face affect the levels of fibronectin and laminin (Dickinson and Sive, 2009). Given the changes to the fibronectin deposition in the mouth with alterations in hedgehog signaling I asked whether Hh was acting in parallel with Wnt in this process or whether one was upstream of the other. The hypothesis based on our perforation and fibronectin data was that a loss of Hedgehog signaling would result in increased Wnt signaling and that the opposite would be true. To test this 100pg Wnt reporter construct super top flash was injected into the 2 anterior cells of a 4cell embryo. These embryos were treated with cyclopamine for 24 hours and a luciferase assay performed. We found that indeed inhibition of hedgehog signaling caused an increase in the levels of Wnt signaling in the embryo (Figure 5.5A).

This was further confirmed by asking whether later up regulation of Wnt signaling could rescue the affects of early hedgehog up regulation. Increased Hedgehog signaling causes early contact between the ectoderm and endoderm in the region of the mouth, giving the enlarged mouth. Up-regulation of Wnt should increase fibronectin levels, preventing the perforation of the mouth. To test this, embryos were treated with purmorphamine at 2cell and washed into BIO, a GSK-3 inhibitor that will increase β-catenin levels, either 12 or 21hours post fertilization (Figure 5.5 E&G). Interestingly, only embryos treated with BIO at stage 19 (Figure 5.5E) showed any rescue of the enlarged mouth phenotype seen in embryos kept in purmorphamine (Figure 5.5C). BIO treatment from stage 12.5 alone causes a loss of the mouth, consistent with increased Wnt signaling. Purmorphamine followed by BIO at this stage also causes a complete loss of the perforated oral opening. Thus up regulation of Wnt was able to not only rescue the expected purmorphamine phenotype but was enough to completely obscure it with a Wnt up-regulation phenotype. BIO treatment at stage 19 has no effect on the size of the mouth (Figure 5.5F). In the tadpoles treated at stage 19 (21hpf) with BIO (Figure 5.5G) we found a reduction in the size of the mouth when compared to purmorphamine alone (Figure 5.5C) but it was still large compared to WT (Figure 5.5B) or BIO alone at this stage (Figure 5.5F). Control

data not shown found that purmorphamine treatment between 2cell stages and stage 12.5 results in an enlarged mouth. Taken together, this suggests that, consistent with previous studies, the mouth is sensitive to both loss and gain of Wnt until the tail bud stages but later, only the loss of Wnt signaling which results in a loss of basement membrane proteins, can perturb mouth size. These data also show that Wnt signaling is upstream of Hh in the anterior of the embryo in these early stages.

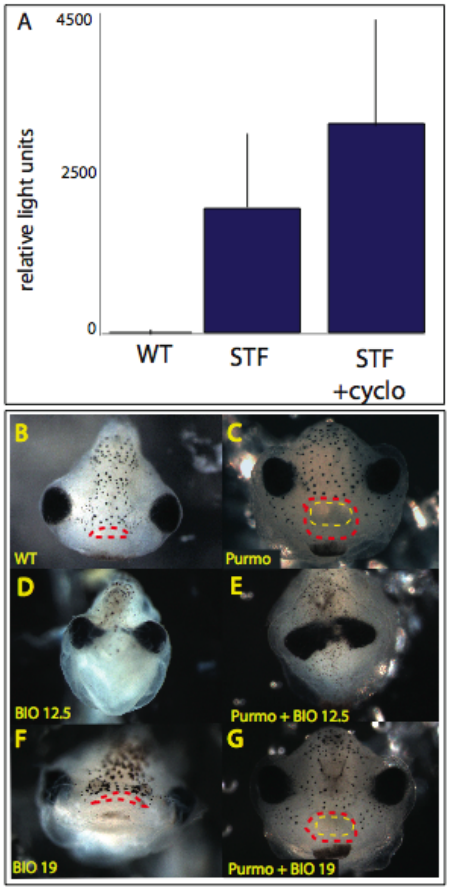

Figure 5.5 Hedgehog is upstream of Wnt in regulating the size of the mouth.

Embryos were injected bilaterally to the anterior 2 cells of a 4 cell embryo with 100pg of STF. They were cultured in a control or in 250μM cyclopamine for 24 hours then lysed in pools of 3 (minimum of 9 pools) and assayed for luciferase activity. (Fig 5.5A) Cyclopamine resulted in increased Wnt activity in this assay suggesting that Hh signaling is downstream of Wnt in the anterior of the embryo at these stages. (n=27)
To address whether Wnt activity was downstream of Hh in the mouth we performed sequential washout experiments.
(Fig 5.5C) Purmorphamine from 2cell stage caused an enlarged mouth.
(Fig 5.5D) GSK-3 inhibitor BIO was used to upregulated Wnt signaling, resulting in a loss of the mouth.
(Fig 5.5E) When Hh was upregulated from 2-cell to stage 12.5 followed by upregulation of Wnt from stage 12.5, the Wnt upregulation completely obscures the purmorphamine phenotype.
Later rescue by Wnt was found to be unsuccessful and by stage 19 the upregulation of Wnt did not effect mouth size or result in a rescue of the enlarged mouth caused by purmorphamine (Fig 5.5G).
Purmorphmine treatment from 2cell to stage 12.5 did result in an enlarged mouth when not followed by BIO treatment (data not shown). (n≥14 for Fig 5.5B-G).

5.3 Discussion and conclusions

I have shown a new and surprising requirement for Hedgehog signaling in the formation of a properly sized primary mouth. The loss of Hh results in a mouth where the cells of the endoderm and ectoderm do not come into contact at the appropriate stage and in a mouth that does not perforate. Excessive signaling causes premature contact between the two apposing tissues resulting in an enlarged mouth that opens prematurely. I believe my work shows that there is no specific region that is determined to be mouth (consistent with work from the Sive lab and studies in other organisms).

The drastic changes seen suggest that localization of the primary mouth opening is closely associated with the amount of Hedgehog exposure. Clearly tight regulation on Hedgehog signaling in the anterior is required to ensure that the oral opening is both present and appropriately sized. It is quite possible that Hedgehog activity is regulating Wnt signaling, which had previously been shown to be important in the primary mouth development (Dickinson and Sive, 2009). In *Shh*$^{-/-}$ mouse mutants decreased Wnt signaling has been reported in the developing cloacal anlagen (Miyagawa et al., 2009). Therefore, the loss of sonic hedgehog signaling in the mouth may also result in a loss in Wnt signaling. Conversely, in conditions where Hedgehog signaling is increased we would expect to see a similar increase in Wnt signaling which would result in a larger mouth (Dickinson and Sive, 2009; Miyagawa et al., 2009).

Premature loss of this fibronectin in the purmorphamine treated tadpoles may also be directly due to altered Wnt signaling. Expression of fibronectin is sensitive to levels of nuclear β–catenin. As it is changed, so is the amount of cell-cell or cell-substrate adhesion (Gradl et al., 1999).

In deuterostomes, there are at least two regions in the body that form by dissolution of a membrane following intercalation of the ectoderm and endoderm: the mouth and the anus. Due to its catastrophic nature, a failure in primary mouth formation is unlikely to be observed in viable pregnancies. However, failure of the cloacal membrane to perforate

does adversely affect a significant number of newborns. Studying the development of these tissues in mouse models is costly and time consuming. *Xenopus* may pose a relatively simple model in which to address development and perforation of these membranes. I propose that the oral opening in *Xenopus* could be used as a model to study the formation and eventual loss of this membrane as well as address the interplay between Hedgehog signaling and Wnt signaling in these tissues. This approach may provide insight into the development of various defects in the urogenital region in humans. It would be of interest to see whether the cloacal membrane behaves in a similar manner in these experiments. Initially, this could be addressed by examining whether embryos are capable of passing waste material from the stomach out through the proctodeum. However, given the severity of the mouth phenotypes embryos treated in cyclopamine or purmorphamine are unlikely to be capable of feeding or surviving much past stage 45 without feeding. In this instance, sections could be made through the posterior embryo to evaluate whether the cloacal membrane has a similar defect. If it does, the buccopharyngeal membrane could be used to assay any abnormal development in the dissolution of both membranes.

Here though, in this simple model using basic washout, we were able to show that not only does Hh have a role in the opening of the mouth but also that Hedgehog signaling is also necessary and sufficient for this process, as loss of Hh prevents mouth formation while gain of Hh can counteract Wnts at later stages. This data, along with recent studies from the Sive lab, suggest that the oral opening in Xenopus may be a tractable model to study the formation and eventual loss of this membrane during development.

6 GSK-3 IS REQUIRED FOR DEVELOPMENT OF ANTERIOR CRANIOFACIAL CARTILAGES

6.1 Summary

I have previously shown, in chapter four, that tadpoles treated with the GSK-3 inhibitor BIO lacked a subset of craniofacial cartilages. In this chapter, I analyze these phenotypes further. I show that GSK-3 inhibition by small molecule and morpholino oligonucleotide (MO) both perturb craniofacial cartilage development. Due to the earlier effects of the MO I returned to using BIO to finely control the timing of inhibition. By applying drug in increasingly shorter time periods, I narrowed down the minimal requirement for GSK-3 in cartilage development as stages 12.5 -19. Inhibition during this period perturbed a very specific region of the craniofacial cartilage while the rest of the embryo remained unaffected. The most anterior neural crest is clearly more sensitive to the loss of GSK-3 activity than the posterior neural crest. To track the migrating neural crest, I examined *twist* and *sox 9* expression. To confirm that these phenotypes are indeed a result of BIO acting on GSK-3 and not off target effects, I first had to identify a full-length clone of *Xenopus laevis GSK-3α*. I then used this cDNA to analyze the expression pattern of GSK-3α and design antisense morpholino oligonucleotides, in order to compare knockdown phenotypes with those seen in BIO treatments. Taken together, my data suggest that GSK-3 is required for appropriate migration of specific neural crest streams. Loss of GSK-3 activity leads to a loss of migration in the anterior streams, which correlates, with the cartilage defect found in stage 45 tadpoles.

6.2 Introduction

6.2.1 Glycogen Synthase Kinase 3

GSK-3 (Glycogen synthase kinase 3) is a serine/threonine protein kinase initially discovered as a regulator of glycogen metabolism. Since its discovery, GSK-3 has been suggested to regulate many processes beyond metabolism, including gene expression, cell cycle regulation, cell migration, development, oncogenesis and neuroprotection. GSK-3 plays a pivotal role in diseases as varied as cancer, Alzheimer's disease and inflammation (Wang et al., 2011) (Wray et al., 2010) (Hur and Zhou, 2010) (Sun et al., 2009).

GSK-3 is evolutionarily conserved. In vertebrates, GSK-3 exists as two gene paralogues, GSK-3α and GSK-3β. GSK-3β is also known to have two splice isoforms, as does the *Drosophila* GSK-3 homologue (Mukai et al., 2002) (Schaffer et al., 2003) (Wood-Kaczmar et al., 2009). Though GSK-3α and GSK-3β are structurally different, in most cases they are functionally redundant (Doble et al., 2007).

Under resting conditions, GSK-3 is a constitutively active kinase. In the presence of active signaling, GSK-3 is usually inhibited. Inhibition of GSK-3 occurs primarily by activation of the PI3K/Akt pathway leading to n-terminal phosphorylation of GSK-3α (Serine 21) or GSK-3β (Serine 9) (Cross et al., 1995) (Cross et al., 1994) (Cross et al., 1997). This inhibition is mediated by Akt (Martin et al., 2005) (Arbibe et al., 2000), PKC (Fang et al., 2002) (Ballou et al., 2001) PKB (van Weeren et al., 1998) or PKA (Fang et al., 2000) (Sheridan et al., 2002) (Tanji et al., 2002) and reviewed in (Harwood, 2001). Phosphorylation on the tyrosine residues Y216 and Y279 (in mammalian GSK-3α and GSK-3β respectively) results in enhanced GSK-3 activity but is not strictly required (Hughes et al., 1993). Along with such phosphorylation, GSK-3 activity can be regulated by other mechanisms such as subcellular localisation and interactions with protein complexes such as the destruction complex in the Wnt pathway. These protein complexes facilitate the actions of GSK-3 with specific substrates. (Jope and Johnson,

2004) (Jope and Roh, 2006) (Ali et al., 2001) (Patel and Woodgett, 2008) (Gordon and Nusse, 2006) (Logan and Nusse, 2004)

6.2.2 GSK-3 prefers pre-phosphorylated targets

GSK-3 recognises the consensus sequence "Ser/Thr – X-X-X-X – Ser_P/Thr_P" and its activity is in part controlled by the phosphorylation state of its targets. GSK-3 has been shown to have a 100-1000 fold stronger preference for pre-primed targets over unprimed substrates (Thomas et al., 1999) (Fiol et al., 1987) but typically, is not responsible for this pre-priming (reviewed in (Doble and Woodgett, 2007)). This preference for pre-phosphorylated substrates is linked to the phosphorylation of GSK-3 itself. When arginine 96 is mutated to alanine, GSK-3β loses the ability to phosphorylate preprimed proteins but not those unprimed substrates (Frame et al., 2001).

Formatted: Font: Symbol, Font color: Auto

6.2.3 GSK-3 activity is regulated by numerous pathways

GSK-3 acts in many different pathways including Wnt and insulin signaling. Its many targets include Gli, glycogen synthase, cyclin D1, tau and β–catenin (reviewed in (Frame and Cohen, 2001). Because GSK-3 is active under normal resting conditions in the cell, it is generally inactivated for signaling to proceed. In many pathways, GSK-3 acts as a negative regulator. For example, in the context of insulin signaling, GSK-3 inhibits at least two proteins. The first, a guanine nucleotide exchange factor eIF2B, is important for controlling protein synthesis while the second is glycogen synthase, preventing glucose storage (Woodgett, 1994) (Welsh et al., 1998). In the presence of insulin ligand, GSK-3 must be shut down to allow downstream activation of eIF2B and glycogen synthase. Similarly, in the absence of Wnt ligand, GSK-3 phosphorylates β–catenin, targeting it for degradation. When Wnts are active, GSK-3 is inhibited and β–catenin can move to the nucleus and act as an transcriptional activator (reviewed (Doble and Woodgett, 2003)). With roles in so many different pathways it is likely that GSK-3 activity is tightly regulated to prevent unwanted cross talk between pathways. Indeed, GSK-3 inhibition by insulin signaling does not affect the levels of nuclear β–catenin, suggesting that GSK-3 in the β–catenin destruction complex is buffered from such

inhibition. Conversely, insulin signaling appears unaffected by Wnt activation (Yuan et al., 1999) (Ding et al., 2000).

While GSK-3 roles in insulin and Wnt signaling are well-established, it may also play roles in a variety of other pathways (Frame and Cohen, 2001). Because the data for other pathways are less clear, I will not summarize them here. However, I will discuss GSK-3 roles in Hedgehog signaling in chapter 7.

6.2.4 Chemical regulation of GSK-3

A number of chemical inhibitors of GSK-3 are currently used in both a research and therapeutic capacity. The best known of these is lithium, which has been used for over 50 years to treat patients with manic depression (bipolar disorder) (Phiel and Klein, 2001) (Jope, 1999). The activity of lithium on GSK-3 is complicated. Although Li+ can very rapidly inhibit GSK-3 by competing with active-site magnesium, the therapeutic value of lithium salts is seen only after treatment for a number of weeks. This suggests either that indirect inhibition of GSK-3 may be causing the desired long-term results in patients with mood disorders (De Sarno et al., 2002) or that Li has another target which causes the appropriate relief from mood disorder symptoms. However, in an unknown mechanism, inhibitory S9 phosphorylation on GSK-3β is increased after long-term administration of lithium (De Sarno et al., 2002). It is quite possible that GSK-3 is not the direct target of lithium at doses used to treat mood disorders, rather that its inhibition is a result of some other, indirect effect.

Due to the unclear mode of action and great potential for off target effects, lithium inhibition of GSK-3 was not included in this study at all. For the chemical perturbations of GSK-3 discussed here, I used a small molecule inhibitor of GSK-3, BIO.

GSK-3 is also being explored as a potential drug target in diabetes, Alzheimer's and other diseases. In diabetes, inhibition of GSK-3 could regulate the rate at which glucose is made into glycogen in the liver. In Alzheimer's disease, hyperphosphorylation of the tau protein by GSK-3 and other kinases is thought to affect disease progression (Hernández et al., 2010). A future challenge for chemists will be to design a GSK-3 inhibitor that

selectively blocks phosphorylation of GSK-3 targets in specific pathways. While this has not yet been achieved, the current generation of compounds targeting GSK-3 are well characterised. These include inositol-phosphate phosphatases (Gould et al., 2004), paullones such as alsterpaullone (Chen et al., 2011; Leost et al., 2000; Tolle and Kunick, 2011) and 6-bromo-substituted indirubins such as BIO (Meijer et al., 2003). BIO acts as a competitive inhibitor for GSK-3 ATP-binding, preventing GSK-3 from phosphorylating any target proteins. BIO shows a high specificity for GSK-3 (IC50 = 4nM) versus similar kinases such as CDK5 (IC50 = 83nM). Therefore, BIO is used extensively in this project (Meijer et al., 2003) (Polychronopoulos et al., 2004).

6.2.5 Possible targets of GSK-3 during neural crest delamination and migration

As outlined in the introduction, Wnt signaling plays a crucial role in induction of the neural crest. GSK-3 activity is important for the proper progression of this induction; however, less is known about subsequent steps in neural crest development. In part, this is due the lack of temporal resolution using previous methods such as overexpression and knockout. It is also worth remembering that all the pathways GSK-3 plays a role (Wnt, Hedgehog, TGF-beta) have been found to be important in the development of neural crest or neural crest derived structures (discussed later). In this project I wanted to bypass earlier effects and ask what role GSK-3 may be playing in later processes such as delamination and migration of neural crest cells. GSK-3 has numerous downstream targets that may affect these events including cell cycle regulators ®-catenin and cyclin D1, substrates implicated in cell migration such as snail, and cytoskeleton regulators such as MAP1 (Frame and Cohen, 2001).

6.3 Results

6.3.1 GSK-3 activity is critical for patterning the early embryo

As demonstrated in chapters 3 and 4, proper timing of activity is crucial for correct patterning and development. The requirements for GSK-3 during gastrulation and early patterning are well established. Because later requirements are unclear, I exploited washout experiments to determine which processes required GSK-3 activity with respect to head and cartilage development.

At stage 45, a normal tadpole has mobile eyes positioned bilaterally on either side of the cranial cartilage structures in the face. The cartilages are visible through the transparent skin of the tadpole (Figure 6.1 A). As a positive control, embryos treated with BIO at the 2-cell stage were cyclopic and lost anterior facial structures Eye defects were severe, resulting in the remnant of a single eye (Figure 6.1B). These results were consisted with an early loss of anterior neural patterning, as addressed previously in Figure 4.3. In contrast, treatment with BIO from stage 12.5 – 19 caused hypoplasia of a subset of craniofacial tissues. Eyes appeared normal; however, heads were narrow and eyes were set abnormally close to the brain (Figure 6.1C). When the drug was applied at stage 19, I found that although the head was slightly narrower and shorter, the tadpoles were appropriately patterned with no obvious tissue loss (Figure 6.1D).

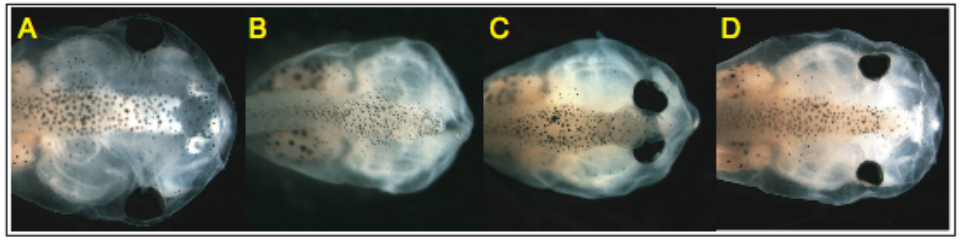

Figure 6.1 Early GSK-3 inhibition affects anterior development

(Fig 6.1A) Dorsal view of representative stage 45 tadpoles treated with carrier control or (Fig 6.1B) 15μM Bio at the 2-cell stage, (Fig 6.1C) stage 12.5 or (Fig 6.1D) stage 19. 2-cell BIO treatment resulted in severe anterior defects with a residual cyclopic eye. Close set eyes and anterior hypoplasia was observed with BIO treatment from stage 12.5. Stage 19 treatment resulted in a slightly smaller but appropriately patterned head.
(n≥70 for each condition shown).

6.3.2 Washout experiments pinpoint stages 12.5 – 16 as a critical period for GSK-3 activity

As previously described, we hypothesized that GSK-3 activity was important for some aspect of neural crest development especially as the facial structures described above rely on outgrowth of the cartilages, derived from the most anterior neural crest streams (chapter 4). To distinguish the critical stages, I performed washout experiments over a number of time points. The data from these suggested that inhibition of GSK-3 activity from stage 12.5 to 23 led to changes in the head and face. To gauge the width of the head I measured between the eyes and at the widest point in the head (schematic, Figure 6.2A). I also tried to compare the extent of facial growth by recording the length of the face from behind the eyes as well as the distance from the front of the eyes to the most anterior point (schematised in Figure 6.2B). When compared to WT and vehicle control I found that only the tadpoles treated between stages 12.5 – 23 were significantly narrower, averaging 0.4mM between the eyes and 1mM total width. This is less than half the width the controls and other treated samples, which ranged from 0.9mM-1.1mM between the eyes and 1.8mM-1.9mM total width (Figure 6.5A). This same treatment window also resulted in tadpoles that had facial truncations. By measuring from the posterior part of the eye to the anterior-most point in the face, I found that treatment from stage 12.5-23 reduced facial size by over 50%, from 0.8-0.95mM in controls to 0.6mM. The majority of the tissue was lost in the region anterior to the eye, where the dimension changed from 0.5mM in controls to 0.25mM in treated tadpoles (Figure 6.5B).

Further experiments were conducted in shorter periods during the already identified critical period of 12.5 - 23. When GSK-3 was inhibited between stages 12.5 – 14 and stages 14 – 16 the tadpoles were smaller than those treated between the stages of 16 - 19 and 19 – 23 in all the measurements taken (Figure 6.3A-C). Head size was dramatically reduced in the abbreviated treatments. The overall width of the tadpoles was reduced by 25% in the tadpoles treated between stages 12.5-14 and by 40% in the stage 14-16 treated samples. Similar changes were seen in the length of the head: approximately 25% in the 12.5-14 treatments and approximately 60% in the 14-16 treatments (Figure 6.3A). Again,

these data suggest that the critical period of activity for GSK-3 encompasses both of these treatment periods. Interestingly we noticed that there was no significant change in the width of the tailfins in the BIO treated tadpoles, though this is also a neural crest derived tissue (Figure 6.3C). In all of these experiments a minimum of 18 embryos in each condition was measured and each experiment was repeated at least three times ($n \leq 18$ per condition, per experiment).

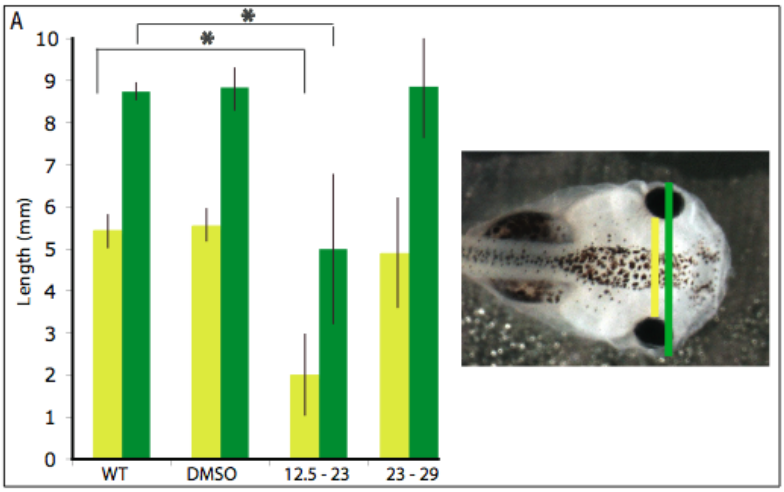

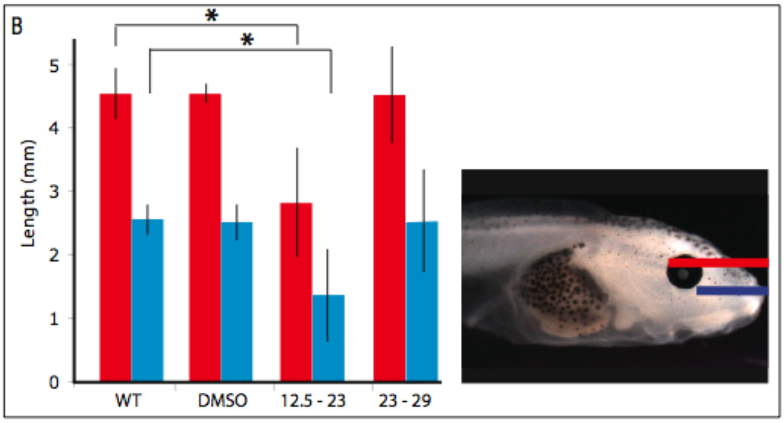

Figure 6.2 Early GSK-3 inhibition perturbs craniofacial growth

(Fig 6.2A, green and yellow lines respectively) Dimensions of the heads of stage 45 tadpoles treated with 15uM BIO between stage 12.5-23 or 23-29 were compared to untreated (WT) or DMSO treated tadpoles. (Fig 6.2A, asterisk) The width of the head at the eyes and between the eyes was measured. BIO treatment between stages 12.5-23 caused a significant reduction in head width compared to other conditions ((yellow line) p=6.15032E-07, (green line) p=1.84111E-07).
(Fig 6.2A) BIO treatment between stages 23-29 had no effect on head width compared to control embryos p=0.740917365
(Fig 6.2B, red and blue lines, respectively) Head length was measured from the anterior most point of the head to either the posterior or anterior extent of the eye.
(Fig 6.2B, asterisk) BIO treatment between stages 12.5-23 caused a significant reduction in the length of the head ((red line) p=5.09014E-06).
(Fig 6.2B) BIO treatment between stages 23-29 did not cause a reduction in head length compared to control tadpoles, p= 0.623238751, (n=12).

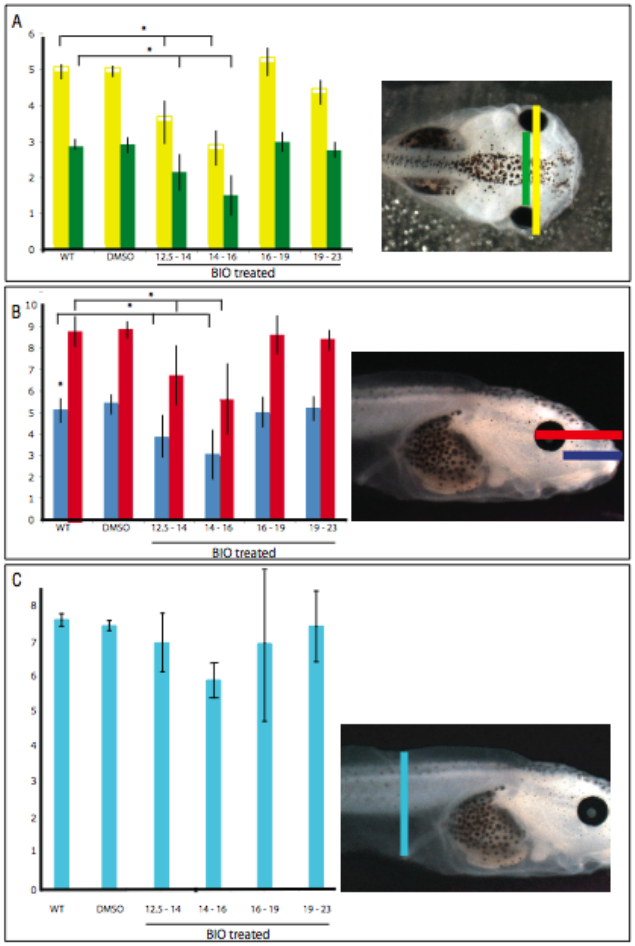

Figure 6.3 When scored at stage 45, application of BIO between stages 12.5-16 decreases tadpole size

Embryos were incubated with 15μM BIO between stages 12.5-14, 14-16, 16-19 or 19-23 and grown to stage 45. The width of the head at the level of the eyes, and the width between the eyes was measured (Figure 6.3A, yellow and green lines respectively). BIO treatment between stages 12.5-14 and 14-16 caused a significant reduction in head width ((stages 12.5-14) p=6.77488E-05, p=0.00006592 * stage 16 - 19 p=3.6403E-06, p=0.00071889).
(Figure 6.3A, asterisk). Control and BIO treatment from stage 16-19 and 19-23 showed little variation in head width, p=0.002735811 and p= 0.041964722.
(Figure 6.3A). Head length was measured from the anterior most point of the head to either the posterior or anterior extent of the eye. (Figure 6.3B, red and blue lines, respectively). BIO treatment between 12.5-14 and 14-16 significantly decreased head length ((red line) p=1.49249E-06, (blue line) p=3.4123E-08) .
(Figure 6.3B, asterisk). Tailfin depth was also measured (blue line) but no significant change was observed, p=0.0466179 (Figure 6.3C).(n=12 in all conditions shown).

6.3.3 Numerous morphological changes were found with loss of GSK-3 activity

To conclude the gross morphological analysis, we scored for other morphological changes in these tadpoles (table 6.1). Defects included loss of ear ossicles, improperly perforated mouths and in some cases loss of nasal pits. As mentioned previously, scoring melanocyte development is challenging given the variation from clutch to clutch but it was apparent that some of these tadpoles had immature, round pigment cells. However, the phenotypes most dramatically changed were those relating to the craniofacial skeleton and midline.

Treatment window	**WT**	**DMSO**	**BIO 12.5 – 14**	**BIO 14 – 16**	**BIO 16 – 19**	**BIO 19 – 23**
Ossicles visible	100	100%	50%	33%	92%	92%
Melanocytes starred	100%	100%	75%	42%	92%	92%
Nasal pits visible	100%	100%	84%	84%	92%	92%
Mouth open	100%	100%	75%	84%	92%	92%
Heart looped	100%	100%	75%	50%	92%	92%
Gut coiled	100%	100%	75%	92%	92%	92%

Table 6.1: Penetrance of phenotypic changes to the gross morphology of tadpoles treated with BIO in small time windows ($n \leq 18$, % to the closest whole number).

6.3.4 BIO–induced truncation in the anterior ventral region is evident by stage 30

Up to this point, our analysis had relied on late-stage phenotypic changes, which we examined some days after drug treatment. Clearly, it was important to identify more direct consequences of our experimental manipulations (adding BIO from stage 12.5-19). The first stage at which I could easily identify a morphological change in treated animals was stage 30 (Figure 6.8A). However it was not possible to accurately measure these changes by examining the length or width of the embryos as I had done with the stage 45 tadpoles. When I measured embryos from the cement gland to the front of the face, from the posterior branchial arch to the front of the face and the width of the head at the posterior branchial arch I found no significant changes (Figure 6.4A). Instead, using the most posterior branchial arch (stained with *twist*) as a landmark, I documented changes to the anterior ventral head by measuring the area of this region in a lateral view (Figure 6.4B-E). Consistent with the above measurements, length of face was unchanged and the anterior-posterior position of the cement gland had not shifted (Figure 6.4C-D) compared to WT (Figure 6.4B). However the area occupied by the stage 12.5 – 19 BIO treated embryos was clearly reduced in the anterior ventral region (yellow, schematic Figure 6.4E) compared to WT (dark green, Figure 6.4E) and stage 19+ BIO treated embryos (light green, Figure 6.4).

The changes to the face are not due to a simple delay in development. Had the BIO resulted in globally delayed embryos it would have been apparent in the development of the tail bud. The embryos were not delayed in their development this structure, used to age embryos as per Nieuwkoop and Faber's stages, and these were no different from the WT or DMSO treated embryos. This data is unsurprising given the relatively normal posterior embryo in the stage 45 tadpoles (see Chapter 3). The question at this point was to ask what was happening to the anterior tissues in the BIO treated embryos.

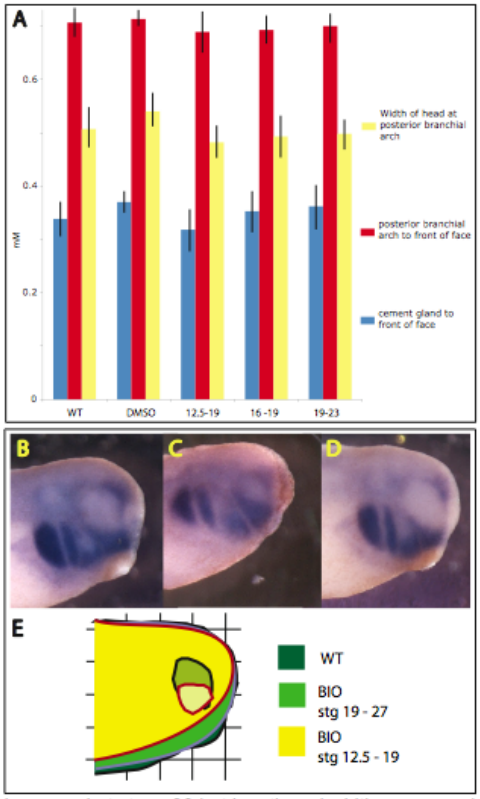

Figure 6.4 Facial changes can be scored at stage 30 but length and width are normal.

Embryos were incubated with 15uM BIO between stages 12.5-14, 14-16, 16-19 or 19-23 and grown to stage 45 and compared to WT, untreated or DMSO treated controls.
(Fig 6.4A, blue bars) The length between the cement gland and the most posterior extent of the face was unchanged in stage 30 BIO treated embryos compared to controls.
(Fig 6.4A, red bars) The length of the embryo from most posterior branchial arch to the anterior extent of the face was unchanged in BIO treated embryos compared to controls.
(Fig 6.A, yellow bars,) Embryo width was measured across the most posterior branchial arch. No significant change in embryo width was observed in BIO treated embryos compared to controls (n=12).

(Fig 6.4B-D) In order to measure the dramatic change in facial shape caused by BIO treatment, embryos were laid over a grid and the area measured. In situ hybridisation for twist stained branchial arches, used as landmarks (Fig 6.4B) in WT, (Fig 6.4C) stage 12.5 - 19 BIO treated and (Fig 6.4D) stage 19 BIO treated. The area from the most posterior branchial arch was measured using a grid and are schematised in Fig 6.4E. WT, dark green BIO 19+ light green, BIO 12.5 - 19 yellow. (n=12).

6.3.5 Inhibition of GSK-3 between stages 12.5 – 19 does not affect neural crest induction

As discussed earlier, one possibility is that treatment with a GSK-3 inhibitor results in inhibition of neural crest induction. To address this, I examined expression of the neural crest marker *slug* expression in embryos treated at stage 9 (during neural crest induction) and stage 12.5. *Slug* is the earliest identified gene expressed in the neural crest (Mayor et al., 1995) (Nieto et al., 1994). Indeed, treatment at stage 9 resulted in a very slight reduction in the lateral and posterior domains of the *slug* expression (Figure 6.5B) compared to WT (Figure 6.5A). In the stage 12.5 treated embryos this posterior reduction was not present and the slug expression appears as normal (Figure 6.5D) when compared to WT (Figure 6.5C). These data suggest that indeed, GSK-3 activity is required for neural crest induction but that by stage 12.5, the window of sensitivity for loss of induction has past.

6.3.6 GSK-3 inhibition does not perturb anterior-posterior patterning

Another possibility is that changes to the anterior-posterior patterning of the neural plate because of altered Wnt signaling resulted in the posteriorization of the anterior neural plate. First, I examined markers for early eye development. The eye field is highly sensitive to any loss of anterior identity and I would predict that if GSK-3 inhibition posteriorized the embryo, expression of eye field markers would be lost (van de Water et al., 2001). While the addition of BIO at stage 12.5 results in a midline defect, cyclopia is only seen in 10% of the tadpoles treated in this time window; the remaining 90% have close-set eyes (see Figure 6.1). Cyclopia has been proposed to be due to loss of the anterior midline. Because the majority of these animals had two eyes, it is unlikely that we have lost anterior or midline identity in these treatments (Durston et al., 1989) (Sampath et al., 1998) (Chiang et al., 1996) (Schier et al., 1996). To confirm that the eye field was dividing appropriately I examined the expression *pax6, six3* and *otx2* (Figure 6.9C-E). Pax6 is expressed in the eye field from stage 12, by stage 15 the expression is segregating and by stage 19 is clearly located in two distinct regions (Figure 6.5E-F). The BIO treated embryos have two distinct fields of expression (Figure 6.5G). *Six3*

expression is unchanged in the BIO treatment (Figure 6.5J) compared to WT and controls (Figure 6.5H-I) as is otx2 expression (Figure 6.5K-M). Therefore, while the later stage tadpoles clearly have close-set eyes, the initial eye field develops appropriately.

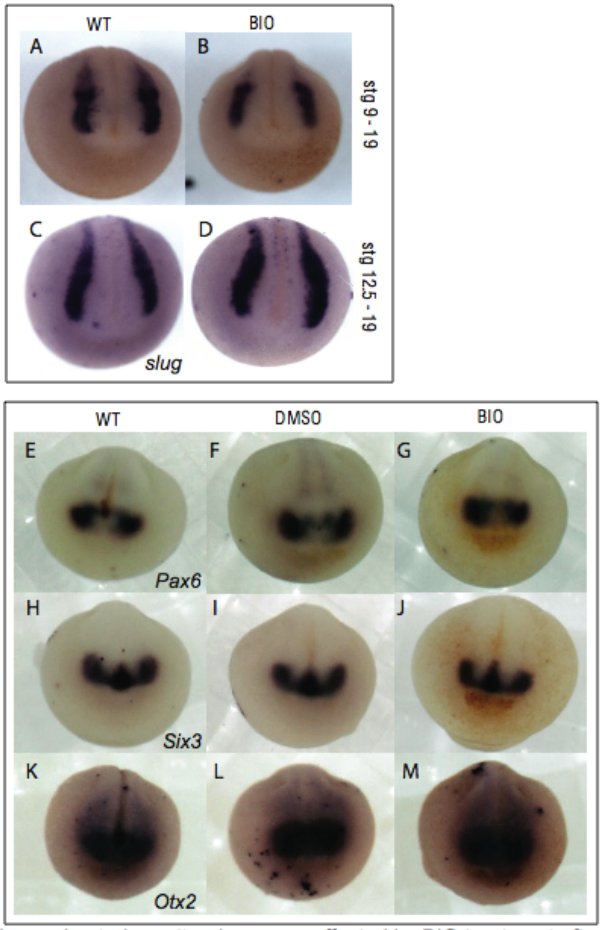

Figure 6.5 NC induction and anterior patterning are unaffected by BIO treatment after stage 12.5

(Fig 6.5A-B) Embryos were incubated in 15μM BIO between stages 9-19 or (Fig 6.5E-M) stages 12.5 - 19. In situ hybridisation was performed against slug, pax6, six3 and otx2.
(Fig 6.5A-B) Slug expression was very slightly reduced in embryos incubated at stage 9 (Fig 6.5B) compared to controls (Fig 6.5A) but not those treated at stage 12.5 (Fig 6.5D) compared to control treated (Fig 6.5C).
(Fig 6.5G,J & M) Pax6, six3 and otx2 were unchanged in embryos treated with BIO between stages 12.5 - 19 compared to WT (Fig 6.5E, H & K) or control treated (Fig 6.5F, I & L).
(n≥25 for each condition shown).

6.3.7 Anterior changes are due to a delay in neural crest migration

Combined, the lack of changes to the induced neural crest at stage 19 along with the normal development of the eye field suggests that anterior – posterior patterning is not changed in these embryos. Based on phenotypes described above, I postulated that the induction of the neural crest was not lost and that the anterior identity was unchanged. Alterations in a number of processes could be causing the phenotype. The neural crest cells might not be delaminating, their migration into the face might be perturbed or the cells are might not be differentiating into cartilage.

I examined *twist* expression, which marks migratory neural crest cells in embryos treated with BIO (stage 12.5 – 19) and fixed at stage 19, 23, and 30. In all the stages examined *twist* expression was found to be less extensive (Figure 6.6). At stage 19, there was a clear delay in the NCCs migrating out of the neural tube in the BIO treated embryos (Figure 6.6C) when compared to controls (Figure 6.6A-B). This continued in the embryos examined at stage 23 (Figure 6.6F). Each of the neural crest streams was affected and all appeared reduced. By stage 26, though cells in the anterior-most stream of NCCs are found surrounding the eye, there is clear reduction in the amount of staining in the streams (Figure 6.6I).

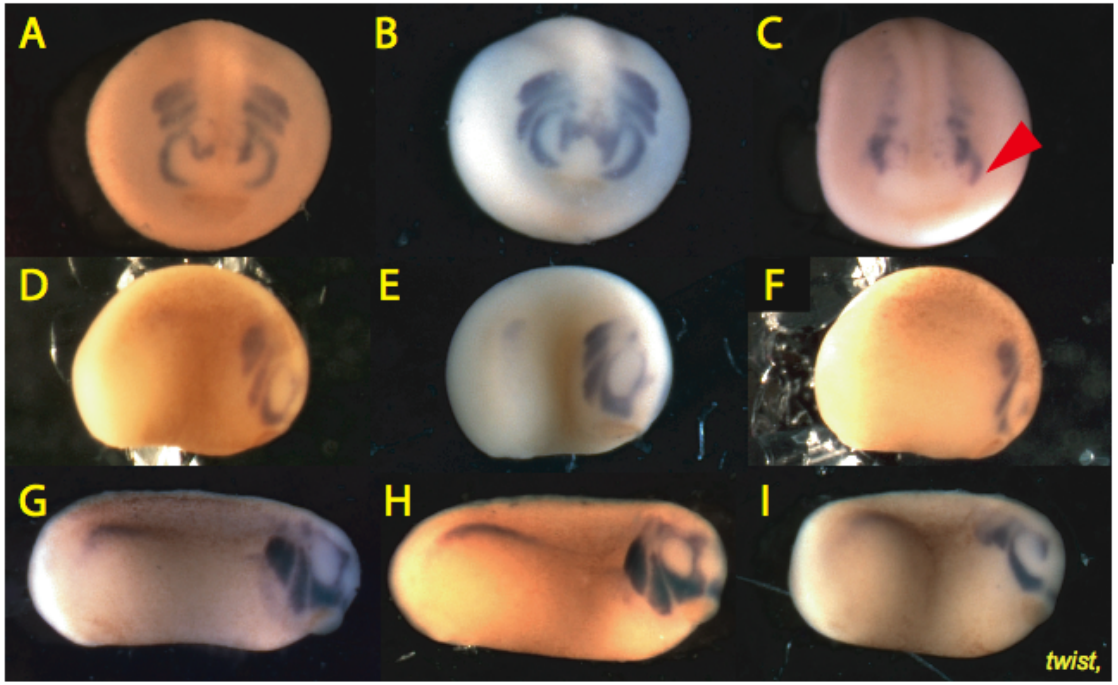

Figure 6.6 Stage 12.5-19 BIO treatments perturb neural crest migration.

Fig 6.6A-C shows frontal views of twist expression at stage 19, whereas Fig 6.6D-F and G-I shows saggital aspects at stages 23 and 26 respectively.
Embryos were incubated in 15μM BIO between stages 12.5-19. At stage 19 BIO treated embryos express twist with migration (red arrow-head, Fig 6.6C) but it was obviously retarded when compared to WT (Fig 6.6A) or DMSO control (Fig 6.6B).
By stage 23 the neural crest cells in the controls have migrated out in 3 clear streams and can be seen in the branchial arches and around the eyes (Fig 6.6D-F). BIO treated embryos have perturbed migration and there is less migratory crest staining (Fig 6.6F).
This continues at stage 26 (Fig 6.6I) compared to WT (Fig 6.6G) and DMSO control (Fig 6.6H).
(n≥35 for each condition shown).

6.3.8 Anterior defects correlate with a very specific loss in Sox9 expression

Sox9 is expressed from about stage 14 in the developing neural crest . It continues to be expressed throughout delamination and migration of the neural crest, becoming localised to the cranial cartilages (O'Donnell et al., 2006). The expression of *sox9* is critical for cartilage formation. When *sox9* expression is lost in the neural crest, cartilage development is perturbed, resulting in malformed cranial cartilages (Spokony et al., 2002).

At stage 26, *sox9* is strongly expressed in the developing otic placode, the eye and the brain along with the migrating neural crest of the WT and control embryos (Figure 6.7A-B). In the BIO treated tadpoles, sox9 expression is slightly weaker in the eye and developing otic placode but is almost entirely lost in the neural crest (Figure 6.7C). By stage 33 this was even more apparent. The control embryos have *Sox9* expression in stripes in the branchial arches (the gill cartilages will arise from this tissue) and very strong staining surrounding the eye and through the brain (Figure 6.7D-E). In the BIO treated embryos expression in the branchial arches is weaker, but present (Figure 6.7F). At stage 36 we can see clearly that the staining in the most posterior branchial arches of the BIO treated tadpoles has recovered (Figure 6.7I) and is comparable to the WT and control (Figure 6.7G-H). Contrast this with the staining that should be in the anterior regions beneath and above the cement gland. These regions are not developed and tissue is absent (Figure 6.7I). In a dorsal view of the stage 36 head it is very clear where the BIO treated tadpoles are dramatically affected (Figure 6.7L). The red arrow points out the sox9 expression in ventro-anterior to the forebrain and above the cement gland. In the control tadpoles this expression is evident but in the BIO treated tadpoles, this domain does not express *Sox9*. Furthermore, the cartilages associated with these regions are the same as those that were lost in the stage 45 tadpoles, consistent with our previous analysis. Based on these data, we believe that GSK-3 is required for maintenance of anterior migratory neural crest. Selective loss of GSK-3 activity then leads to an associated loss of ventral facial structures in the tadpole.

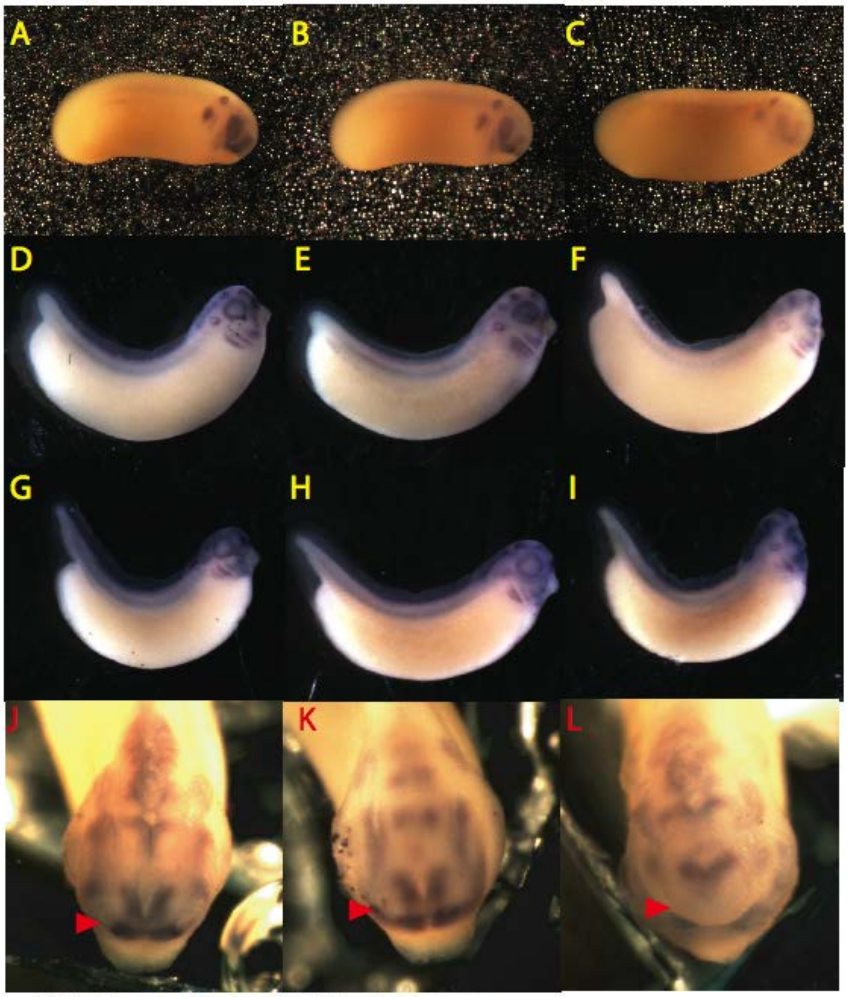

Figure 6.7 Anterior sox9 is lost in BIO treated tadpoles.

Representative stage 23, 33 and 36 (Fig 6.7A-C, D-F and G-I, respectively) probed for sox9 expression after control or 15μM BIO treatment from stage 12.5-19.
BIO treatment caused severe reduction in anterior sox9 expression compared to WT and DMSO treated controls in stage 23 (Fig 6.7C, A and B, respectively), 33 (Fig 6.7F, D and E, respectively) and 36 tadpoles (Fig 6.7 G&J, H&K, and I&L, respectively) (n≥9 for all conditions shown)
Dorso-anterior views of stage 36 tadpoles show severe anterior defects in sox9 expression in BIO treated embryos compared to controls (Fig 6.7J, 6.7K-L, red arrowheads). (n=9).

6.3.9 Identification of full length GSK-3α

One of the challenges of using a small molecule is the possibility that the phenotype examined is an artifact generated by off target effects. In order to confirm that the phenotype I was seeing was consistent with a loss of GSK-3 activity, I needed to compare BIO treatment with another knockdown method. To do this, I wanted to design morpholino oligonucleotides (MOs) to reduce *Xenopus laevis* GSK-3 protein. Although both GSK-3α and GSK-3β were initially identified in 1995 (He et al., 1995), the complete GSK-3α cDNA had not been reported. Therefore, we set out to identify full-length GSK-3⟨. An expressed sequence tag (EST) clone, which contained the cDNA, was identified (AccNo: BA364215). Comparison to *Xenopus laevis* GSK-3® and to the genomic sequence of GSK-3⟨ from *Xenopus tropicalis* confirmed a full-length insert for the cDNA sequence for *X laevis* GSK-3⟨ (Figure 6.8)

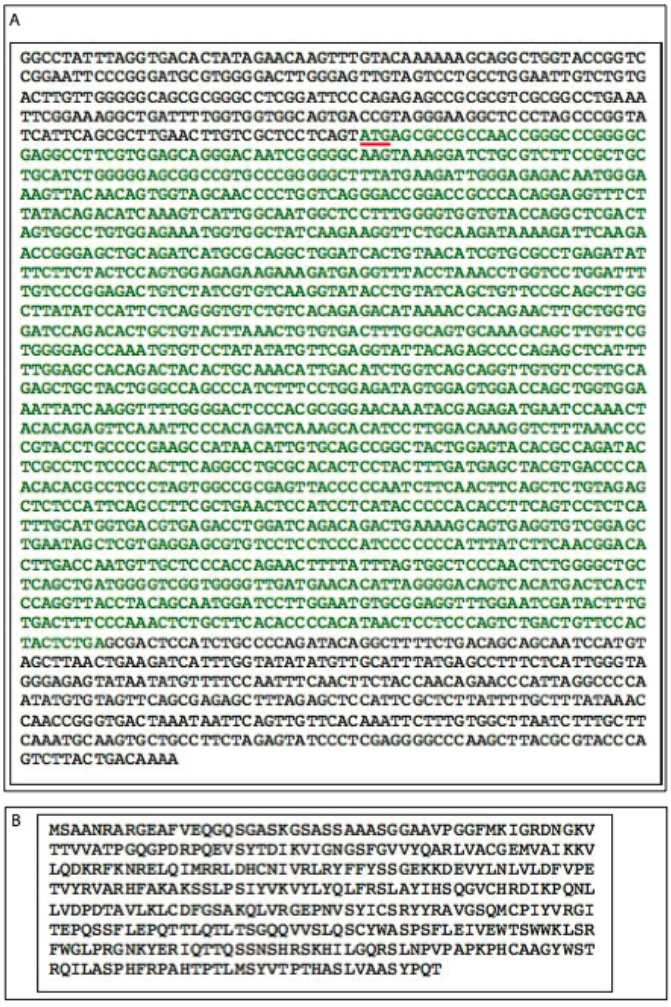

Figure 6.8 Identification of Xenopus GSK-3α
GSK-3α was identified in an expressed sequence tag (EST) clone (AccNo: BA364215) and the 1215 nucleotide coding region identified (Green, Fig 6.8A) The start site ATG is underlined in red. The translated protein sequence is shown (Fig 6.8B).

The coding region (in green, Figure 6.8) is 1215 nucleotides long. Our data included 268 nucleotides of 5'UTR and 361 nucleotides of 3'UTR. Along with sequence alignments, a phylogenetic tree of human, mouse, zebrafish, *Xenopus laevis* and *Xenopus tropicalis* GSK-3α and GSK-3β was generated. It showed that the clone identified was closely related to the GSK-3〈 in the other species, more closely related to GSK-3® (Figure 6.9). Using NCBI alignment tools, I found that in *X. laevis* the sequence identity between GSK-3〈 and GSK-3® is 69%. The overall amino acid similarity between GSK-3〈 and GSK-3® is 72.5%. As expected, the similarity in the kinase domain is much higher than outside the kinase domain (96%, schematised in Figure 6.8). Also conserved is the inhibitory serine at position 21 (red arrows, schematic Figure 6.10) The conserved activating tyrosine is be predicted at to be at position 233, based on the canonical phosphorylation motif "VSYIC" (green arrows, schematic Figure 6.10).

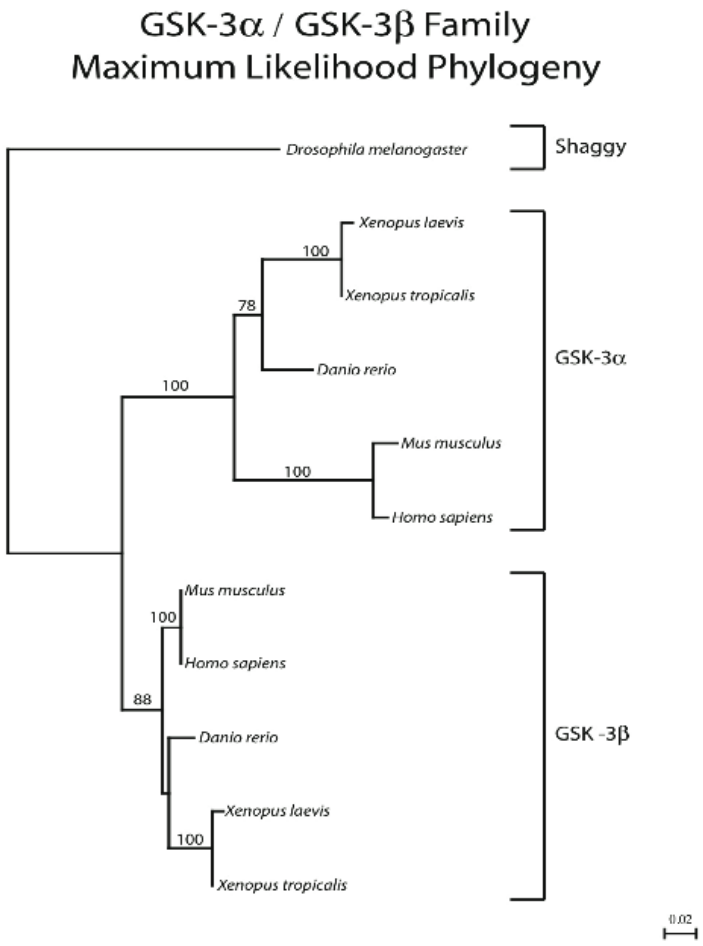

Figure 6.9 Phylogenetic tree of human, mouse, zebrafish, Xenopus laevis and Xenopus tropicalis GSK-3α and GSK-3β protein sequences.

GSK-3α protein sequences from the above species are more closely related to each other than GSK-3β of the same species. GSK-3 family tree was generated from 333 amino acid characters. Tree was reconstructed with PHYML v. 2.4.4. using the JTT substitution matrix with rates across sites modeled on a discrete gamma distribution modeled using 4 categories of variable sites and no categories of invariable sites (alpha parameter =0.216). Numbers above nodes are PHYML bootstrap values generated from 100 bootstrapped replicates using the same parameters. Courtesy of Matthew B Rogers.

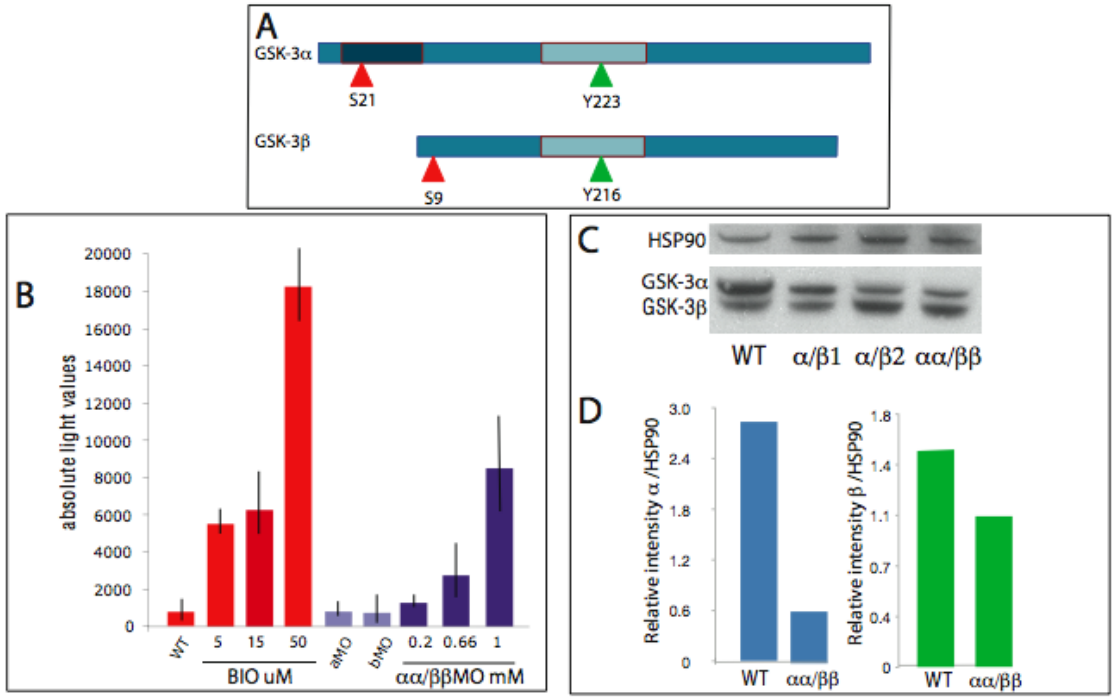

Figure 6.10 Characterisation of GSK-3 and it's activity

Schematic of X. laevis GSK-3a and GSK-3b (Fig 6.10A). Inhibitory serines are shown in red and activating tyrosines in green. Embryos injected at the 2-cell stage with 100pg Supertopflash (STF) were incubated with 5μM, 15μM or 50μM BIO for 24 hours. Luciferase activity was assayed. BIO treatment caused a dose dependent increase in luciferase activity (red bars, Fig 6.10B) (n=21).

Embryos co-injected with 100pg STF and GSK3α and GSK3β MOs, individually or in combination at 1mM, 0.66mM or 0.2mM. After 24 hours luciferase activity was not changed upon GSK3α or β MO alone. Co-injection of GSK3α and β MO's increased luciferease activity in a dose dependent manner after 24-hours (blue bars, Fig 6.10B) (n=21).

Mo specificity was tested by Western blot against GSK3α and β antibodies (Fig 6.10C). 1mM injection of set 1 α/β MO's, or set 2 α/β MO's or all four MO's showed reduced GSK3α and β protein levels compared to uninjected control, relative to HSP90 loading. Quantification of relative intensity of GSK3α or β over HSP90 loading control (Fig 6.10D) shows that GSK3β protein is more effectively reduced by the injection of αα/ββ MO. (n=9).

Based on the sequence analysis in Figure 6.9, I designed two MOs targeting GSK-3α, one blocking the translational start site and another based on a putative intron-exon boundary (determined by alignment with Xenopus tropicalis GSK-3α). Morpholino oligonucleotides act to knock down gene function by preventing the proper translation of a protein from mRNA. They can do this in one of two ways, by interfering with the binding of the ribosome to the mRNA sequence at the start codon or by preventing the splicing of introns from the mRNA. Such misplaced mRNA is then not translated into protein (Draper et al., 2001; Heasman, 2002).

A MO targeting the start site in GSK-3® had been previously described (Onai et al., 2004). I also designed a GSK-3β splice-blocking MO. In order to assay the amount of GSK-3 protein in animals injected with MO, we performed western blot analysis (Figure 6.10B). We found that the 1mM injection of MO's resulted in a small reduction of GSK-3 on the western blot. Injections of a higher concentration were lethal to the developing embryo, suggesting that any more complete knock down of GSK-3 function was not compatible with life. Shown in Figure 6.10B are western blots on protein lysates from 3 embryos. The embryos were collected and lysed together in order to reduce any embryo variability. In embryos injected with all four MOs (labeled αα/ββMO) we can clearly see that the GSK-3α knockdown was more effective than GSK-3β, relative to loading control, HSP90 (Figure 6.10C).

6.3.10 Treatment with BIO and GSK-3 MOs have comparable effects

At this point, I wanted to compare the effect of BIO and morpholino oligonucleotides on a Wnt responsive luciferase reporter, SuperTOPFLASH (STF) (Mikels and Nusse, 2006). This reporter contains multiple β–catenin dependent TCF/LEF binding sites driving expression of the firefly luciferase gene. This allows a quantitative assessment of Wnt/β–catenin activity under various conditions. STF was injected into both cells of 2-cell stage embryos and these were treated with various concentrations of BIO or co-injected with combinations of GSK-3α and GSK-3β MOs (Figure 6.10A). The embryos were cultured until stage 14 when they were lysed for luciferase assays. Embryos were lysed in pools of 3 and a minimum of 9 pools used in each experiment. I showed that BIO increased STF activity dramatically (in red, Figure 6.10). Increasing

concentrations of BIO increased this response. At the highest doses (50uM) BIO incubations produced a massive response but killed the embryos within a few days. In MO treated embryos we can clearly see that inhibition of either GSK-3α or GSK-3β alone does not affect reporter activity (in navy, Figure 6.10). However, combining GSK-3α and GSK-3β MOs produced a significant dose dependent induction of the reporter. Therefore, inhibition of both genes is required to activate Wnt/b-catenin signaling. In fact, the use of two α morpholinos and two β morpholinos was found to result in the most profound phenotype.

To confirm that BIO's effects on cartilage are due to loss of GSK-3 activity, I used the MO's to examine the cartilage development in tadpoles where GSK-3 activity has been lost in the anterior of the embryo. MO knockdowns did indeed perturb cartilage development. MO's were injected unilaterally into the anterior of a 4-cell embryo. These morphants were grown to stage 45 and examined for changes to cranial cartilages (schematised, Figure 6.11D). I found that in both the α/β set 1 and the αα/ββ MO injected tadpoles the craniofacial cartilages have been reduced, when compared to the control tadpoles (Figure 6.11A). In the tadpoles injected with a single set of MOs Meckel's cartilage and the palatoquadrate were reduced (Figure 6.11B). The cartilages are catastrophically disrupted in tadpoles injected with both sets of MO (αα/ββ) (Figure 6.11C). On the injected side, marked with a red star, most of the tissue is lost, of the anterior cartilages only a portion of the parahyoid on the non-injected side can be seen (yellow *, Figure 6.11C) and the cartilages surrounding the ear ossicle (red star, Figure 6.11).

6.4 Discussion and Conclusions

In this chapter, I have shown that GSK-3 has a role for patterning of the very anterior neural crest and that when GSK-3 activity is inhibited this anterior tissue is lost, resulting in dramatic and specific changes to the craniofacial cartilages. To some extent, this is not surprising, as Wnt activation had already been implicated in early development. Indeed, early knockdown of GSK-3 activity (2-cell treatments) are reminiscent of *dkk-1* knockdown mutants (Glinka et al., 1998). In the *dkk-1* mutant embryos Wnt inhibition in the anterior is lost and subsequently the head structures are lost. What is more intriguing is the requirement of GSK-3 activity during periods of neural crest migration. This had not been previously characterized, in part because injection of mRNA or MOs does not allow that level of temporal refinement, and also because conditional mouse mutants have not previously been available. In fact, in the majority of experiments in this chapter, I used BIO exclusively to inhibit GSK-3 activity, because it was technically impossible to do these experiments using the MOs.

Specificity of the treatments

To confirm that BIO treatment and MO injections are targeting Wnt/β-catenin signaling, I used a TCF/LEF responsive luciferase reporter. High levels of inhibition were toxic, suggesting that loss of GSK-3 activity results in catastrophic consequences during embryonic development. Indeed, knockout of both GSK-3 genes in the mouse leads to preimplantation lethality.

Using intermediate doses of BIO and/or the MOs, we can assume that we are achieving a partial knockdown of GSK-3 activity. In this way, we can learn which processes or regions in the embryo are more sensitive to the loss of GSK-3. It is also possible that subcellularly, GSK-3 sequestration changes its drug accessibility. In fact it is known that protein interactions (such as those in the destruction complex) and cellular localisation (such as leading edge of growth cone) are important regulators of GSK-3 activity (Green, 2004) (Dominguez and Green, 2001) (Dominguez and Green, 2000) (Sun et al., 2009). Thus, it is not inconceivable to imagine then that BIO is prohibited from acting on certain GSK-3 molecules at the expense of others depending on their binding and location. I think the very dramatic increase in luciferase activity in the 50uM treated samples compared to the limited changes between the 15uM and 5uM

treated samples supports this idea. Perhaps cytosolic GSK-3 or GSK-3 in other complexes is more readily available while GSK-3 in the Wnt destruction complex (with axin and APC) is only accessible at higher concentrations.

What is GSK-3 doing in the neural crest?

GSK-3 may have a number of roles in neural crest development between stages 12.5 – 19. The absence of strong changes to *slug* expression suggest that induction of the neural crest is unaffected, supporting the hypothesis that the phenotype is caused by delayed EMT or delayed migration. Instead, GSK-3 activity is important in regulating the delamination and migration of neural crest. Several GSK-3 phosphorylation targets are important in neural crest delamination and migration including cyclin D1, ®-catenin, TCF and snail/slug (Alt et al., 2000) (van Noort and Clevers, 2002) (Doble and Woodgett, 2003) (Burstyn-Cohen et al., 2004) (Zhou et al., 2004) (Zhou and Hung, 2005) (Doble and Woodgett, 2007). Cyclin D1, a protein required for progression of the cell cycle from G1 to S phase, is a direct target of GSK-3. Phosphorylation by GSK-3 leads to the relocalisation and degradation of cyclin D1 during S phase (Diehl et al., 1997). Inhibition of GSK-3 results in stabilisation and nuclear accumulation of cyclin D1 (Alt et al., 2000).

GSK-3 may also phosphorylate multiple targets during epithelial to mesenchymal transitions (EMT). In epithelial cells, E-cadherin is down regulated during EMT. ®-catenin, another direct target of GSK-3 phosphorylation, acts as a repressor of E-cadherin transcription (Doble and Woodgett, 2007). A second target, Snail, is a zinc-finger transcription factor that represses E-cadherin expression. Snail is also required for delamination. Phosphorylation by GSK-3 results in the nuclear export of snail and its degradation (Ko et al., 2007). Combined, these data suggest that GSK-3 is critical for EMT consistent with the observed delay in delamination. These events take place during the treatment window I describe and would result in the reported changes to *sox9*.

Along with a possible role in delamination GSK-3 may also have a role in regulating cell migration (Eickholt et al., 2002). GSK-3 has been shown to be important in regulating neuronal responses to slit and robo during neuronal migration; therefore it is possible that GSK-3 has a similar role in neural crest migration. During neuronal migration,

inactive GSK-3 is specifically maintained in the growth cone of neurons (Owen and Gordon-Weeks, 2003). Antagonists of GSK-3 have been shown to inhibit sema3 dependent collapse of neuronal growth cones suggesting that tight regulation of active/inactive GSK-3 localisation is required for neuron outgrowth (Eickholt et al., 2002). Although migrating neural crest cells do not have a growth cone they have an active protrusion (Jesuthasan, 1996). It is unknown whether GSK-3 behaves similarly at this active protrusion in neural crest. However, if GSK-3 inhibition perturbed migration of the neural crest, I would have expected to see phenotypes in the tadpoles treated from stage 19 onwards. As this was not the case, it seems unlikely that phenotypes observed were due to the effect of GSK-3 activity on these putative cell protrusions.

The *Sox-9* phenotype is very dramatic. It is well documented that Sox-9 is required for cartilage development and is expressed in procartilagenous tissue. There is a clear correlation between loss of anterior *Sox-9* positive tissues with the later loss of cartilage. As I clearly highlighted, this change in *Sox-9* expressing cells precedes a change in the anterior growth of the face and occurs after the reduction in *twist* positive cells migrating into the anterior face. As such, I believe that the later cartilage defect is due to an absence of tissue derived from the anterior most streams of neural crest. To this regard, I have overlooked the possible role for GSK-3 in regulating TGF-beta in craniofacial cartilage development (Guo et al., 2008; Ito et al., 2002). While it has been shown that GSK-3 has a role in the regulation of TGF-beta signalling, TGF is required during the later stages of cartilage development, chondrogenesis (Guo et al., 2008). I believe that the phenotype I have described here is different as the key window for GSK-3 requirement is too early for our experiments to have been directly perturbing chondrogenesis.

This chapter has outlined for us a requirement for GSK-3 in facial development. Having identified this loss of tissue the question remains, what signaling pathways could be responsible? We have not addressed signals regulating GSK-3 in this context. In part, this is due to an assumption that GSK-3 roles in the early embryo are primarily regulating Wnt signal transduction. However, as described in the introduction, GSK-3 plays pivotal roles in multiple signaling pathways. The following chapter addresses the challenges of deciphering potential roles for GSK-3 in the Hedgehog pathway, which others and I have shown to be critical for proper development of the head structures.

7 A ROLE FOR GSK-3 IN VERTEBRATE HEDGEHOG SIGNALING

7.1 Summary

GSK-3, introduced in the previous chapter, is a highly promiscuous kinase that has the potential to play key regulatory roles in many signaling pathways. One such pathway is the Hedgehog (Hh) signaling pathway. In *Drosophila*, the Kruppel-like transcription factor Cubitus interruptus (Ci) is phosphorylated by the GSK-3 homologue shaggy leading to Ci degradation. This is a key step in the negative regulation of Hh signaling (Jia et al., 2002) (Price and Kalderon, 2002). It is unclear whether phosphorylation of Ci by GSK-3 leads to a similar role in vertebrates. In vertebrates the single *Ci* gene has diverged into three homologues (*Gli1, Gli2 and Gli3*). These proteins have different roles in modulation of the pathway and are differentially processed. Therefore, regulation of protein activity and stability is more complex. Many aspects, including the role of GSK-3 activity, are still unclear. Our lab is currently using several approaches, such as biochemical analysis, activity assays and mouse genetics to address these issues.

At the protein level, *Xenopus* is the ideal model for testing the activity and processing of Gli proteins in response to GSK-3 modulation. By combining mRNA injection (Gli over-expression) and BIO treatment (GSK-3 inhibition), I am able to demonstrate a requirement for GSK-3 in reduction of Gli activity. When GSK-3 is inhibited by BIO, I see a dose dependent increase in Gli reporter responses as well as phenotypic readouts such as epithelial tumours.

The data in this chapter are preliminary and comprise a small portion of a collaborative project. However, our results are novel and interesting. Therefore, I will describe the background evidence and provide an analysis of the current work. Necessary experiments and future work will be considered in the discussion.

7.2 Introduction

In the previous chapter I outlined the role for GSK-3 in the development of the anterior cartilages of the face. I showed that GSK-3 activity is essential for proper migration of the *twist* positive neural crest cells and for expression of *Sox-9* in the pre-cartilaginous tissue. In this chapter I will ask how levels of GSK-3 activity affect Gli function.

7.2.1 Hh signal transduction and GSK-3

An overview of Hh signaling was presented in the introduction. Here I examine the evidence suggesting that GSK-3 may have a role in modulating signaling downstream of Hh. In Hedgehog signaling, there are two distinct forms of Ci: a full-length activator that is 155kD and a 75kD truncated repressor that lacks the c-terminal domain (Aza-Blanc et al., 1997). In *Drosophila*, the two different forms have distinct roles. For example, in the wing disc, a short repressor form is important in the anterior domain where it blocks the expression of a subset of Hh-responsive genes (Méthot and Basler, 1999). In cells near the anterior-posterior boundary, the presence of Hh ligand inhibits Ci processing allowing full length Ci to translocate to the nucleus. Here it acts as a transcriptional activator driving expression of Hh target genes such as *patched* and *engrailed* (Méthot and Basler, 1999)

The truncation of Ci requires that the full-length protein be phosphorylated, a process that involves multiple kinases. Loss of the cAMP-dependent protein kinase A (PKA) is important in the proteolytic processing of Ci. PKA loss of function mutants have constitutively active Hh signaling (Pan and Rubin, 1995) (Li et al., 1995) (Lepage et al., 1995) (Jiang and Struhl, 1995). PKA phosphorylates serine and threonine residues on the C-terminal end of Ci and this phosphorylation is essential for further processing (Wang and Holmgren, 1999) (Chen et al., 1999) (Price and Kalderon, 2002).

More recently two other kinases have been suggested to act in the Hh pathway; GSK-3 and casein kinase 1 (Jia et al., 2002) (Price and Kalderon, 2002). *In vitro* biochemical evidence suggests that GSK-3 can phosphorylate Ci. Inhibition of GSK-3 activity using

LiCl reduced the levels of Ci phosphorylation in embryonic extracts and in cell culture (Klein and Melton, 1996) (Price and Kalderon, 2002) (Jia et al., 2002).

In vivo, Jia et al. also showed that *sgg* mutants have mild Hh overactivation phenotypes including an accumulation of Ci-155, increased and mislocalised expression of Hh responsive genes, and anterior wing duplication. Furthermore, loss of *suppressor of fused* (*Sufu*), a negative regulator of Hh signaling, further exacerbated the *sgg* phenotypes (see Figure 1.4). Therefore, phosphorylation of Ci by shaggy appears to inhibit Ci function leading to an increase in hedgehog activity (Jia et al., 2002) (Price and Kalderon, 2002).

In vertebrates, Hh signals are mediated by three Gli orthologues: Gli1, Gli2 and Gli3. To further complicate matters, each Gli is regulated differently. Unlike Ci, which is cleaved from an activator form to a shorter repressor form, Gli1 does not contain a repressor domain and is therefore only able to act as an activator of Hh signaling (Dai et al., 1999). In contrast, Gli2 can be cleaved to the repressor form *in vitro;* however, this process is highly inefficient, suggesting that *in vivo* the vast majority of Gli2 activity is as an activator (Pan et al., 2006). Instead, Gli2 appears to be highly regulated by degradation. In unstimulated cells, phosphorylation of Gli2 is dependent on PKA and other kinases (Pan et al., 2006). Hedgehog signal inhibits this degradation and allows Gli2 to translocate to the nucleus and induce transcription (Nguyen et al., 2005) (Bai et al., 2004; Lei et al., 2004). Finally, Gli3 is very efficiently processed and is usually found *in vivo* as a truncated repressor. Indeed Gli3 does not rescue Gli2 function when expressed in the Gli2 locus (Bai et al., 2004). In addition, alteration of any one of the six putative PKA sites in Gli3 completely blocks its processing in cell culture, suggesting that this Gli3 processing requires extensive phosphorylation at multiple sites (Wang et al. 2000).

Mutations in the different *Gli* genes also demonstrate their functional divergence. Gli1 was originally isolated from gliomas and is upregulated in many cancers including basal cell carcinoma (BCC) (Altaba et al.). Targeted over expression of Gli1 in the *Xenopus* ectoderm causes epithelial tumours, suggesting that Gli1 activity is sufficient to for tumorigenesis (Dahmane et al., 1997). However, mice with homozygous *Gli1* mutations appear normal, suggesting that *Gli1* is not required for normal development (Park et al., 2000). Both *Gli2* and *Gli3* are required for embryonic development. Loss of Gli2 results in an array of developmental problems, with neural tube defects evident

by e10.5, while Gli3 mutants display by polydactyly and exencephaly (Hui and Joyner, 1993).

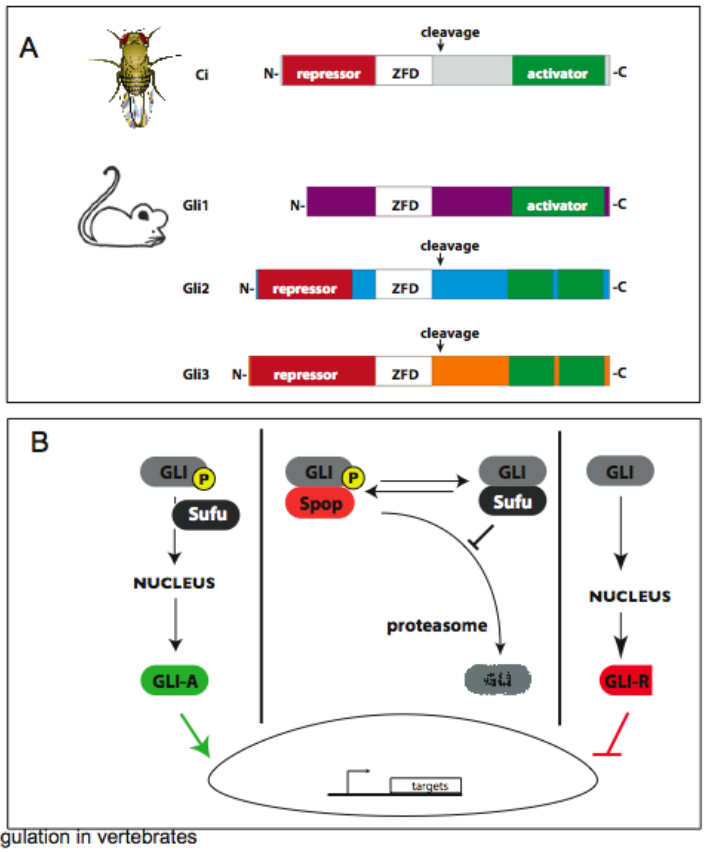

Figure 7.1 Gli regulation in vertebrates

Intracellular Hh signaling is mediated by cubitus interuptus (Ci) in drosophila and one of three Gli genes in vertebrates (Fig 7.1A). Ci contains both an activator and repressor region (green and red respectively). Vertebrate Gli1 (shown in purple, Fig 7.1A) does not contain a repressor region and acts as a transcriptional activator. Gli2 (shown in blue, Fig 7.1A) contains both activator and repressor regions but mainly functions as transcriptional activator. Gli3 (shown in orange, Fig 7.1A) acts mainly as a repressor of transcriptional signaling. In the absence of Hh ligand ptc inhibits smo, preventing activation of hedgehog signaling. Gli is phosphorylated by glycogen synthase kinase (GSK-3), protein kinase A (PKA) and protein kinase CK1 (CK1). The results in the cleavage of Gli3 into a repressor form which enters the nucleus and inhibits Hh target gene expression (orange circle, Fig 7.2B).
Intracellularly, in the presence of Hh ligand, full length Gli1/2 interacts with suppressor of fused (SuFu), is phosphorylated and can translocate to the nucleus where it activates downstream transcription of targets including patched1 or gli1. Further regulation of Gli activity involves its interaction with Spop which targets Gli for proteosomal degradation. This degradation can be inhibited by SuFu. Gli2 is heavily regulated in this way.

In addition to playing critical roles during development, Hedgehog dysregulation is also associated with adult cancers such as basal cell carcinoma (BCC, reviewed in (Daya-Grosjean and Couvé-Privat, 2005)). BCC is a slow growing form of skin cancer that starts in the epidermis, which expresses *Shh* (Bitgood and McMahon, 1995; Chiang et al., 1999). BCCs are the most common skin cancer, making up 75% of all diagnosed cases and affecting 750,000 people in the US each year (Epstein, 2008). Though most BCCs occur spontaneously, in almost all cases they arise from ectopic activation of Hh signaling. This may be due to Smo-activating mutations (Xie et al., 1998) (Lam et al., 1999), inactivation of Ptch (Gailani et al., 1996) or in other proteins in the pathway such as SuFu (Reifenberger et al., 2005). In *Xenopus*, overexpression of Gli1 mRNA causes epithelial tumours (Dahmane et al., 1997). This activity can be used to assay the effects of GSK-3 inhibition on Gli activity in *Xenopus*.

7.3 Results

7.3.1 Inhibition of GSK-3 increases Gli-dependent reporter activity

If GSK-3 is indeed an important regulator of vertebrate Hedgehog signaling, we should see a change in Gli-dependent transcriptional activation in response to BIO treatment. To do this, I used a Gli responsive luciferase reporter (GliBS, figure 7.2). Embryos were injected in both cells at the 2-cell stage with GliBS. As a positive control, we first tested this reporter activity in the presence of cyclopamine and purmorphamine, which inhibit and activate Hedgehog signaling respectively. As predicted, cyclopamine reduced the luciferase response while purmorphamine increased it in stage 14 embryos ($p < 0.05$, Figure 7.2A). At 5μM, 15μM and 50μM, BIO treatment resulted in a dose-dependent increase in Gli-responsive luciferase activity, an almost 3-fold increase when embryos were incubated with 50μM BIO ($p < 0.05$, Figure 7.2A).

7.3.1.1 Kinetics of Hedgehog response to BIO

As described in the introduction, the Hedgehog pathway autoregulates by activating expression a feedback inhibitor, *patched* (Kalderon, 2000) (Taipale et al., 2002) (Rohatgi and Scott, 2007). This suggests that early activation of Hh signal transduction, seen at stage 14 above, might lead to loss of Hh target genes several stages later. Therefore, I treated embryos from stages 12.5 – 19 with BIO and examined *ptc-2* expression at stages 19 and 21. Indeed, I found that expression of *ptc-2* at stage 21 was strongly reduced through the neural tube (Figure 7.2C, n=6) compared to controls (Figure 7.2A-B, n=4 & 5 respectively). Expression in the very anterior region (presumptive eye field) is less perturbed. Hedgehog also controls expression of the ligand *Shh*. Again, I found that expression this target gene was reduced in response to BIO treatment (Figure 7.2 E-G) Taken together, these data suggest that initially, BIO treatment leads to an activation of Hedgehog signal transduction; feedback via the repressor Ptc leads to a subsequent loss of Hedgehog dependent genes. As mentioned, this data is preliminary so in order to fully quantify this response RT PCR is required to determine the actual changes in expression of Gli responsive genes at both time points.

However it should be noted that Hh signaling is present and active in the embryo by stage 14 so the different response at stage 14 and stage 21 are not due to the absence of Hh at the earlier stage (discussed further, Figure 7.5).

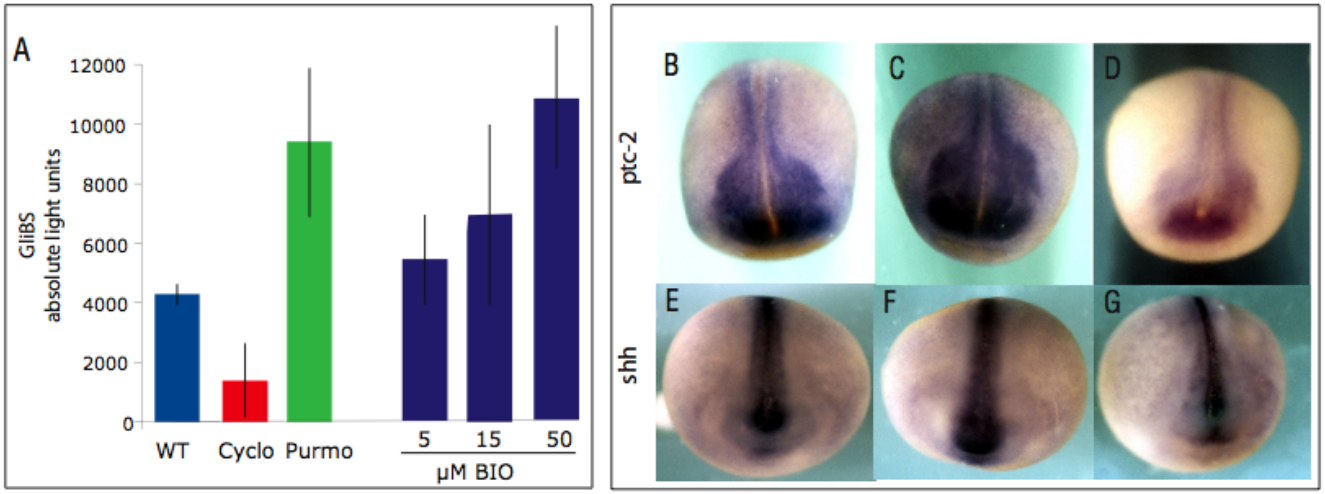

Figure 7.2 Inhibition of GSK-3 leads to an early increase in Hh signaling, followed by a loss of Hh

(Fig 7.2A) Embryos were injected with 100pg GliBS-luciferase DNA at the 2-cell stage. Embryos were then treated with the indicated small molecules, grown to stage 14, lysed in pools of 3 (at least 9 pools) then assayed for luciferase activity (n=27).
250μM cyclopamine treatment from the 2-cell stage decreased luciferase activity compared to controls. Increased luciferase activity was observed in response to 100μM purmorphamine compared to controls. Luciferase activity increased in a dose dependent manner in embryo lysates treated with 5, 15 and 50μM BIO.
Embryos treated with 15μM BIO from stages 12.5 - 19 were collected at stage 21. In situ hybridisation against patched-2 (ptc-2) and sonic hedgehog (shh) were performed. Ptc-2 expression at stage 21 was reduced in the BIO treated embryos (Fig 7.2D) compared to WT (Fig 7.2B) and DMSO controls (Fig 7.2C). Shh expression was down regulated at stage 21 (Fig 7.2G) compared to controls (7.2E-F). (n≥21 in all conditions shown).

7.3.2 GSK-3 inhibition increases Gli activator function

As mentioned previously, ectopic hedgehog signaling causes BCCs. Similarly, injections of 2ng *Gli* mRNA targeted to the ectoderm resulted in tumour formation in most embryos (Dahmane et al., 1997). This provides a useful *in vivo* assay for Gli activity. To test for modulation of Gli activity I injected *Gli* mRNAs at subphenotypic levels (0.5ng). I could then culture with or without BIO at stage 9 and score for the presence of tumours, which can be identified as raised, darkened lumps on the injected flank of the embryo (see red arrows, Figure 7.3). I found that in all cases inhibition of GSK-3 increased the number of tumours, suggesting an increase in Gli activity. This was most obvious with Gli1 overexpression where over 80% of the injected BIO treated embryos developed tumours compared to 20% of the control embryos (Figure 7.3D, graphed, red columns). Similar results were seen with Gli2 overexpression with 50% developing tumours after BIO treatment compared to 15% in controls (Figure 7.3F, graphed in blue). Gli3 has been reported to cause tumours in this assay. We did observe similar effects with Gli3; however, the phenotype was comparatively weak, with only 30% induction after BIO incubation and less than 15% in controls (Figure 7.3H, green columns).

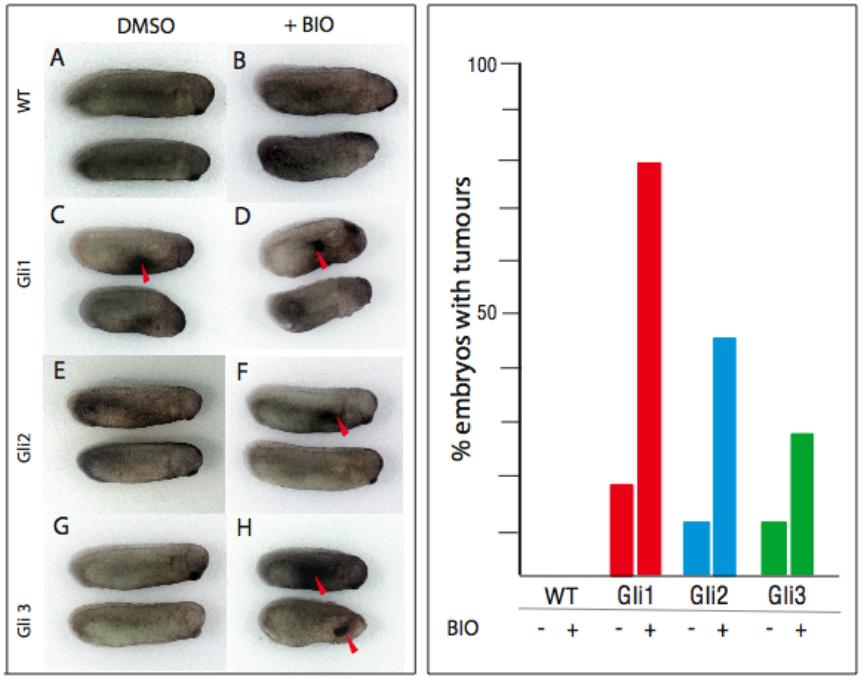

Figure 7.3 GSK3 inhibition exacerbates Gli induced ectodermal tumours

Embryos were injected with 0.5ug Gli1 (Fig 7.3 C-D), Gli 2 (Fig 7.3 E-F) or Gli 3 (Fig 7.3 G-H) mRNA into the animal pole at the 2 cell stage and treated with 15uM BIO (B,D,F&H) or carrier control from stage 9.
Tumours, defined as dark, raised and bumpy growths on the ectoderm, were observed in embryos injected with Gli1, 2 and 3 mRNA with or without BIO treatment (red arrowheads, Fig 7.3C, D, F and H).
No tumours were seen on embryos treated only with BIO (Fig 7.3B). In the absence of BIO, Gli1, 2 and 3 mRNA injection caused tumours in 20%, 15% and 15% of embryos, respectively (Fig 7.3D,F, H).
15μM BIO treatment increased the incidence of tumours in Gli1, 2 and 3 mRNA injected embryos to 80%, 45% and 30%, respectively (Fig 7.3I). (n≥14 in all conditions shown).

7.3.3 At cleavage stages, GSK-3 activity is required to repress Gli induced dorsalisation

For many decades, *Xenopus* has been a powerful tool for studying early axial patterning. Common phenotypes include ultraviolet irradiation induced ventralisation, which leads to a loss of the dorsal organiser and lithium-induced hyperdorsalisation, which results in embryos with expanded cement glands and enlarged eyes. To easily score these phenotypes, Kao and Elinson (1988) developed a dorsoanterior index (DAI), ranging from 0 (ventralised) to 10 (dorsalised) (simplified in Figure 7.4, (Kao and Elinson, 1988)).

Over expression of Gli mRNAs has not been reported to affect initial dorsal-ventral patterning of the early embryo. Early inhibition of GSK-3 by LiCl from (32-128 cell stages) strongly dorsalises embryos, resulting in phenotypes scoring 9 or 10 on the dorsoanterior index (DAI) (Cooke and Smith, 1988). Although BIO also inhibits GSK-3, we never see much dorsalisation at the concentrations used (Figure 7.4). This could be due to the doses used in our treatments, or to a different mode of drug action.

To my surprise, Gli overexpression followed by early GSK-3 inhibition (at the 8-cell stage) resulted in severely hyperdorsalised animals (Figure 7.4D,F&H)', DAI phenotypes scored in 7.4I). Neither individual treatment led to such dramatic phenotypes (Figure 7.4A-B).

Clearly GSK-3 is required for dampening the Wnt signaling in the embryo (Dominguez and Green, 2000). It is possible that these DAI phenotypes were due to expansion of the dorsal identity via upregulation of Wnt. Indeed, I have previously shown that treatment with BIO induced β–catenin dependent STF activity, suggesting that Wnt signaling is upregulated in these treatments (Figure 6.3A). However, our BIO alone controls were, at best, mildly dorsalised (Figure 7.4A-B).

A second possibility is that increasing Hedgehog activity leads to hyperdorsalisation. However, we have also never observed these phenotypes when using Hedgehog modulators, either loss of function (cyclopamine), or gain of function (purmorphamine) (Chapter 5). This suggests that modulation of the Hedgehog pathway at the receptor level is insufficient for dorsalisation during cleavage stages,

possibly due to a lack of endogenous Hh signal transduction. As a result, exogenous Gli is required to induce this dorsalisation activity. To address this, I compiled published microarray data on expression levels of Hedgehog pathway genes (Figure 7.5). Consistent with my hypothesis, most of these genes are not expressed prior to gastrulation. *Sonic hedgehog* and *desert hedgehog* are expressed at very low levels until stage 10 when there is a sharp increase (green and purple, Figure 7.5). *Indian hedgehog* is not turned on until neurulation (yellow, Figure 7.5). The *Gli* genes maintain the same trend. The only gene that is expressed at high levels from fertilisation is the negative regulator *Ptc1*, supporting the idea that Hh signaling must be kept off prior to gastrulation.

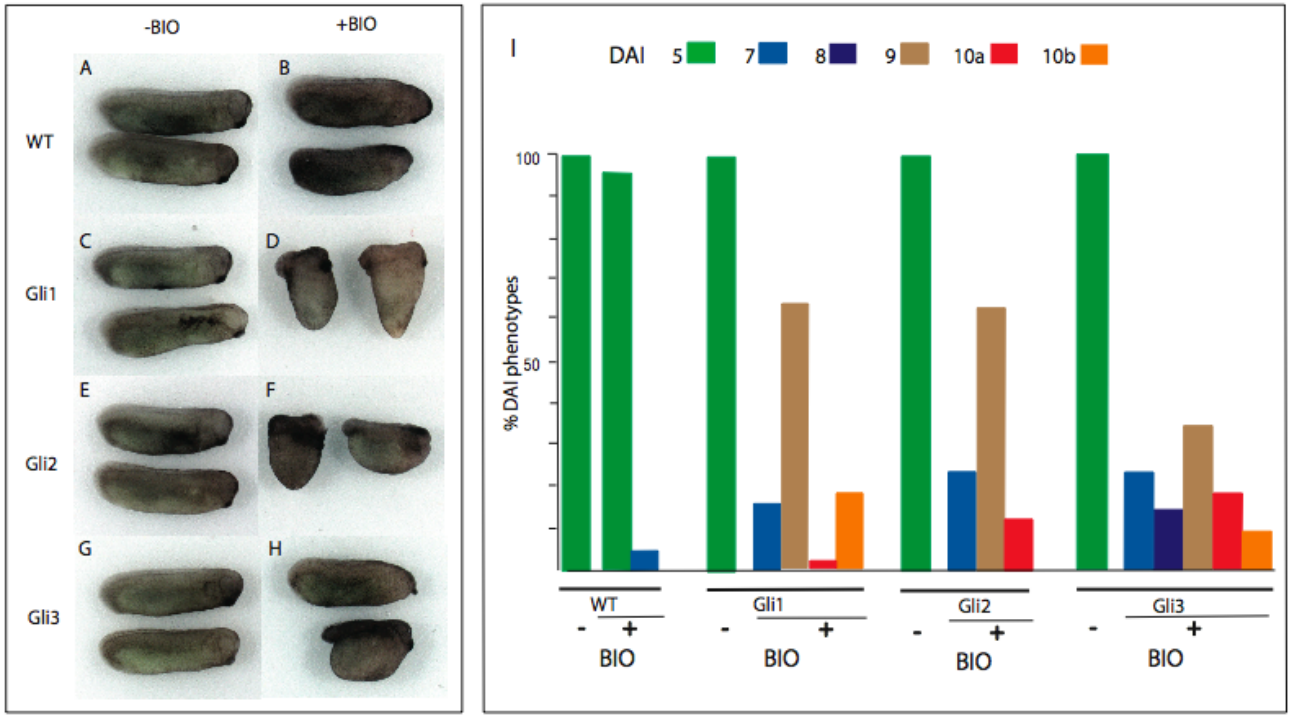

Figure 7.4 Inhibition of GSK-3 from 8cell stage in Gli over expressing embryos causes severe dorsoanterior transformations

Embryos injected at the 2-cell stages with 0.5ug Gli1 (Fig 7.4C-D), Gli 2 (Fig 7.E-F) or Gli 3 (Fig 7.4G-H) mRNA and treated with 15μM BIO at the 8-cell stage (Fig 7.4 B,D,F,H).
Embryos were allowed to develop to free swimming tadpole stage when they were scored for dorsoanterior defects. DAI phenotypes were noted in all Gli o/e + BIO treated tadpoles (Fig 7.4 D,F &H).
No dorsoanterior phenotypes were found in Gli o/e (Fig 7.4B). 5% of BIO treated tadpoles had mild DAI phenotypes (Fig 7.4B & I).
100% of BIO treated + Gli injected embryos (Fig 7.4I). (n≥21 in all treatments, % pooled from 3 experiments).

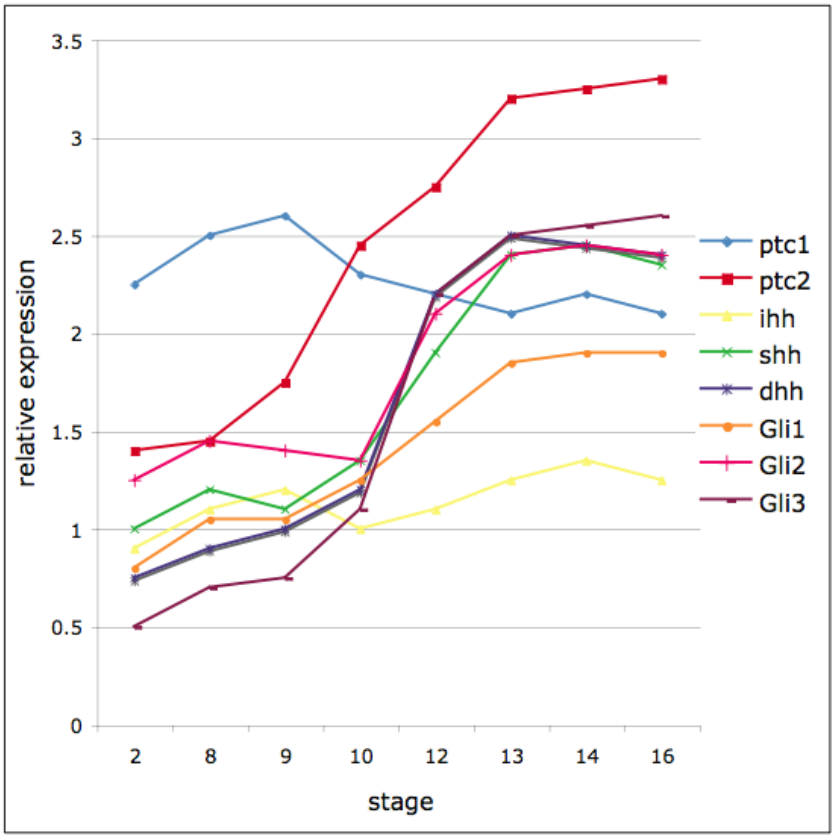

Figure 7.5 Expression profiles of Hh genes in Xenopus leavis

Published microarray data {Yanai, 2011, p04532} was collected for common Hh genes in the gastrulating embryo between stages 2 and 16. Expression of sonic hedgehog (shh) and desert hedgehog (dhh) (green and purple, respectively) is low before stage 10 and increases sharply thereafter. Indian hedgehog (Ihh) (yellow) is expressed at low levels between stages 2-16. Gli1-3 (orange, pink and maroon, respectively) are also expressed at low levels before stage 9/10 and increase thereafter. Relative levels of Ihh, dhh and Gli1, 2 and 3 are expressed at similar levels after stage 10. Patched-1 and -2 (ptc1 and 2) (Blue and red, respectively) is more highly expressed than other Hh components. Ptc1 is highly expressed between stages 2 and 16, whereas Ptc-2 increases steadily.

Discussion and conclusion

Though preliminary, my data suggest that GSK-3 can modulate the Hedgehog pathway in vertebrates. Inhibition of GSK-3 causes an increase in Hh activity at both the transcriptional level and in Hh-dependent assays, such as induction of epithelial tumours. This chapter also demonstrates a previously unknown ability of GSK-3 to dampen Hh signaling in the early embryo, which may or may not be required endogenously. As this project is ongoing, I will outline the current conclusions and some future work for this project.

GSK-3 may have a role in controlling the cleavage of Gli from activator to repressor form in the absence of Hh ligand. Increased Gli-responsive signaling in the presence of BIO suggests that inhibition of GSK-3 does result in more activator Glis. The effect of BIO on the individual Gli proteins is less clear. Phenotypically, all three Gli proteins demonstrated increased "activator" function (in the form of epithelial masses) following BIO incubation. In the case of Gli2, which is most similar to Ci, GSK-3 should be regulating cleavage and degradation kinetics. When GSK-3 is inhibited, increased activity could be attributed to an increase in stable Gli2 protein. Similarly, in the case of Gli3, which is usually cleaved to a stable repressor form, GSK-3 inhibition may lead to some accumulation of full-length activator Gli3. However, as Gli1 is not normally cleaved to a short repressor form, GSK-3-dependent cleavage may not explain this increased activity. I hypothesize that GSK-3 may regulate stability of full-length activator Gli1.

First, I will examine expression of Gli responsive genes by quantitative RT-PCR and by comparing GliBS reporter activity. I will also compare the effects of Gli overexpression in embryos response to BIO versus proteosome inhibitors. I would predict that if the increase in Gli activity in the presence of BIO was due to decreased degradation, I would be able to phenocopy this in embryos treated with a proteosome inhibitor. We should then be able to distinguish this from an increase in Gli activity due to decreased processing.

A second interesting question that arises from my data is the possibility of temporal changes in GSK-3-dependent Hh signaling. As the Hh pathway autoregulates through

patched expression, it is possible that in a 24hour experiment, such as those described in this chapter, immediate transcriptional changes will have been overlooked. To explore this further, I will confirm the kinetics of GliBS activation in response Gli proteins +/- BIO. To do this, I am examining immediate responses (one to three hours after BIO treatment) and compare to long-term responses (16 hours). I could further separate primary and secondary responses using a translational inhibitor such as cycloheximide.

Finally, it would be important to acknowledge that the DAI phenotypes typically arise with excess Wnt. Here I show that severe DAI phenotypes are induced with early GSK-3 inhibition in the presence of ectopic Gli. We could use this system to ask whether Hh is acting upstream of Wnt in this case or whether Hh signaling is capable of disrupting early patterning directly.

8 FINAL SUMMARY

My thesis is a study of temporal requirements for signaling pathways in development using the *Xenopus laevis* tadpole. To do this, I began by designing a pilot screen to test these signaling pathways in development of neural crest derived structures or craniofacial features. This screen then led me to identify previously unknown molecular requirements in several interesting biological processes: Hh in the development of the primary mouth, and GSK-3 in the patterning of the anterior cranial cartilages. Finally, I show preliminary experiments uncovering novel crosstalk between GSK-3 and Hedgehog signaling.

I described the use of *Xenopus* tadpoles as an *in vivo* chemical biology assay. This method has many advantages and we can learn much from using small molecules in this way. In combination with transgenic technology, such as GFP reporter animals, or overexpression assays, this could be a very powerful system. As an assay for craniofacial development, I think *Xenopus* has shown itself to be a useful developmental model. However, it has not been as possible to scale-up this project as intended. I had hoped that this type of screen could be performed using many hundreds if not thousands of chemicals. I believe the initial set up (embryos into dishes with timed application of drug) would be relatively straightforward. However there are a number of limitations.

Firstly, each individual well needs to be kept rigorously clean so that the tadpoles can survive for the 7+ days it takes to reach feeding stages. In the treatments where drugs are applied for short periods of time and washed out, this does not pose too much of a problem as a complete solution change occurs at twice in the culture. In the experiments where incubation was for a longer period, for example in the 2 cell onwards treatments, embryos were cultured in the same media for a prolonged period of time and required twice daily monitoring to remove any dead embryos.

Secondly, as the tadpoles grow, over crowding becomes more of an issue. In fact, I found that a maximum of 10 tadpoles per well in a 12 well plate developed successfully. When embryos were cultured in 24 well plates, up to 3 embryos would grow to stage 45. I did not find that the 48 well plates were compatible with culture to that late stage. By the late

stage 30's, even with only one individual per well, the embryos were dying. It may be possible that *Xenopus tropicalis*, smaller than *X. laevis*, could do better in the smaller wells to a later stage but that was beyond the scope of this project.

Finally, because of the 3D nature of the stage 45 tadpoles, I believe that automated analysis of the *in situ* results or of the Alcian Blue cartilage staining or of the immunohistochemistry is not feasible at this point. As such, all scoring of phenotypes would be done manually. In my opinion this would limit the screen to fewer than 200 drugs in order to allow the researcher time to score the various phenotypes of interest. Despite these limitations I think that if the small molecules were selected carefully then this type of screen can generate vast quantities of data, which is not so readily attainable in other systems. Perhaps if a smaller number of time points were chosen it would simplify the expansion of the screen and allow for refinement based on positive readouts as determined by the tissue or pathway of interest.

These screens are quite data intensive. Even in the small screen I carried out two novel phenotypes were identified. The first shows a previously unidentified role for Hedgehog signaling in regulating the perforation and size of the primary mouth in *Xenopus*. I show that decreases in the levels of Hedgehog signaling reduce the size of the mouth and that increases expand the mouth dramatically. This is true until after stage 28, highlighting the late plasticity of this structure. Increased Hedgehog signal causes early contact between the ectoderm and endoderm, resulting in premature loss of basal lamina identity. Loss of Hedgehog alters cell shape in the endoderm and delays/inhibits perforation of the mouth.

The second novel discovery is a narrow temporal requirement for GSK-3 signaling in the very anterior embryo that is essential for proper development of the craniofacial cartilages. GSK-3 inhibition during neurula stages perturbs neural crest cell migration, most strongly in the anterior. These changes to neural crest cell migration result in a loss of *sox9* positive tissue and subsequent hypoplasia of the anterior cartilages, the infrarostral cartilage, Meckel's cartilage and the palatoquadrate. This work proved very interesting and it would be quite possible to pursue it with the MO tools we designed and more targeted injections. However, the lab has, after many years of breeding, developed extensive mouse lines that provide a better tool to ask the more targeted questions of

'what role is GSK-3 playing in the delamination and migration of the neural crest'. A number of experiments that we discussed and determined to have value for this project, may be carried out by another student. In these, conditional knockouts plus both GSK-3 mutants can be used to target specific tissues in the development of the murine NC. This project would likely have been too expensive to do without the support from the preliminary data from the *Xenopus* screen.

Finally, as part of a larger collaborative project in our lab, I show that inhibition of GSK-3 in *Xenopus* increases Gli-responsive luciferase activity and increases the number of Gli induced "tumours". This chapter also highlights further advantages to *Xenopus* as a model organism: how simple alterations in experimental design (addition of drug at an early time point, 8-cell stage, or later time point, stage 8) can be used to ask drastically different questions. This project is ongoing so I have suggested some future work. Taken together with other work from the lab, these data should shed further light on potential roles of GSK-3 in the context of vertebrate Hedgehog signaling and Gli processing.

9 REFERENCES

Abreu, J. G., Ketpura, N. I., Reversade, B. and De Robertis, E. M. (2002). Connective-tissue growth factor (CTGF) modulates cell signalling by BMP and TGF-beta. In *Nat Cell Biol*, vol. 4 (ed., pp. 599-604.

Abzhanov, A., Tzahor, E., Lassar, A. B. and Tabin, C. J. (2003). Dissimilar regulation of cell differentiation in mesencephalic (cranial) and sacral (trunk) neural crest cells in vitro. *Development* **130**, 4567-79.

Ahlgren, S. and Bronner-Fraser, M. (1999). Inhibition of sonic hedgehog signaling in vivo results in craniofacial neural crest cell death. *Curr Biol* **9**, 1304-14.

Alexandre, C., Jacinto, A. and Ingham, P. W. (1996). Transcriptional activation of hedgehog target genes in Drosophila is mediated directly by the cubitus interruptus protein, a member of the GLI family of zinc finger DNA-binding proteins. *Genes Dev* **10**, 2003-13.

Alfandari, D., Cousin, H., Gaultier, A., Smith, K., White, J. M., Darribère, T. and DeSimone, D. W. (2001). Xenopus ADAM 13 is a metalloprotease required for cranial neural crest-cell migration. In *Curr Biol*, vol. 11 (ed., pp. 918-30.

Ali, A., Hoeflich, K. P. and Woodgett, J. R. (2001). Glycogen synthase kinase-3: properties, functions, and regulation. *Chem Rev* **101**, 2527-40.

Alt, J. R., Cleveland, J. L., Hannink, M. and Diehl, J. A. (2000). Phosphorylation-dependent regulation of cyclin D1 nuclear export and cyclin D1-dependent cellular transformation. *Genes Dev* **14**, 3102-14.

Anderson, K. V. (2000). Finding the genes that direct mammalian development : ENU mutagenesis in the mouse. *Trends Genet* **16**, 99-102.

Andrésson, T. and Ruderman, J. V. (1998). The kinase Eg2 is a component of the Xenopus oocyte progesterone-activated signaling pathway. *EMBO J* **17**, 5627-37.

Arbibe, L., Mira, J. P., Teusch, N., Kline, L., Guha, M., Mackman, N., Godowski, P. J., Ulevitch, R. J. and Knaus, U. G. (2000). Toll-like receptor 2-mediated NF-kappa B activation requires a Rac1-dependent pathway. *Nat Immunol* **1**, 533-40.

Aybar, M., Glavic, A. and Mayor, R. (2002). Extracellular signals, cell interactions and transcription factors involved in the induction of the neural crest cells. *Biol Res* **35**, 267-75.

Aza-Blanc, P., Ramírez-Weber, F. A., Laget, M. P., Schwartz, C. and Kornberg, T. B. (1997). Proteolysis that is inhibited by hedgehog targets Cubitus interruptus protein to the nucleus and converts it to a repressor. *Cell* **89**, 1043-53.

Bachiller, D., Klingensmith, J., Kemp, C., Belo, J. A., Anderson, R. M., May, S. R., McMahon, J. A., McMahon, A. P., Harland, R. M., Rossant, J. et al. (2000). The organizer factors Chordin and Noggin are required for mouse forebrain development. In *Nature*, vol. 403 (ed., pp. 658-61.

Bachler, M. and Neubüser, A. (2001). Expression of members of the Fgf family and their receptors during midfacial development. *Mech Dev* **100**, 313-6.

Bai, C. B., Stephen, D. and Joyner, A. L. (2004). All mouse ventral spinal cord patterning by hedgehog is Gli dependent and involves an activator function of Gli3. *Dev Cell* **6**, 103-15.

Ballou, L. M., Tian, P. Y., Lin, H. Y., Jiang, Y. P. and Lin, R. Z. (2001). Dual regulation of glycogen synthase kinase-3beta by the alpha1A-adrenergic receptor. *J Biol Chem* **276**, 40910-6.
Baltzinger, M., Ori, M., Pasqualetti, M., Nardi, I. and Rijli, F. M. (2005). Hoxa2 knockdown in Xenopus results in hyoid to mandibular homeosis. *Dev Dyn* **234**, 858-67.
Beachy, P. A., Cooper, M. K., Young, K. E., von Kessler, D. P., Park, W. J., Hall, T. M., Leahy, D. J. and Porter, J. A. (1997). Multiple roles of cholesterol in hedgehog protein biogenesis and signaling. *Cold Spring Harb Symp Quant Biol* **62**, 191-204.
Birgbauer, E., Sechrist, J., Bronner-Fraser, M. and Fraser, S. (1995). Rhombomeric origin and rostrocaudal reassortment of neural crest cells revealed by intravital microscopy. *Development* **121**, 935-45.
Bitgood, M. J. and McMahon, A. P. (1995). Hedgehog and Bmp genes are coexpressed at many diverse sites of cell-cell interaction in the mouse embryo. *Dev Biol* **172**, 126-38.
Bonstein, L., Elias, S. and Frank, D. (1998). Paraxial-fated mesoderm is required for neural crest induction in Xenopus embryos. *Dev Biol* **193**, 156-68.
Brault, V., Moore, R., Kutsch, S., Ishibashi, M., Rowitch, D. H., McMahon, A. P., Sommer, L., Boussadia, O. and Kemler, R. (2001). Inactivation of the beta-catenin gene by Wnt1-Cre-mediated deletion results in dramatic brain malformation and failure of craniofacial development. *Development* **128**, 1253-64.
Briscoe, J. (2004). Hedgehog signaling: measuring ligand concentrations with receptor ratios. *Curr Biol* **14**, R889-91.
Briscoe, J., Chen, Y., Jessell, T. M. and Struhl, G. (2001). A hedgehog-insensitive form of patched provides evidence for direct long-range morphogen activity of sonic hedgehog in the neural tube. *Mol Cell* **7**, 1279-91.
Brito, J. M., Teillet, M.-A. and Le Douarin, N. M. (2006). An early role for sonic hedgehog from foregut endoderm in jaw development: ensuring neural crest cell survival. *Proc Natl Acad Sci USA* **103**, 11607-12.
Brugmann, S. A., Cordero, D. R. and Helms, J. A. (2010). Craniofacial ciliopathies: A new classification for craniofacial disorders. *Am J Med Genet A* **152A**, 2995-3006.
Bürglin, T. R. and Kuwabara, P. E. (2006). Homologs of the Hh signalling network in C. elegans. *WormBook*, 1-14.
Burns, A. J. and Douarin, N. M. (1998). The sacral neural crest contributes neurons and glia to the post-umbilical gut: spatiotemporal analysis of the development of the enteric nervous system. *Development* **125**, 4335-47.
Burstyn-Cohen, T., Stanleigh, J., Sela-Donenfeld, D. and Kalcheim, C. (2004). Canonical Wnt activity regulates trunk neural crest delamination linking BMP/noggin signaling with G1/S transition. *Development* **131**, 5327-39.
Cabrera, C. V., Alonso, M. C., Johnston, P., Phillips, R. G. and Lawrence, P. A. (1987). Phenocopies induced with antisense RNA identify the wingless gene. *Cell* **50**, 659-63.
Calloni, G., Glavieux-Pardanaud, C., Le Douarin, N. and Dupin, E. (2007). Sonic Hedgehog promotes the development of multipotent neural crest progenitors endowed with both mesenchymal and neural potentials. *Proc Natl Acad Sci USA* **104**, 19879-84.
Carmona-Fontaine, C., Acuña, G., Ellwanger, K., Niehrs, C. and Mayor, R. (2007). Neural crests are actively precluded from the anterior neural fold by a novel inhibitory

mechanism dependent on Dickkopf1 secreted by the prechordal mesoderm. *Dev Biol* **309**, 208-21.
Carmona-Fontaine, C., Theveneau, E., Tzekou, A., Tada, M., Woods, M., Page, K. M., Parsons, M., Lambris, J. D. and Mayor, R. (2011). Complement fragment C3a controls mutual cell attraction during collective cell migration. In *Dev Cell*, vol. 21 (ed., pp. 1026-37.
Carpenter, D., Stone, D. M., Brush, J., Ryan, A., Armanini, M., Frantz, G., Rosenthal, A. and de Sauvage, F. J. (1998). Characterization of two patched receptors for the vertebrate hedgehog protein family. *Proc Natl Acad Sci USA* **95**, 13630-4.
Cha, S.-W., Tadjuidje, E., Tao, Q., Wylie, C. and Heasman, J. (2008). Wnt5a and Wnt11 interact in a maternal Dkk1-regulated fashion to activate both canonical and non-canonical signaling in Xenopus axis formation. *Development* **135**, 3719-29.
Cha, S.-W., Tadjuidje, E., White, J., Wells, J., Mayhew, C., Wylie, C. and Heasman, J. (2009). Wnt11/5a complex formation caused by tyrosine sulfation increases canonical signaling activity. *Curr Biol* **19**, 1573-80.
Chalmers, A. D. and Slack, J. M. (2000). The Xenopus tadpole gut: fate maps and morphogenetic movements. *Development* **127**, 381-92.
Chang, C. and Hemmati-Brivanlou, A. (1998). Neural crest induction by Xwnt7B in Xenopus. *Dev Biol* **194**, 129-34.
Chen, J., Taipale, J., Cooper, M. and Beachy, P. (2002). Inhibition of Hedgehog signaling by direct binding of cyclopamine to Smoothened. *Genes Dev* **16**, 2743-8.
Chen, M.-H., Li, Y.-J., Kawakami, T., Xu, S.-M. and Chuang, P.-T. (2004). Palmitoylation is required for the production of a soluble multimeric Hedgehog protein complex and long-range signaling in vertebrates. *Genes Dev* **18**, 641-59.
Chen, Q., Cui, W., Cheng, Y., Zhang, F. and Ji, M. (2011). Studying the mechanism that enables paullones to selectively inhibit glycogen synthase kinase 3 rather than cyclin-dependent kinase 5 by molecular dynamics simulations and free-energy calculations. *J Mol Model* **17**, 795-803.
Chen, Y., Cardinaux, J. R., Goodman, R. H. and Smolik, S. M. (1999). Mutants of cubitus interruptus that are independent of PKA regulation are independent of hedgehog signaling. *Development* **126**, 3607-16.
Chiang, C., Litingtung, Y., Lee, E., Young, K. E., Corden, J. L., Westphal, H. and Beachy, P. A. (1996). Cyclopia and defective axial patterning in mice lacking Sonic hedgehog gene function. *Nature* **383**, 407-13.
Chiang, C., Swan, R. Z., Grachtchouk, M., Bolinger, M., Litingtung, Y., Robertson, E. K., Cooper, M. K., Gaffield, W., Westphal, H., Beachy, P. A. et al. (1999). Essential role for Sonic hedgehog during hair follicle morphogenesis. *Dev Biol* **205**, 1-9.
Chow, R. L. and Lang, R. A. (2001). Early eye development in vertebrates. *Annu Rev Cell Dev Biol* **17**, 255-96.
Christian, J. L., McMahon, J. A., McMahon, A. P. and Moon, R. T. (1991). Xwnt-8, a Xenopus Wnt-1/int-1-related gene responsive to mesoderm-inducing growth factors, may play a role in ventral mesodermal patterning during embryogenesis. *Development* **111**, 1045-55.
Collazo, A., Bronner-Fraser, M. and Fraser, S. E. (1993). Vital dye labelling of Xenopus laevis trunk neural crest reveals multipotency and novel pathways of migration. *Development* **118**, 363-76.

Cooke, J. and Smith, E. J. (1988). The restrictive effect of early exposure to lithium upon body pattern in Xenopus development, studied by quantitative anatomy and immunofluorescence. *Development* **102**, 85-99.
Cross, D. A., Alessi, D. R., Cohen, P., Andjelkovich, M. and Hemmings, B. A. (1995). Inhibition of glycogen synthase kinase-3 by insulin mediated by protein kinase B. *Nature* **378**, 785-9.
Cross, D. A., Alessi, D. R., Vandenheede, J. R., McDowell, H. E., Hundal, H. S. and Cohen, P. (1994). The inhibition of glycogen synthase kinase-3 by insulin or insulin-like growth factor 1 in the rat skeletal muscle cell line L6 is blocked by wortmannin, but not by rapamycin: evidence that wortmannin blocks activation of the mitogen-activated protein kinase pathway in L6 cells between Ras and Raf. *Biochem J* **303 (Pt 1)**, 21-6.
Cross, D. A., Watt, P. W., Shaw, M., van der Kaay, J., Downes, C. P., Holder, J. C. and Cohen, P. (1997). Insulin activates protein kinase B, inhibits glycogen synthase kinase-3 and activates glycogen synthase by rapamycin-insensitive pathways in skeletal muscle and adipose tissue. *FEBS Lett* **406**, 211-5.
Dahmane, N., Lee, J., Robins, P., Heller, P. and Ruiz i Altaba, A. (1997). Activation of the transcription factor Gli1 and the Sonic hedgehog signalling pathway in skin tumours. *Nature* **389**, 876-81.
Dai, P., Akimaru, H., Tanaka, Y., Maekawa, T., Nakafuku, M. and Ishii, S. (1999). Sonic Hedgehog-induced activation of the Gli1 promoter is mediated by GLI3. *J Biol Chem* **274**, 8143-52.
Dale, R. M., Sisson, B. E. and Topczewski, J. (2009). The emerging role of Wnt/PCP signaling in organ formation. *Zebrafish* **6**, 9-14.
Daya-Grosjean, L. and Couvé-Privat, S. (2005). Sonic hedgehog signaling in basal cell carcinomas. *Cancer Lett* **225**, 181-92.
De Sarno, P., Li, X. and Jope, R. S. (2002). Regulation of Akt and glycogen synthase kinase-3 beta phosphorylation by sodium valproate and lithium. *Neuropharmacology* **43**, 1158-64.
Derynck, R. and Zhang, Y. E. (2003). Smad-dependent and Smad-independent pathways in TGF-beta family signalling. In *Nature*, vol. 425 (ed., pp. 577-84.
Dickinson, A. J. G. and Sive, H. (2006). Development of the primary mouth in Xenopus laevis. *Dev Biol* **295**, 700-13.
Dickinson, A. J. G. and Sive, H. L. (2009). The Wnt antagonists Frzb-1 and Crescent locally regulate basement membrane dissolution in the developing primary mouth. *Development* **136**, 1071-81.
Dickinson, M., Selleck, M., McMahon, A. and Bronner-Fraser, M. (1995). Dorsalization of the neural tube by the non-neural ectoderm. *Development* **121**, 2099-106.
Diehl, J., Zindy, F. and Sherr, C. (1997). Inhibition of cyclin D1 phosphorylation on threonine-286 prevents its rapid degradation via the ubiquitin-proteasome pathway. *Genes Dev* **11**, 957-72.
Ding, V. W., Chen, R. H. and McCormick, F. (2000). Differential regulation of glycogen synthase kinase 3beta by insulin and Wnt signaling. *J Biol Chem* **275**, 32475-81.
Dirk Nieuwkoop, P. (1994). Normal table of Xenopus laevis (Daudin): a systematical and chronological .... 252.

Doble, B. W., Patel, S., Wood, G. A., Kockeritz, L. K. and Woodgett, J. R. (2007). Functional redundancy of GSK-3alpha and GSK-3beta in Wnt/beta-catenin signaling shown by using an allelic series of embryonic stem cell lines. *Dev Cell* **12**, 957-71.
Doble, B. W. and Woodgett, J. R. (2003). GSK-3: tricks of the trade for a multi-tasking kinase. *J Cell Sci* **116**, 1175-86.
Doble, B. W. and Woodgett, J. R. (2007). Role of glycogen synthase kinase-3 in cell fate and epithelial-mesenchymal transitions. *Cells Tissues Organs (Print)* **185**, 73-84.
Domingos, P. M., Itasaki, N., Jones, C. M., Mercurio, S., Sargent, M. G., Smith, J. C. and Krumlauf, R. (2001). The Wnt/beta-catenin pathway posteriorizes neural tissue in Xenopus by an indirect mechanism requiring FGF signalling. *Dev Biol* **239**, 148-60.
Dominguez, I. and Green, J. B. (2000). Dorsal downregulation of GSK3beta by a non-Wnt-like mechanism is an early molecular consequence of cortical rotation in early Xenopus embryos. *Development* **127**, 861-8.
Dominguez, I. and Green, J. B. (2001). Missing links in GSK3 regulation. *Dev Biol* **235**, 303-13.
Doray, B., Langer, B. and Stoll, C. (1999). Two cases of Townes-Brocks syndrome. *Genet Couns* **10**, 359-67.
Dorsky, R., Moon, R. and Raible, D. (1998). Control of neural crest cell fate by the Wnt signalling pathway. *Nature* **396**, 370-3.
Douarin, N. (1999). The Neural Crest.
Draper, B. W., Morcos, P. A. and Kimmel, C. B. (2001). Inhibition of zebrafish fgf8 pre-mRNA splicing with morpholino oligos: a quantifiable method for gene knockdown. In *Genesis*, vol. 30 (ed., pp. 154-6.
Durston, A. J., Timmermans, J. P., Hage, W. J., Hendriks, H. F., de Vries, N. J., Heideveld, M. and Nieuwkoop, P. D. (1989). Retinoic acid causes an anteroposterior transformation in the developing central nervous system. *Nature* **340**, 140-4.
Dush, M. K., McIver, A. L., Parr, M. A., Young, D. D., Fisher, J., Newman, D. R., Sannes, P. L., Hauck, M. L., Deiters, A. and Nascone-Yoder, N. (2011). Heterotaxin: a TGF-β signaling inhibitor identified in a multi-phenotype profiling screen in Xenopus embryos. In *Chem Biol*, vol. 18 (ed., pp. 252-63.
Echelard, Y., Epstein, D. J., St-Jacques, B., Shen, L., Mohler, J., McMahon, J. A. and McMahon, A. P. (1993). Sonic hedgehog, a member of a family of putative signaling molecules, is implicated in the regulation of CNS polarity. *Cell* **75**, 1417-30.
Eickholt, B. J., Mackenzie, S. L., Graham, A., Walsh, F. S. and Doherty, P. (1999). Evidence for collapsin-1 functioning in the control of neural crest migration in both trunk and hindbrain regions. *Development* **126**, 2181-9.
Eickholt, B. J., Walsh, F. S. and Doherty, P. (2002). An inactive pool of GSK-3 at the leading edge of growth cones is implicated in Semaphorin 3A signaling. *J Cell Biol* **157**, 211-7.
Ellies, D., Tucker, A. and Lumsden, A. (2002). Apoptosis of premigratory neural crest cells in rhombomeres 3 and 5: consequences for patterning of the branchial region. *Dev Biol* **251**, 118-28.
Epperlein, H. H., Krotoski, D., Halfter, W. and Frey, A. (1990). Origin and distribution of enteric neurones in Xenopus. *Anat Embryol* **182**, 53-67.
Epstein, E. H. (2008). Basal cell carcinomas: attack of the hedgehog. *Nat Rev Cancer* **8**, 743-54.

Fang, X., Yu, S., Tanyi, J. L., Lu, Y., Woodgett, J. R. and Mills, G. B. (2002). Convergence of multiple signaling cascades at glycogen synthase kinase 3: Edg receptor-mediated phosphorylation and inactivation by lysophosphatidic acid through a protein kinase C-dependent intracellular pathway. *Mol Cell Biol* **22**, 2099-110.
Fang, X., Yu, S. X., Lu, Y., Bast, R. C., Woodgett, J. R. and Mills, G. B. (2000). Phosphorylation and inactivation of glycogen synthase kinase 3 by protein kinase A. *Proc Natl Acad Sci USA* **97**, 11960-5.
Fiol, C. J., Mahrenholz, A. M., Wang, Y., Roeske, R. W. and Roach, P. J. (1987). Formation of protein kinase recognition sites by covalent modification of the substrate. Molecular mechanism for the synergistic action of casein kinase II and glycogen synthase kinase 3. *J Biol Chem* **262**, 14042-8.
Fliegauf, M., Benzing, T. and Omran, H. (2007). When cilia go bad: cilia defects and ciliopathies. *Nat Rev Mol Cell Biol* **8**, 880-93.
Frame, S. and Cohen, P. (2001). GSK3 takes centre stage more than 20 years after its discovery. *Biochem J* **359**, 1-16.
Frame, S., Cohen, P. and Biondi, R. M. (2001). A common phosphate binding site explains the unique substrate specificity of GSK3 and its inactivation by phosphorylation. *Mol Cell* **7**, 1321-7.
Fu, M., Lui, V. C. H., Sham, M. H., Pachnis, V. and Tam, P. K. H. (2004). Sonic hedgehog regulates the proliferation, differentiation, and migration of enteric neural crest cells in gut. *J Cell Biol* **166**, 673-84.
Fuchs, S. and Sommer, L. (2007). The neural crest: understanding stem cell function in development and disease. *Neurodegener Dis* **4**, 6-12.
Gailani, M. R., Ståhle-Bäckdahl, M., Leffell, D. J., Glynn, M., Zaphiropoulos, P. G., Pressman, C., Undén, A. B., Dean, M., Brash, D. E., Bale, A. E. et al. (1996). The role of the human homologue of Drosophila patched in sporadic basal cell carcinomas. *Nat Genet* **14**, 78-81.
Gammill, L., Gonzalez, C., Gu, C. and Bronner-Fraser, M. (2006). Guidance of trunk neural crest migration requires neuropilin 2/semaphorin 3F signaling. *Development* **133**, 99-106.
Gammill, L. S., Gonzalez, C. and Bronner-Fraser, M. (2007). Neuropilin 2/semaphorin 3F signaling is essential for cranial neural crest migration and trigeminal ganglion condensation. *Dev Neurobiol* **67**, 47-56.
García-Castro, M. and Bronner-Fraser, M. (1999). Induction and differentiation of the neural crest. *Curr Opin Cell Biol* **11**, 695-8.
García-Castro, M. I., Marcelle, C. and Bronner-Fraser, M. (2002). Ectodermal Wnt function as a neural crest inducer. *Science* **297**, 848-51.
Gawkrodger, D. J., Ormerod, A. D., Shaw, L., Mauri-Sole, I., Whitton, M. E., Watts, M. J., Anstey, A. V., Ingham, J. and Young, K. (2010). Vitiligo: concise evidence based guidelines on diagnosis and management. *Postgrad Med J* **86**, 466-71.
Glinka, A., Wu, W., Delius, H., Monaghan, A. P., Blumenstock, C. and Niehrs, C. (1998). Dickkopf-1 is a member of a new family of secreted proteins and functions in head induction. *Nature* **391**, 357-62.
Goetz, J. A., Singh, S., Suber, L. M., Kull, F. J. and Robbins, D. J. (2006). A highly conserved amino-terminal region of sonic hedgehog is required for the formation of its freely diffusible multimeric form. *J Biol Chem* **281**, 4087-93.

Goetz, S. C. and Anderson, K. V. (2010). The primary cilium: a signalling centre during vertebrate development. *Nat Rev Genet* **11**, 331-44.
Goetz, S. C., Ocbina, P. J. R. and Anderson, K. V. (2009). The primary cilium as a Hedgehog signal transduction machine. *Methods Cell Biol* **94**, 199-222.
Gordon, M. D. and Nusse, R. (2006). Wnt signaling: multiple pathways, multiple receptors, and multiple transcription factors. *J Biol Chem* **281**, 22429-33.
Gould, T. D., Zarate, C. A. and Manji, H. K. (2004). Glycogen synthase kinase-3: a target for novel bipolar disorder treatments. *J Clin Psychiatry* **65**, 10-21.
Gradl, D., Kühl, M. and Wedlich, D. (1999). The Wnt/Wg signal transducer beta-catenin controls fibronectin expression. *Mol Cell Biol* **19**, 5576-87.
Grammer, T. C., Liu, K. J., Mariani, F. V. and Harland, R. M. (2000). Use of large-scale expression cloning screens in the Xenopus laevis tadpole to identify gene function. *Dev Biol* **228**, 197-210.
Green, J. B. A. (2004). Lkb1 and GSK3-beta: kinases at the center and poles of the action. *Cell Cycle* **3**, 12-4.
Grocott, T., Johnson, S., Bailey, A. and Streit, A. (2011). Neural crest cells organize the eye via TGF- β and canonical Wnt signalling. *Nat Commun* **2**, 265.
Guo, X., Ramirez, A., Waddell, D. S., Li, Z., Liu, X. and Wang, X.-F. (2008). Axin and GSK3- control Smad3 protein stability and modulate TGF- signaling. In *Genes Dev*, vol. 22 (ed., pp. 106-20.
Gurdon, J. B. and Hopwood, N. (2000). The introduction of Xenopus laevis into developmental biology: of empire, pregnancy testing and ribosomal genes. *Int J Dev Biol* **44**, 43-50.
Hall, B. K. (2008). The neural crest and neural crest cells: discovery and significance for theories of embryonic organization. *J Biosci* **33**, 781-93.
Haraguchi, R., Motoyama, J., Sasaki, H., Satoh, Y., Miyagawa, S., Nakagata, N., Moon, A. and Yamada, G. (2007). Molecular analysis of coordinated bladder and urogenital organ formation by Hedgehog signaling. *Development* **134**, 525-33.
Harland, R. (2008). Induction into the Hall of Fame: tracing the lineage of Spemann's organizer. *Development* **135**, 3321-3.
Harland, R. and Gerhart, J. (1997). Formation and function of Spemann's organizer. *Annu Rev Cell Dev Biol* **13**, 611-67.
Harwood, A. J. (2001). Regulation of GSK-3: a cellular multiprocessor. *Cell* **105**, 821-4.
Hassoun, R., Schwartz, P., Rath, D., Viebahn, C. and Männer, J. (2010). Germ layer differentiation during early hindgut and cloaca formation in rabbit and pig embryos. *J Anat* **217**, 665-78.
He, X., Saint-Jeannet, J. P., Woodgett, J. R., Varmus, H. E. and Dawid, I. B. (1995). Glycogen synthase kinase-3 and dorsoventral patterning in Xenopus embryos. *Nature* **374**, 617-22.
Heasman, J. (2002). Morpholino oligos: making sense of antisense? In *Dev Biol*, vol. 243 (ed., pp. 209-14.
Heasman, J., Crawford, A., Goldstone, K., Garner-Hamrick, P., Gumbiner, B., McCrea, P., Kintner, C., Noro, C. Y. and Wylie, C. (1994). Overexpression of cadherins and underexpression of beta-catenin inhibit dorsal mesoderm induction in early Xenopus embryos. *Cell* **79**, 791-803.

Heasman, J., Kofron, M. and Wylie, C. (2000). Beta-catenin signaling activity dissected in the early Xenopus embryo: a novel antisense approach. *Dev Biol* **222**, 124-34.
Henion, P. and Weston, J. (1997). Timing and pattern of cell fate restrictions in the neural crest lineage. *Development* **124**, 4351-9.
Henion, P. D., Raible, D. W., Beattie, C. E., Stoesser, K. L., Weston, J. A. and Eisen, J. S. (1996). Screen for mutations affecting development of Zebrafish neural crest. *Dev Genet* **18**, 11-7.
Hernández, F., Gómez de Barreda, E., Fuster-Matanzo, A., Lucas, J. J. and Avila, J. (2010). GSK3: a possible link between beta amyloid peptide and tau protein. *Exp Neurol* **223**, 322-5.
Hogan, B. L. (1996). Bone morphogenetic proteins in development. In *Curr Opin Genet Dev*, vol. 6 (ed., pp. 432-8.
Holland, L. Z. and Holland, N. D. (2001). Evolution of neural crest and placodes: amphioxus as a model for the ancestral vertebrate? *J Anat* **199**, 85-98.
Honore, S., Aybar, M. and Mayor, R. (2003). Sox10 is required for the early development of the prospective neural crest in Xenopus embryos. *Dev Biol* **260**, 79-96.
Hopwood, N. D., Pluck, A. and Gurdon, J. B. (1989). A Xenopus mRNA related to Drosophila twist is expressed in response to induction in the mesoderm and the neural crest. *Cell* **59**, 893-903.
Hrabé de Angelis, M. H., Flaswinkel, H., Fuchs, H., Rathkolb, B., Soewarto, D., Marschall, S., Heffner, S., Pargent, W., Wuensch, K., Jung, M. et al. (2000). Genome-wide, large-scale production of mutant mice by ENU mutagenesis. *Nat Genet* **25**, 444-7.
Hu, D. and Helms, J. (1999). The role of sonic hedgehog in normal and abnormal craniofacial morphogenesis. *Development* **126**, 4873-84.
Hughes, K., Nikolakaki, E., Plyte, S., Totty, N. and Woodgett, J. (1993). Modulation of the glycogen synthase kinase-3 family by tyrosine phosphorylation. *EMBO J* **12**, 803-8.
Hui, C. C. and Joyner, A. L. (1993). A mouse model of greig cephalopolysyndactyly syndrome: the extra-toesJ mutation contains an intragenic deletion of the Gli3 gene. *Nat Genet* **3**, 241-6.
Hui, C. C., Slusarski, D., Platt, K. A., Holmgren, R. and Joyner, A. L. (1994). Expression of three mouse homologs of the Drosophila segment polarity gene cubitus interruptus, Gli, Gli-2, and Gli-3, in ectoderm- and mesoderm-derived tissues suggests multiple roles during postimplantation development. *Dev Biol* **162**, 402-13.
Hur, E.-M. and Zhou, F.-Q. (2010). GSK3 signalling in neural development. *Nat Rev Neurosci* **11**, 539-51.
Ikeya, M., Lee, S. M., Johnson, J. E., McMahon, A. P. and Takada, S. (1997). Wnt signalling required for expansion of neural crest and CNS progenitors. *Nature* **389**, 966-70.
Ingham, P. W. and McMahon, A. P. (2001). Hedgehog signaling in animal development: paradigms and principles. *Genes Dev* **15**, 3059-87.
Ingham, P. W., Nakano, Y. and Seger, C. (2011). Mechanisms and functions of Hedgehog signalling across the metazoa. *Nat Rev Genet* **12**, 393-406.

Ingham, P. W., Taylor, A. M. and Nakano, Y. (1991). Role of the Drosophila patched gene in positional signalling. *Nature* **353**, 184-7.
Ito, Y., Bringas, P., Mogharei, A., Zhao, J., Deng, C. and Chai, Y. (2002). Receptor-regulated and inhibitory Smads are critical in regulating transforming growth factor beta-mediated Meckel's cartilage development. In *Dev Dyn*, vol. 224 (ed., pp. 69-78.
Jeong, J., Mao, J., Tenzen, T., Kottmann, A. H. and McMahon, A. P. (2004). Hedgehog signaling in the neural crest cells regulates the patterning and growth of facial primordia. *Genes Dev* **18**, 937-51.
Jesuthasan, S. (1996). Contact inhibition/collapse and pathfinding of neural crest cells in the zebrafish trunk. *Development* **122**, 381-9.
Jia, J., Amanai, K., Wang, G., Tang, J., Wang, B. and Jiang, J. (2002). Shaggy/GSK3 antagonizes Hedgehog signalling by regulating Cubitus interruptus. *Nature* **416**, 548-52.
Jiang, J. and Struhl, G. (1995). Protein kinase A and hedgehog signaling in Drosophila limb development. *Cell* **80**, 563-72.
Johnson, R. L., Rothman, A. L., Xie, J., Goodrich, L. V., Bare, J. W., Bonifas, J. M., Quinn, A. G., Myers, R. M., Cox, D. R., Epstein, E. H. et al. (1996). Human homolog of patched, a candidate gene for the basal cell nevus syndrome. *Science* **272**, 1668-71.
Johnston, M. C. and Bronsky, P. T. (1995). Prenatal craniofacial development: new insights on normal and abnormal mechanisms. *Crit Rev Oral Biol Med* **6**, 368-422.
Jope, R. S. (1999). Anti-bipolar therapy: mechanism of action of lithium. *Mol Psychiatry* **4**, 117-28.
Jope, R. S. and Johnson, G. V. W. (2004). The glamour and gloom of glycogen synthase kinase-3. *Trends Biochem Sci* **29**, 95-102.
Jope, R. S. and Roh, M.-S. (2006). Glycogen synthase kinase-3 (GSK3) in psychiatric diseases and therapeutic interventions. *Current drug targets* **7**, 1421-34.
Kalderon, D. (2000). Transducing the hedgehog signal. *Cell* **103**, 371-4.
Kang, P. and Svoboda, K. K. H. (2005). Epithelial-mesenchymal transformation during craniofacial development. *J Dent Res* **84**, 678-90.
Kang, S., Graham, J. M., Olney, A. H. and Biesecker, L. G. (1997). GLI3 frameshift mutations cause autosomal dominant Pallister-Hall syndrome. *Nat Genet* **15**, 266-8.
Kao, K. R. and Elinson, R. P. (1988). The entire mesodermal mantle behaves as Spemann's organizer in dorsoanterior enhanced Xenopus laevis embryos. *Dev Biol* **127**, 64-77.
Kazanskaya, O., Glinka, A. and Niehrs, C. (2000). The role of Xenopus dickkopf1 in prechordal plate specification and neural patterning. *Development* **127**, 4981-92.
Kelsh, R. N., Brand, M., Jiang, Y. J., Heisenberg, C. P., Lin, S., Haffter, P., Odenthal, J., Mullins, M. C., van Eeden, F. J., Furutani-Seiki, M. et al. (1996). Zebrafish pigmentation mutations and the processes of neural crest development. *Development* **123**, 369-89.
Kim, J., Kim, P. and Hui, C. C. (2001). The VACTERL association: lessons from the Sonic hedgehog pathway. *Clin Genet* **59**, 306-15.
Kimmel, S. G., Mo, R., Hui, C. C. and Kim, P. C. (2000). New mouse models of congenital anorectal malformations. *J Pediatr Surg* **35**, 227-30; discussion 230-1.
Kingsley, D. M. (1994). What do BMPs do in mammals? Clues from the mouse short-ear mutation. In *Trends Genet*, vol. 10 (ed., pp. 16-21.

Kirsch, T., Nickel, J. and Sebald, W. (2000). BMP-2 antagonists emerge from alterations in the low-affinity binding epitope for receptor BMPR-II. In *EMBO J*, vol. 19 (ed., pp. 3314-24.
Klein, P. S. and Melton, D. A. (1996). A molecular mechanism for the effect of lithium on development. *Proc Natl Acad Sci USA* **93**, 8455-9.
Knecht, A. K. and Bronner-Fraser, M. (2002). Induction of the neural crest: a multigene process. *Nat Rev Genet* **3**, 453-61.
Ko, H., Kim, H., Kim, N., Lee, S., Kim, K., Hong, S. and Yook, J. (2007). Nuclear localization signals of the E-cadherin transcriptional repressor Snail. *Cells Tissues Organs* **185**, 66-72.
Kuriyama, S. and Mayor, R. (2008). Molecular analysis of neural crest migration. *Philos Trans R Soc Lond, B, Biol Sci* **363**, 1349-62.
LaBonne, C. and Bronner-Fraser, M. (1998). Neural crest induction in Xenopus: evidence for a two-signal model. *Development* **125**, 2403-14.
LaBonne, C. and Bronner-Fraser, M. (1999). Molecular mechanisms of neural crest formation. *Annu Rev Cell Dev Biol* **15**, 81-112.
Lam, C. W., Xie, J., To, K. F., Ng, H. K., Lee, K. C., Yuen, N. W., Lim, P. L., Chan, L. Y., Tong, S. F. and McCormick, F. (1999). A frequent activated smoothened mutation in sporadic basal cell carcinomas. *Oncogene* **18**, 833-6.
Lane, M. C. and Sheets, M. D. (2000). Designation of the anterior/posterior axis in pregastrula Xenopus laevis. *Dev Biol* **225**, 37-58.
Le Douarin, N. and Kalcheim, C. (1999). The neural crest. 445.
Lee, H., Kleber, M., Hari, L., Brault, V., Suter, U., Taketo, M., Kemler, R. and Sommer, L. (2004). Instructive role of Wnt/beta-catenin in sensory fate specification in neural crest stem cells. *Science* **303**, 1020-3.
Lee, J. J., Ekker, S. C., von Kessler, D. P., Porter, J. A., Sun, B. I. and Beachy, P. A. (1994). Autoproteolysis in hedgehog protein biogenesis. *Science* **266**, 1528-37.
Lei, Q., Zelman, A. K., Kuang, E., Li, S. and Matise, M. P. (2004). Transduction of graded Hedgehog signaling by a combination of Gli2 and Gli3 activator functions in the developing spinal cord. *Development* **131**, 3593-604.
Leitner, J., Drobits, K., Pickl, W. F., Majdic, O., Zlabinger, G. and Steinberger, P. (2011). The effects of Cyclosporine A and azathioprine on human T cells activated by different costimulatory signals. In *Immunol Lett*, vol. 140 (ed., pp. 74-80.
Leost, M., Schultz, C., Link, A., Wu, Y. Z., Biernat, J., Mandelkow, E. M., Bibb, J. A., Snyder, G. L., Greengard, P., Zaharevitz, D. W. et al. (2000). Paullones are potent inhibitors of glycogen synthase kinase-3beta and cyclin-dependent kinase 5/p25. *Eur J Biochem* **267**, 5983-94.
Lepage, T., Cohen, S. M., Diaz-Benjumea, F. J. and Parkhurst, S. M. (1995). Signal transduction by cAMP-dependent protein kinase A in Drosophila limb patterning. *Nature* **373**, 711-5.
Levitt, M. A., Bischoff, A. and Peña, A. (2011). Pitfalls and challenges of cloaca repair: how to reduce the need for reoperations. *J Pediatr Surg* **46**, 1250-5.
Lewis, J. L., Bonner, J., Modrell, M., Ragland, J. W., Moon, R. T., Dorsky, R. I. and Raible, D. W. (2004). Reiterated Wnt signaling during zebrafish neural crest development. *Development* **131**, 1299-308.

Lewis, P. M., Dunn, M. P., McMahon, J. A., Logan, M., Martin, J. F., St-Jacques, B. and McMahon, A. P. (2001). Cholesterol modification of sonic hedgehog is required for long-range signaling activity and effective modulation of signaling by Ptc1. *Cell* **105**, 599-612.
Li, H., Tierney, C., Wen, L., Wu, J. Y. and Rao, Y. (1997). A single morphogenetic field gives rise to two retina primordia under the influence of the prechordal plate. *Development* **124**, 603-15.
Li, W., Ohlmeyer, J. T., Lane, M. E. and Kalderon, D. (1995). Function of protein kinase A in hedgehog signal transduction and Drosophila imaginal disc development. *Cell* **80**, 553-62.
Linker, C., Bronner-Fraser, M. and Mayor, R. (2000). Relationship between gene expression domains of Xsnail, Xslug, and Xtwist and cell movement in the prospective neural crest of Xenopus. *Dev Biol* **224**, 215-25.
Liu, J., Wu, X., Mitchell, B., Kintner, C., Ding, S. and Schultz, P. G. (2005). A small-molecule agonist of the Wnt signaling pathway. *Angew Chem Int Ed Engl* **44**, 1987-90.
Logan, C. and Nusse, R. (2004). The Wnt signaling pathway in development and disease. *Annu Rev Cell Dev Biol* **20**, 781-810.
Lynch, K. (1990). Development and innervation of the abdominal muscle in embryonic Xenopus laevis. *Am J Anat* **187**, 374-92.
MacDonald, B. T., Adamska, M. and Meisler, M. H. (2004). Hypomorphic expression of Dkk1 in the doubleridge mouse: dose dependence and compensatory interactions with Lrp6. *Development* **131**, 2543-52.
Mancilla, A. and Mayor, R. (1996). Neural crest formation in Xenopus laevis: mechanisms of Xslug induction. *Dev Biol* **177**, 580-9.
Mao, B., Wu, W., Li, Y., Hoppe, D., Stannek, P., Glinka, A. and Niehrs, C. (2001). LDL-receptor-related protein 6 is a receptor for Dickkopf proteins. *Nature* **411**, 321-5.
Marchant, L., Linker, C., Ruiz, P., Guerrero, N. and Mayor, R. (1998). The inductive properties of mesoderm suggest that the neural crest cells are specified by a BMP gradient. *Dev Biol* **198**, 319-29.
Marigo, V., Davey, R. A., Zuo, Y., Cunningham, J. M. and Tabin, C. J. (1996). Biochemical evidence that patched is the Hedgehog receptor. *Nature* **384**, 176-9.
Martin, B. L. and Harland, R. M. (2001). Hypaxial muscle migration during primary myogenesis in Xenopus laevis. *Dev Biol* **239**, 270-80.
Martin, M., Rehani, K., Jope, R. S. and Michalek, S. M. (2005). Toll-like receptor-mediated cytokine production is differentially regulated by glycogen synthase kinase 3. *Nat Immunol* **6**, 777-84.
Massagué, J. (2000). How cells read TGF-beta signals. In *Nat Rev Mol Cell Biol*, vol. 1 (ed., pp. 169-78.
Massagué, J. and Chen, Y. G. (2000). Controlling TGF-beta signaling. In *Genes Dev*, vol. 14 (ed., pp. 627-44.
Massagué, J. and Wotton, D. (2000). Transcriptional control by the TGF-beta/Smad signaling system. In *EMBO J*, vol. 19 (ed., pp. 1745-54.
Mayor, R., Morgan, R. and Sargent, M. (1995). Induction of the prospective neural crest of Xenopus. *Development* **121**, 767-77.
McCormick, M. (1987). Sib selection. *Meth Enzymol* **151**, 445-9.

Meijer, L., Skaltsounis, A.-L., Magiatis, P., Polychronopoulos, P., Knockaert, M., Leost, M., Ryan, X. P., Vonica, C. A., Brivanlou, A., Dajani, R. et al. (2003). GSK-3-selective inhibitors derived from Tyrian purple indirubins. *Chem Biol* **10**, 1255-66.
Méthot, N. and Basler, K. (1999). Hedgehog controls limb development by regulating the activities of distinct transcriptional activator and repressor forms of Cubitus interruptus. *Cell* **96**, 819-31.
Meulemans, D. and Bronner-Fraser, M. (2007). Insights from amphioxus into the evolution of vertebrate cartilage. In *PLoS ONE*, vol. 2 (ed., pp. e787.
Mikels, A. J. and Nusse, R. (2006). Purified Wnt5a protein activates or inhibits beta-catenin-TCF signaling depending on receptor context. *PLoS Biol* **4**, e115.
Mine, N., Anderson, R. M. and Klingensmith, J. (2008). BMP antagonism is required in both the node and lateral plate mesoderm for mammalian left-right axis establishment. In *Development*, vol. 135 (ed., pp. 2425-34.
Miyagawa, S., Moon, A., Haraguchi, R., Inoue, C., Harada, M., Nakahara, C., Suzuki, K., Matsumaru, D., Kaneko, T., Matsuo, I. et al. (2009). Dosage-dependent hedgehog signals integrated with Wnt/beta-catenin signaling regulate external genitalia formation as an appendicular program. *Development* **136**, 3969-78.
Mo, R., Kim, J. H., Zhang, J., Chiang, C., Hui, C. C. and Kim, P. C. (2001). Anorectal malformations caused by defects in sonic hedgehog signaling. *Am J Pathol* **159**, 765-74.
Moury, J. D. and Jacobson, A. G. (1990). The origins of neural crest cells in the axolotl. *Dev Biol* **141**, 243-53.
Mukai, F., Ishiguro, K., Sano, Y. and Fujita, S. (2002). Alternative splicing isoform of tau protein kinase I/glycogen synthase kinase 3beta. *J Neurochem* **81**, 1073-83.
Nagy, V., Steiber, Z., Takacs, L., Vereb, G., Berta, A., Bereczky, Z. and Pfliegler, G. (2006). Trombophilic screening for nonarteritic anterior ischemic optic neuropathy. In *Graefes Arch Clin Exp Ophthalmol*, vol. 244 (ed., pp. 3-8.
Neuhauss, S. C., Solnica-Krezel, L., Schier, A. F., Zwartkruis, F., Stemple, D. L., Malicki, J., Abdelilah, S., Stainier, D. Y. and Driever, W. (1996). Mutations affecting craniofacial development in zebrafish. *Development* **123**, 357-67.
Nguyen, V., Chokas, A. L., Stecca, B. and Ruiz i Altaba, A. (2005). Cooperative requirement of the Gli proteins in neurogenesis. *Development* **132**, 3267-79.
Nie, X., Luukko, K. and Kettunen, P. (2006). FGF signalling in craniofacial development and developmental disorders. *Oral Dis* **12**, 102-11.
Nieto, M., Sargent, M., Wilkinson, D. and Cooke, J. (1994). Control of cell behavior during vertebrate development by Slug, a zinc finger gene. *Science* **264**, 835-9.
Nieto, M. A. (2002). The snail superfamily of zinc-finger transcription factors. *Nat Rev Mol Cell Biol* **3**, 155-66.
Nolan, P. M., Peters, J., Strivens, M., Rogers, D., Hagan, J., Spurr, N., Gray, I. C., Vizor, L., Brooker, D., Whitehill, E. et al. (2000). A systematic, genome-wide, phenotype-driven mutagenesis programme for gene function studies in the mouse. *Nat Genet* **25**, 440-3.
Nusse, R. and Varmus, H. E. (1982). Many tumors induced by the mouse mammary tumor virus contain a provirus integrated in the same region of the host genome. *Cell* **31**, 99-109.

Nüsslein-Volhard, C. and Wieschaus, E. (1980). Mutations affecting segment number and polarity in Drosophila. *Nature* **287**, 795-801.
O'Donnell, M., Hong, C.-S., Huang, X., Delnicki, R. J. and Saint-Jeannet, J.-P. (2006). Functional analysis of Sox8 during neural crest development in Xenopus. *Development* **133**, 3817-26.
Olesnicky Killian, E. C., Birkholz, D. A. and Artinger, K. B. (2009). A role for chemokine signaling in neural crest cell migration and craniofacial development. In *Dev Biol*, vol. 333 (ed., pp. 161-72.
Onai, T., Sasai, N., Matsui, M. and Sasai, Y. (2004). Xenopus XsalF: anterior neuroectodermal specification by attenuating cellular responsiveness to Wnt signaling. *Dev Cell* **7**, 95-106.
Oro, A. E., Higgins, K. M., Hu, Z., Bonifas, J. M., Epstein, E. H. and Scott, M. P. (1997). Basal cell carcinomas in mice overexpressing sonic hedgehog. *Science* **276**, 817-21.
Osborne, N., Begbie, J., Chilton, J., Schmidt, H. and Eickholt, B. (2005). Semaphorin/neuropilin signaling influences the positioning of migratory neural crest cells within the hindbrain region of the chick. *Dev Dyn* **232**, 939-49.
Owen, R. and Gordon-Weeks, P. R. (2003). Inhibition of glycogen synthase kinase 3beta in sensory neurons in culture alters filopodia dynamics and microtubule distribution in growth cones. *Mol Cell Neurosci* **23**, 626-37.
Pan, D. and Rubin, G. M. (1995). cAMP-dependent protein kinase and hedgehog act antagonistically in regulating decapentaplegic transcription in Drosophila imaginal discs. *Cell* **80**, 543-52.
Pan, Y., Bai, C. B., Joyner, A. L. and Wang, B. (2006). Sonic hedgehog signaling regulates Gli2 transcriptional activity by suppressing its processing and degradation. *Mol Cell Biol* **26**, 3365-77.
Park, H. L., Bai, C., Platt, K. A., Matise, M. P., Beeghly, A., Hui, C. C., Nakashima, M. and Joyner, A. L. (2000). Mouse Gli1 mutants are viable but have defects in SHH signaling in combination with a Gli2 mutation. *Development* **127**, 1593-605.
Park, T. J., Haigo, S. L. and Wallingford, J. B. (2006). Ciliogenesis defects in embryos lacking inturned or fuzzy function are associated with failure of planar cell polarity and Hedgehog signaling. *Nat Genet* **38**, 303-11.
Parkin, C. A., Allen, C. E. and Ingham, P. W. (2009). Hedgehog signalling is required for cloacal development in the zebrafish embryo. *Int J Dev Biol* **53**, 45-57.
Patel, S. and Woodgett, J. (2008). Glycogen synthase kinase-3 and cancer: good cop, bad cop? *Cancer Cell* **14**, 351-3.
Pepinsky, R. B., Zeng, C., Wen, D., Rayhorn, P., Baker, D. P., Williams, K. P., Bixler, S. A., Ambrose, C. M., Garber, E. A., Miatkowski, K. et al. (1998). Identification of a palmitic acid-modified form of human Sonic hedgehog. *J Biol Chem* **273**, 14037-45.
Pera, E. M. and Kessel, M. (1997). Patterning of the chick forebrain anlage by the prechordal plate. *Development* **124**, 4153-62.
Perriton, C. L., Powles, N., Chiang, C., Maconochie, M. K. and Cohn, M. J. (2002). Sonic hedgehog signaling from the urethral epithelium controls external genital development. *Dev Biol* **247**, 26-46.

Peyrot, S. M., Wallingford, J. B. and Harland, R. M. (2011). A revised model of Xenopus dorsal midline development: differential and separable requirements for Notch and Shh signaling. *Dev Biol* **352**, 254-66.
Phiel, C. J. and Klein, P. S. (2001). Molecular targets of lithium action. *Annu Rev Pharmacol Toxicol* **41**, 789-813.
Polychronopoulos, P., Magiatis, P., Skaltsounis, A.-L., Myrianthopoulos, V., Mikros, E., Tarricone, A., Musacchio, A., Roe, S. M., Pearl, L., Leost, M. et al. (2004). Structural basis for the synthesis of indirubins as potent and selective inhibitors of glycogen synthase kinase-3 and cyclin-dependent kinases. *J Med Chem* **47**, 935-46.
Price, M. A. and Kalderon, D. (2002). Proteolysis of the Hedgehog signaling effector Cubitus interruptus requires phosphorylation by Glycogen Synthase Kinase 3 and Casein Kinase 1. *Cell* **108**, 823-35.
Ragland, J. W. and Raible, D. W. (2004). Signals derived from the underlying mesoderm are dispensable for zebrafish neural crest induction. *Dev Biol* **276**, 16-30.
Rao, T. P. and Kühl, M. (2010). An updated overview on Wnt signaling pathways: a prelude for more. *Circ Res* **106**, 1798-806.
Reardon, W., Winter, R. M., Rutland, P., Pulleyn, L. J., Jones, B. M. and Malcolm, S. (1994). Mutations in the fibroblast growth factor receptor 2 gene cause Crouzon syndrome. *Nat Genet* **8**, 98-103.
Reifenberger, J., Wolter, M., Knobbe, C. B., Köhler, B., Schönicke, A., Scharwächter, C., Kumar, K., Blaschke, B., Ruzicka, T. and Reifenberger, G. (2005). Somatic mutations in the PTCH, SMOH, SUFUH and TP53 genes in sporadic basal cell carcinomas. *Br J Dermatol* **152**, 43-51.
Rezzoug, F., Seelan, R. S., Bhattacherjee, V., Greene, R. M. and Pisano, M. M. (2011). Chemokine-mediated migration of mesencephalic neural crest cells. In *Cytokine*, vol. 56 (ed., pp. 760-8.
Riddle, R. D., Johnson, R. L., Laufer, E. and Tabin, C. (1993). Sonic hedgehog mediates the polarizing activity of the ZPA. *Cell* **75**, 1401-16.
Rijsewijk, F., Schuermann, M., Wagenaar, E., Parren, P., Weigel, D. and Nusse, R. (1987). The Drosophila homolog of the mouse mammary oncogene int-1 is identical to the segment polarity gene wingless. *Cell* **50**, 649-57.
Robinson, V., Smith, A., Flenniken, A. M. and Wilkinson, D. G. (1997). Roles of Eph receptors and ephrins in neural crest pathfinding. In *Cell Tissue Res*, vol. 290 (ed., pp. 265-74.
Roessler, E., Belloni, E., Gaudenz, K., Jay, P., Berta, P., Scherer, S. W., Tsui, L. C. and Muenke, M. (1996). Mutations in the human Sonic Hedgehog gene cause holoprosencephaly. *Nat Genet* **14**, 357-60.
Rohatgi, R. and Scott, M. P. (2007). Patching the gaps in Hedgehog signalling. *Nat Cell Biol* **9**, 1005-9.
Rosen, N. G., Hong, A. R., Soffer, S. Z., Rodriguez, G. and Peña, A. (2002). Rectovaginal fistula: a common diagnostic error with significant consequences in girls with anorectal malformations. *J Pediatr Surg* **37**, 961-5; discussion 961-5.
Sadaghiani, B. and Thiébaud, C. H. (1987). Neural crest development in the Xenopus laevis embryo, studied by interspecific transplantation and scanning electron microscopy. *Dev Biol* **124**, 91-110.

Saint-Jeannet, J. P., He, X., Varmus, H. E. and Dawid, I. B. (1997). Regulation of dorsal fate in the neuraxis by Wnt-1 and Wnt-3a. *Proc Natl Acad Sci USA* **94**, 13713-8.
Salic, A., Lee, E., Mayer, L. and Kirschner, M. (2000). Control of beta-catenin stability: reconstitution of the cytoplasmic steps of the wnt pathway in Xenopus egg extracts. *Mol Cell* **5**, 523-32.
Sampath, K., Rubinstein, A. L., Cheng, A. M., Liang, J. O., Fekany, K., Solnica-Krezel, L., Korzh, V., Halpern, M. E. and Wright, C. V. (1998). Induction of the zebrafish ventral brain and floorplate requires cyclops/nodal signalling. *Nature* **395**, 185-9.
Saneyoshi, T., Kume, S., Amasaki, Y. and Mikoshiba, K. (2002). The Wnt/calcium pathway activates NF-AT and promotes ventral cell fate in Xenopus embryos. *Nature* **417**, 295-9.
Santiago, A. and Erickson, C. A. (2002). Ephrin-B ligands play a dual role in the control of neural crest cell migration. In *Development*, vol. 129 (ed., pp. 3621-32.
Sasai, N., Mizuseki, K. and Sasai, Y. (2001). Requirement of FoxD3-class signaling for neural crest determination in Xenopus. *Development* **128**, 2525-36.
Sasaki, H., Nishizaki, Y., Hui, C., Nakafuku, M. and Kondoh, H. (1999). Regulation of Gli2 and Gli3 activities by an amino-terminal repression domain: implication of Gli2 and Gli3 as primary mediators of Shh signaling. *Development* **126**, 3915-24.
Sauer, B. (1987). Functional expression of the cre-lox site-specific recombination system in the yeast Saccharomyces cerevisiae. In *Mol Cell Biol*, vol. 7 (ed., pp. 2087-96.
Sauka-Spengler, T. and Bronner-Fraser, M. (2008). A gene regulatory network orchestrates neural crest formation. *Nat Rev Mol Cell Biol* **9**, 557-68.
Schaffer, B., Wiedau-Pazos, M. and Geschwind, D. H. (2003). Gene structure and alternative splicing of glycogen synthase kinase 3 beta (GSK-3beta) in neural and non-neural tissues. *Gene* **302**, 73-81.
Schier, A. F., Joyner, A. L., Lehmann, R. and Talbot, W. S. (1996). From screens to genes: prospects for insertional mutagenesis in zebrafish. *Genes Dev* **10**, 3077-80.
Seals, D. F. and Courtneidge, S. A. (2003). The ADAMs family of metalloproteases: multidomain proteins with multiple functions. In *Genes Dev*, vol. 17 (ed., pp. 7-30.
Seifert, A. W., Bouldin, C. M., Choi, K.-S., Harfe, B. D. and Cohn, M. J. (2009). Multiphasic and tissue-specific roles of sonic hedgehog in cloacal septation and external genitalia development. *Development* **136**, 3949-57.
Selleck, M. A. and Bronner-Fraser, M. (1995). Origins of the avian neural crest: the role of neural plate-epidermal interactions. *Development* **121**, 525-38.
Serbedzija, G., Bronner-Fraser, M. and Fraser, S. (1994). Developmental potential of trunk neural crest cells in the mouse. *Development* **120**, 1709-18.
Sheridan, C. M., Heist, E. K., Beals, C. R., Crabtree, G. R. and Gardner, P. (2002). Protein kinase A negatively modulates the nuclear accumulation of NF-ATc1 by priming for subsequent phosphorylation by glycogen synthase kinase-3. *J Biol Chem* **277**, 48664-76.
Sieber-Blum, M. and Zhang, J. (1997). Growth factor action in neural crest cell diversification. *J Anat* **191 (Pt 4)**, 493-9.
Slack, J. and Tannahill, D. (1992). Mechanism of anteroposterior axis specification in vertebrates. Lessons from the amphibians. *Development* **114**, 285-302.

Slattery, C., Campbell, E., McMorrow, T. and Ryan, M. P. (2005). Cyclosporine A-induced renal fibrosis: a role for epithelial-mesenchymal transition. *Am J Pathol* **167**, 395-407.
Smith, A., Robinson, V., Patel, K. and Wilkinson, D. G. (1997). The EphA4 and EphB1 receptor tyrosine kinases and ephrin-B2 ligand regulate targeted migration of branchial neural crest cells. *Curr Biol* **7**, 561-70.
Smith, J. C. and Slack, J. M. (1983). Dorsalization and neural induction: properties of the organizer in Xenopus laevis. *J Embryol Exp Morphol* **78**, 299-317.
Smith, W. C. and Harland, R. M. (1992). Expression cloning of noggin, a new dorsalizing factor localized to the Spemann organizer in Xenopus embryos. *Cell* **70**, 829-40.
Spokony, R. F., Aoki, Y., Saint-Germain, N., Magner-Fink, E. and Saint-Jeannet, J.-P. (2002). The transcription factor Sox9 is required for cranial neural crest development in Xenopus. *Development* **129**, 421-32.
Steventon, B., Carmona-Fontaine, C. and Mayor, R. (2005). Genetic network during neural crest induction: from cell specification to cell survival. *Semin Cell Dev Biol* **16**, 647-54.
Stone, D. M., Hynes, M., Armanini, M., Swanson, T. A., Gu, Q., Johnson, R. L., Scott, M. P., Pennica, D., Goddard, A., Phillips, H. et al. (1996). The tumour-suppressor gene patched encodes a candidate receptor for Sonic hedgehog. *Nature* **384**, 129-34.
Stone, J. R. and Hall, B. K. (2004). Latent homologues for the neural crest as an evolutionary novelty. *Evol Dev* **6**, 123-9.
Stottmann, R. W., Anderson, R. M. and Klingensmith, J. (2001). The BMP antagonists Chordin and Noggin have essential but redundant roles in mouse mandibular outgrowth. In *Dev Biol*, vol. 240 (ed., pp. 457-73.
Stukenberg, P. T., Lustig, K. D., McGarry, T. J., King, R. W., Kuang, J. and Kirschner, M. W. (1997). Systematic identification of mitotic phosphoproteins. *Curr Biol* **7**, 338-48.
Sun, T., Rodriguez, M. and Kim, L. (2009). Glycogen synthase kinase 3 in the world of cell migration. *Dev Growth Differ* **51**, 735-42.
Svensson, M. E. and Haas, A. (2005). Evolutionary innovation in the vertebrate jaw: A derived morphology in anuran tadpoles and its possible developmental origin. *Bioessays* **27**, 526-32.
Szabo-Rogers, H., Geetha-Loganathan, P., Nimmagadda, S., Fu, K. and Richman, J. (2008). FGF signals from the nasal pit are necessary for normal facial morphogenesis. *Dev Biol* **318**, 289-302.
Taïeb, A. (2005). Tacrolimus and the pigmentary system. *Dermatology (Basel)* **210**, 177-8.
Taipale, J., Cooper, M. K., Maiti, T. and Beachy, P. A. (2002). Patched acts catalytically to suppress the activity of Smoothened. *Nature* **418**, 892-7.
Takahama, H., Sasaki, F. and Watanabe, K. (1988). Morphological changes in the oral (buccopharyngeal) membrane in urodelan embryos: development of the mouth opening. *J Morphol* **195**, 59-69.

Take-uchi, M., Clarke, J. and Wilson, S. (2003). Hedgehog signalling maintains the optic stalk-retinal interface through the regulation of Vax gene activity. *Development* **130**, 955-68.
Tanji, C., Yamamoto, H., Yorioka, N., Kohno, N., Kikuchi, K. and Kikuchi, A. (2002). A-kinase anchoring protein AKAP220 binds to glycogen synthase kinase-3beta (GSK-3beta) and mediates protein kinase A-dependent inhibition of GSK-3beta. *J Biol Chem* **277**, 36955-61.
Tao, Q., Yokota, C., Puck, H., Kofron, M., Birsoy, B., Yan, D., Asashima, M., Wylie, C. C., Lin, X. and Heasman, J. (2005). Maternal wnt11 activates the canonical wnt signaling pathway required for axis formation in Xenopus embryos. *Cell* **120**, 857-71.
Tetsu, O. and McCormick, F. (1999). Beta-catenin regulates expression of cyclin D1 in colon carcinoma cells. *Nature* **398**, 422-6.
Théveneau, E., Duband, J.-L. and Altabef, M. (2007). Ets-1 confers cranial features on neural crest delamination. *PLoS ONE* **2**, e1142.
Theveneau, E. and Mayor, R. (2012). Neural crest migration: interplay between chemorepellents, chemoattractants, contact inhibition, epithelial–mesenchymal transition, and collective cell migration. In *Dev Biol*, (ed.
Thomas, G. M., Frame, S., Goedert, M., Nathke, I., Polakis, P. and Cohen, P. (1999). A GSK3-binding peptide from FRAT1 selectively inhibits the GSK3-catalysed phosphorylation of axin and beta-catenin. *FEBS Lett* **458**, 247-51.
Tobin, J. L., Di Franco, M., Eichers, E., May-Simera, H., Garcia, M., Yan, J., Quinlan, R., Justice, M. J., Hennekam, R. C., Briscoe, J. et al. (2008a). Inhibition of neural crest migration underlies craniofacial dysmorphology and Hirschsprung's disease in Bardet-Biedl syndrome. *Proc Natl Acad Sci U S A* **105**, 6714-9.
Tobin, J. L., Di Franco, M., Eichers, E., May-Simera, H., Garcia, M., Yan, J., Quinlan, R., Justice, M. J., Hennekam, R. C., Briscoe, J. et al. (2008b). Inhibition of neural crest migration underlies craniofacial dysmorphology and Hirschsprung's disease in Bardet-Biedl syndrome. *Proc Natl Acad Sci USA* **105**, 6714-9.
Tolle, N. and Kunick, C. (2011). Paullones as inhibitors of protein kinases. In *Curr Top Med Chem*, vol. 11 (ed., pp. 1320-32.
Topf, K. F., Kletter, G. B., Kelch, R. P., Brunberg, J. A. and Biesecker, L. G. (1993). Autosomal dominant transmission of the Pallister-Hall syndrome. *J Pediatr* **123**, 943-6.
Trainor, P. A. (2010). Craniofacial birth defects: The role of neural crest cells in the etiology and pathogenesis of Treacher Collins syndrome and the potential for prevention. *Am J Med Genet A* **152A**, 2984-94.
Trainor, P. A., Dixon, J. and Dixon, M. J. (2009). Treacher Collins syndrome: etiology, pathogenesis and prevention. *Eur J Hum Genet* **17**, 275-83.
Tucker, R. P. (2004). Neural crest cells: a model for invasive behavior. *Int J Biochem Cell Biol* **36**, 173-7.
Ulleland, C. N. (1972). The offspring of alcoholic mothers. *Ann N Y Acad Sci* **197**, 167-9.
Ungos, J. M., Karlstrom, R. O. and Raible, D. W. (2003). Hedgehog signaling is directly required for the development of zebrafish dorsal root ganglia neurons. *Development* **130**, 5351-62.
Urist, M. R. (1965). Bone: formation by autoinduction. In *Science*, vol. 150 (ed., pp. 893-9.

Vallin, J., Thuret, R., Giacomello, E., Faraldo, M., Thiery, J. and Broders, F. (2001). Cloning and characterization of three Xenopus slug promoters reveal direct regulation by Lef/beta-catenin signaling. *J Biol Chem* **276**, 30350-8.
van de Water, S., van de Wetering, M., Joore, J., Esseling, J., Bink, R., Clevers, H. and Zivkovic, D. (2001). Ectopic Wnt signal determines the eyeless phenotype of zebrafish masterblind mutant. *Development* **128**, 3877-88.
van Noort, M. and Clevers, H. (2002). TCF transcription factors, mediators of Wnt-signaling in development and cancer. *Dev Biol* **244**, 1-8.
van Weeren, P. C., de Bruyn, K. M., de Vries-Smits, A. M., van Lint, J. and Burgering, B. M. (1998). Essential role for protein kinase B (PKB) in insulin-induced glycogen synthase kinase 3 inactivation. Characterization of dominant-negative mutant of PKB. *J Biol Chem* **273**, 13150-6.
Vega, S., Morales, A. V., Ocaña, O. H., Valdés, F., Fabregat, I. and Nieto, M. A. (2004). Snail blocks the cell cycle and confers resistance to cell death. *Genes Dev* **18**, 1131-43.
Vokes, S. A., Ji, H., McCuine, S., Tenzen, T., Giles, S., Zhong, S., Longabaugh, W. J. R., Davidson, E. H., Wong, W. H. and McMahon, A. P. (2007). Genomic characterization of Gli-activator targets in sonic hedgehog-mediated neural patterning. *Development* **134**, 1977-89.
Vokes, S. A., Ji, H., Wong, W. H. and McMahon, A. P. (2008). A genome-scale analysis of the cis-regulatory circuitry underlying sonic hedgehog-mediated patterning of the mammalian limb. *Genes Dev* **22**, 2651-63.
Wada, H. (2001). Origin and evolution of the neural crest: a hypothetical reconstruction of its evolutionary history. *Dev Growth Differ* **43**, 509-20.
Wada, N., Javidan, Y., Nelson, S., Carney, T. J., Kelsh, R. N. and Schilling, T. F. (2005). Hedgehog signaling is required for cranial neural crest morphogenesis and chondrogenesis at the midline in the zebrafish skull. *Development* **132**, 3977-88.
Walsh, S. B., Xu, J., Xu, H., Kurundkar, A. R., Maheshwari, A., Grizzle, W. E., Timares, L., Huang, C. C., Kopelovich, L., Elmets, C. A. et al. (2011). Cyclosporine a mediates pathogenesis of aggressive cutaneous squamous cell carcinoma by augmenting epithelial-mesenchymal transition: Role of TGF β signaling pathway. *Mol Carcinog* **50**, 516-27.
Wang, H., Brown, J. and Martin, M. (2011). Glycogen synthase kinase 3: a point of convergence for the host inflammatory response. *Cytokine* **53**, 130-40.
Wang, Q. T. and Holmgren, R. A. (1999). The subcellular localization and activity of Drosophila cubitus interruptus are regulated at multiple levels. *Development* **126**, 5097-106.
Wasmeier, C., Hume, A. N., Bolasco, G. and Seabra, M. C. (2008). Melanosomes at a glance. In *J Cell Sci*, vol. 121 (ed., pp. 3995-9.
Waterman, R. E. (1977). Ultrastructure of oral (buccopharyngeal) membrane formation and rupture in the hamster embryo. *Dev Biol* **58**, 219-29.
Waterman, R. E. (1985). Formation and perforation of closing plates in the chick embryo. *Anat Rec* **211**, 450-7.
Waterman, R. E. and Schoenwolf, G. C. (1980). The ultrastructure of oral (buccopharyngeal) membrane formation and rupture in the chick embryo. *Anat Rec* **197**, 441-70.

Welsh, G. I., Miller, C. M., Loughlin, A. J., Price, N. T. and Proud, C. G. (1998). Regulation of eukaryotic initiation factor eIF2B: glycogen synthase kinase-3 phosphorylates a conserved serine which undergoes dephosphorylation in response to insulin. *FEBS Lett* **421**, 125-30.
Wheeler, G. and Brändli, A. (2009). Simple vertebrate models for chemical genetics and drug discovery screens: lessons from zebrafish and Xenopus. *Dev Dyn* **238**, 1287-308.
Wilson, C. W. and Stainier, D. Y. R. (2010). Vertebrate Hedgehog signaling: cilia rule. *BMC Biol* **8**, 102.
Wilson, Y., Richards, K., Ford-Perriss, M., Panthier, J. and Murphy, M. (2004). Neural crest cell lineage segregation in the mouse neural tube. *Development* **131**, 6153-62.
Wodarz, A. and Nusse, R. (1998). Mechanisms of Wnt signaling in development. *Annu Rev Cell Dev Biol* **14**, 59-88.
Wolda, S. L., Moody, C. J. and Moon, R. T. (1993). Overlapping expression of Xwnt-3A and Xwnt-1 in neural tissue of Xenopus laevis embryos. *Dev Biol* **155**, 46-57.
Wood-Kaczmar, A., Kraus, M., Ishiguro, K., Philpott, K. L. and Gordon-Weeks, P. R. (2009). An alternatively spliced form of glycogen synthase kinase-3beta is targeted to growing neurites and growth cones. *Mol Cell Neurosci* **42**, 184-94.
Woodgett, J. R. (1994). Regulation and functions of the glycogen synthase kinase-3 subfamily. *Semin Cancer Biol* **5**, 269-75.
Wrana, J. L., Tran, H., Attisano, L., Arora, K., Childs, S. R., Massagué, J. and O'Connor, M. B. (1994). Two distinct transmembrane serine/threonine kinases from Drosophila melanogaster form an activin receptor complex. In *Mol Cell Biol*, vol. 14 (ed., pp. 944-50.
Wray, J., Kalkan, T. and Smith, A. G. (2010). The ground state of pluripotency. *Biochem Soc Trans* **38**, 1027-32.
Wu, J., Saint-Jeannet, J.-P. and Klein, P. S. (2003). Wnt-frizzled signaling in neural crest formation. *Trends Neurosci* **26**, 40-5.
Wu, J., Yang, J. and Klein, P. S. (2005). Neural crest induction by the canonical Wnt pathway can be dissociated from anterior-posterior neural patterning in Xenopus. *Dev Biol* **279**, 220-32.
Wurdak, H., Ittner, L. M. and Sommer, L. (2006). DiGeorge syndrome and pharyngeal apparatus development. *Bioessays* **28**, 1078-86.
Xie, J., Murone, M., Luoh, S. M., Ryan, A., Gu, Q., Zhang, C., Bonifas, J. M., Lam, C. W., Hynes, M., Goddard, A. et al. (1998). Activating Smoothened mutations in sporadic basal-cell carcinoma. *Nature* **391**, 90-2.
Yamaguchi, T. P. (2001). Heads or tails: Wnts and anterior-posterior patterning. *Curr Biol* **11**, R713-24.
Yang, Y., Drossopoulou, G., Chuang, P. T., Duprez, D., Marti, E., Bumcrot, D., Vargesson, N., Clarke, J., Niswander, L., McMahon, A. et al. (1997). Relationship between dose, distance and time in Sonic Hedgehog-mediated regulation of anteroposterior polarity in the chick limb. *Development* **124**, 4393-404.
Yu, H. and Moens, C. (2005). Semaphorin signaling guides cranial neural crest cell migration in zebrafish. *Dev Biol* **280**, 373-85.

Yu, J.-K., Meulemans, D., McKeown, S. J. and Bronner-Fraser, M. (2008). Insights from the amphioxus genome on the origin of vertebrate neural crest. In *Genome Res*, vol. 18 (ed., pp. 1127-32.
Yuan, H., Mao, J., Li, L. and Wu, D. (1999). Suppression of glycogen synthase kinase activity is not sufficient for leukemia enhancer factor-1 activation. *J Biol Chem* **274**, 30419-23.
Zaghloul, N. A. and Katsanis, N. (2009). Mechanistic insights into Bardet-Biedl syndrome, a model ciliopathy. *J Clin Invest* **119**, 428-37.
Zeng, X., Goetz, J. A., Suber, L. M., Scott, W. J., Schreiner, C. M. and Robbins, D. J. (2001). A freely diffusible form of Sonic hedgehog mediates long-range signalling. *Nature* **411**, 716-20.
Zhou, B. P., Deng, J., Xia, W., Xu, J., Li, Y. M., Gunduz, M. and Hung, M.-C. (2004). Dual regulation of Snail by GSK-3beta-mediated phosphorylation in control of epithelial-mesenchymal transition. *Nat Cell Biol* **6**, 931-40.
Zhou, B. P. and Hung, M.-C. (2005). Wnt, hedgehog and snail: sister pathways that control by GSK-3beta and beta-Trcp in the regulation of metastasis. *Cell Cycle* **4**, 772-6.